IN²UB
ANNUAL MEETING
BOOK OF ABSTRACTS

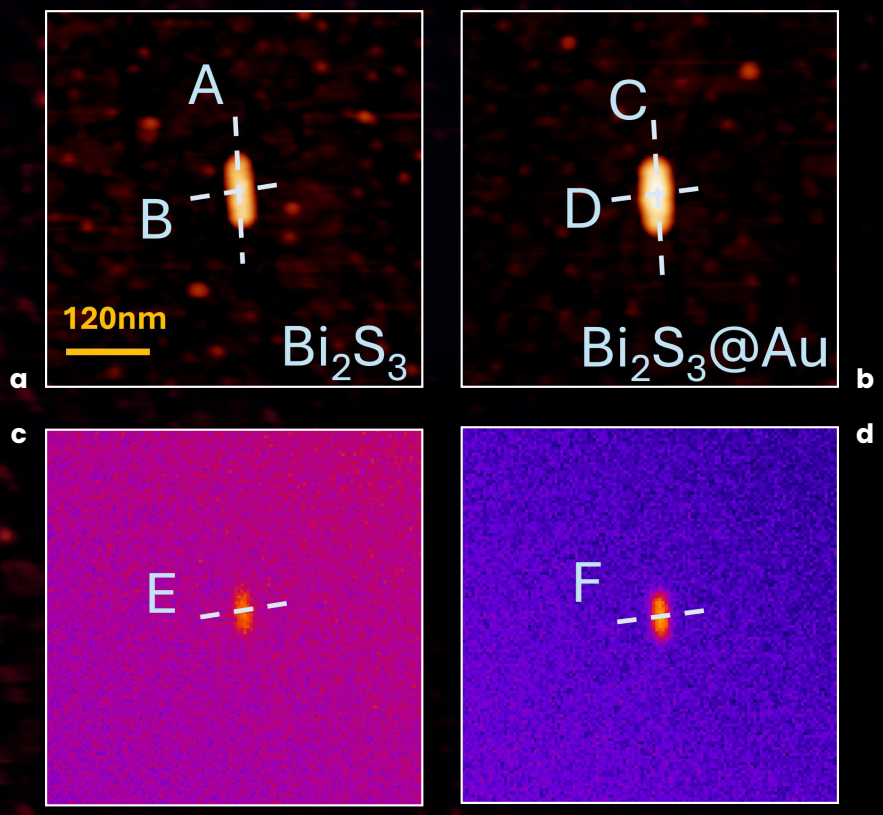

10th JULY 2025

Aula Magna, Solar Atrium and Hall
of the Faculties of Chemistry and Physics

Institut de Nanociència i Nanotecnologia

UNIVERSITAT DE BARCELONA

Institut de Nanociència i Nanotecnologia

UNIVERSITAT DE BARCELONA

Editorial Board and Scientific Management: IN^{2}UB

Graphic Design and Layout: Cristina M. Idoate

Cover image: Nanoscale topographic and dielectric characterization of individual Bi_2S_3 and Bi_2S_3@Au NRs. a, b) Atomic force microscopy topographic images of Bi_2S_3 and Bi_2S_3@Au NRs, respectively. c, d) Electrostatic force microscopy images acquired in constant height mode at tip–sample distances of 23 ± 2 nm for Bi_2S_3 and 26 ± 2 nm for Bi_2S_3@Au. Kindly provided by Dra. Adriana Isabel Figueroa in frame of ATR-2022 IN^{2}UB call.

FOREWORD

Dear IN²UB Fellows,

As every year, it is a great pleasure to welcome you to the 2025 IN²UB Annual Workshop. I invite you to explore the program and book of abstracts, which once again reflect the vibrant and diverse research carried out across our institute. We are deeply encouraged by your enthusiastic response and the richness of your contributions, which make this gathering so meaningful.

The primary goal of this workshop remains to showcase the breadth and depth of the scientific endeavors within our community and to promote fruitful exchanges that strengthen collaboration among our members.

I would like to express my sincere gratitude to all those who have dedicated their time and effort to organizing this event, as well as to all contributors for their valuable scientific work.

As this marks my final year as Director of the Institute, I would also like to take this opportunity to thank everyone who has supported me throughout this journey. It has been an honor to serve in this role, one I have approached with honesty and fairness. These years have been among the most rewarding and inspiring of my academic career at the University of Barcelona.

Warm regards,
GUILLEM AROMÍ
Director of the Institute of Nanoscience and Nanotechnology
of the University of Barcelona (IN²UB)

CONTENTS INDEX

PROGRAM 8 - 9

ART 10 - 15

ART1
Light-Responsive Magnetic Nanorods: Design, Stabilization, And Local Photothermal Ablation Experiments

ART2
Impact Of Spin Orbit Coupling On Decoherence In Molecular Quantum Bits

ART3
Biodegradable, Antioxidant & Antimicrobial Active Food Packaging Films By Acylation Of Biomass Cellulose Over Ion-Exchange Resins: Challenges, Facts And Opportunities

ORALS 16 - 27

O1
High-Resolution 3D Printed Hydrogels In Microfluidic Devices For Biomimetic Angiogenesis Modeling (NanoBio)

O2
Micelle Movement And Fiber Vibrations In Bis-Imidazolium Supramolecular Hydrogels (NanoPharmaMed)

O3
The Coupling Of Polarization And Oxygen Vacancy Migration In Ferroelectric $Hf_{0.5}Zr_{0.5}O_2$ Thin Films Enables Electrically Controlled Thermal Memories Above Room Temperature (NanoPhotoElectro)

O5
Study of Active Nematic Dynamics: Transition from 3D to 2D Structures and Self-Assembly Processes (NanosMat)

O4
Unveiling High-Temperature Pigments in 16th–17th Century Bizen Ceramics: A Multiscale Analytical Approach (NanoMet)

O6
Cyclometalated Pt(Ii) Co-Crystals: Luminescence Tuning And Weak Interaction Analysis (NanosMat)

O7
Characterizing The Hard And Soft Nanoparticle-Protein Corona With Multilayer Adsorption (NanoMet)

O8
Synthesis And Modification Of BiOI-Based Materials For Water Decontamination (NanosMat)

O9
Magnetic Wrinkles For Magnonics (NanoEnergy)

O10
Understanding Magnetic Hyperthermia Performance Within Physiological Safety Field Limits (NanoMagnetics)

O11
Anchoring Transition Of A Smectic Film And Pattern Formation Of Focal Conic Domains In Liquid Crystal Flow Cell Geometry

POSTERS 28 - 105

NanoMet **29**

P1 Crystalline Phase-Dependent Dielectric Properties Of HfO_2: A Tem And Eels Study

NanoBio **31**

P2 Dwell Time Dispersion In DNA Translocation Through Nanopores

P3 Cannabidiol On Synthetic Neuronal Membranes

P4 Nanostructured Topographies For Cardiomyocyte Alignment Using Two-Photon Polymerization

P5 PCSK9 Inhibition By Polypurine Reverse Hoogsteen Hairpins

P6 Micro And Manoengineered Heart-On-A-Chip For In Vitro Study And Treatment Screening Of Catecholaminergic Polymorphic Ventricular Tachycardia

P7 TRIFAPYs As Lipid-Based Delivery Of PPRHs Targeting Survivin In Cancer And Brain Endothelial Cells

NanoPharmaMed **37**

P8 3D Spheroids Induced By Superhydrophobicity As Both In Vitro Diagnostic And Therapeutic Tools

P9 Synthesis Of TPE-Based Aie Fluorescent Probes And Their Application In Bioimaging

P10 Halloysite Based Nanomaterials For Potential Theranostic Application

P11 Biological Profiling Of ZnO And TiO_2 Nanoparticles: Hemocompatibility And Phototoxicity Compared

P12 Molecular Photoswitching: Energy Storage And Controlled Release In Light-Induced Trans-Cis Isomerization

P13 Responsive-Functionalized Silicon Oxide Microchips As A Sensing Platform For Intracellular Recognition Of Glutathione

P14 Nanotechnological Breakthrough For ALS: Multifunctional pVEC-PEG-PLGA Nanoparticles For Targeted Riluzole Delivery To Motor Neuron Diseases

P15 Self-Assembled Porphyrin Gels For Enhanced Singlet Oxygen Generation For Photodynamic Therapy

P16 Advanced Nanocarrier Platforms For The Delivery Of Bakuchiol, Encapsulation Efficiency And Release Profiling

P17 Robust Calix[4]Arene–Polyethyleneimine Functionalized Iron Oxide Nanoparticles For Efficient Recovery Of Gold And Platinum Chloride Complexes

P18 In Vitro Release And Ex Vivo Permeation Study Of Lipid Solution For Topical Treatment Of Psoriasis

NanoMagnetics **52**

P19 Design Of An Optomagnomechanical Crystal For The Investigation Of Novel Quantum States Of Matter

P20 Synthesizing SMM And/Or Magnetocoolant Rings By Slight Schiff-Base Tuning

P21 Magnetic Induced Transparency In Cavity-Magnon Polaritons

P22 A Triclinic Co(II)–Polyoxometalate Complex $(C_9H_{13}N_2O_2)_2[(Co(H_2O)_5)_2Temo_6O_{24}]\cdot 2h_2O$: Synthesis, Structure And SMM Properties

P23 Raylegih-Jeans Condensation Of Magnons In An Optomagnomechanical System

P24 The Role Of Terahertz Vibrations In The Spin Relaxation Of Cerium-Based Metal-Organic Frameworks[1]

P25 2D Materials: Metallic/Molecular Heterostructures For Spintronics Applications

P26 Orbital Currents Generated By Surface Acoustic Waves In FM/NM Bilayers

P27 Design Of Hydrogen-Bonded Supramolecular Switchable Magnetic Materials

P28 Exploring Structural Diversity In Lanthanide-Based Metal-Organic Frameworks For Advanced Functional Applications

P29 Stroboscopic Kerr Imaging Of Magnetoacustic Waves In Ferromagnetic Thin Films

P30 Versatile Supramolecular Architectures As Host/Guest Systems

P31 Antiferromagnetism At The Nanoscale

P32 Spin Dynamics In Ag(II) Molecular Systems

P33 Biocatalysis And Photothermal Efficiency Using Semiconducting Nanoparticles

P34 Deep Learning For Magnetitzation Dynamics

P35 How Ligand Surroundings Affect The Coherence Of An Electron Spin Qubit

P36 Tunable Functionalization Of Host-Guest Supramolecular Assemblies Via Selective Metal Ion Employment

P37 Chiroptical Response Through Multipolar Plasmonic Modes In Twisted Triskelion Stacks

P38 Molecular Flexibility-Driven Spin-Crossover Modulation In A Single-Crystal Fe(II) Complex

P39 Electric Control Of Switching Fields In FM Thin Films Using Surface Acoustic Waves

P40 Study Of The Spin Dynamics Of A New Family Of Schiff Base Heterometallic Mn(V)-4f Complexes

NanoPhotoElectro **75**

P41 Development Of ZIF-8 Thin Film Sensors For The Detection Of Volatile Organic Compunds

P42 Inkjet-Printed $CsCu_2I_3$ Perovskite Photodetectors: Synthesis, Optical Characterization, And Device Performance

P43 Novel Gas Sensors Based On (MGCONICUZN)O High-Entropy Oxide

P44 Influence Of Pulsed Current Driving On The Lifetime And Efficiency Of $CsPbBr_3$-Based PeLEDs

P45 Depth Sensible Instrument For Mueller Matrix Imaging

P46 Effect Of Relative Humidity And Temperature On The Chemoresisitive Gas Sensing Of $Ni_3(HHTP)_2$ MOF

P47 Full Stokes Imaging Using Wavelength-Dependent Retardation In A Polarization Camera

NanosMat **83**

P48 C-Bridged Diphosphanes With A Substituted Backbone

P49 Systematic Investigation Of Deposition And Thermal Treatment Parameters For Mo_2C Thin-Film HER Catalysts

P50 Supercapacitive Performance Of Electrodes Based On Graphene Nanowalls Anchored On Titanium-Mxene

P51 Nanostructured CNT@SINW Hybrid Anodes For Next-Generation Lithium-Ion Batteries

P52 Ru/CNTs Prepared By Electroless Deposition For Heterogeneous Catalysis Application

P53 Magnetic Control Of Driven Colloids Dispersed In Liquid Crystals

P54 Exploring Structural–Photophysical Property Relationships In Gold(I)-Phosphine Complexes

P55 Tuning Photophysical Properties Of Au(I) Pillarplexes Through Anion Variation

P56 New Organometallic Precursors For Enantioselective Catalysis

P57 Inkjet Printing Of Metal Halide Perovskites: Linking Thin Film Formation To Photodetector Device Performance

P58 Electrodeposited Cu, Ni, Ru, And Their Binary/Ternary Alloys For Enhanced Electrocatalytic Reduction Of Levulinic Acid Into Value-Added Chemical Platforms

P59 WITHDRAWN

NanoEnergy **96**

P60 Dielectric-Metal-Dielectric Thin Film Structures As Transparent Electrodes For Solar Cells

P61 Evaluation Of Tio_2–HCl Inks For Chemical Sintering In Direct Ink Writing (DIW) 3D Printing Processes For Water Treatment Applications

P62 New Technologies Of Transparent Solar Cells With Oxides For Advanced Photovoltaic Integrations

P63 Carbide-Based Materials As Catalysts For The CO_2 Reduction To Syngas Processes

Research Areas Collaborations **103**

P64 Corona Personalisation Via Iterative Exposure To Media Modulates Nanoparticle Toxicity (NanoMet & NanoPharmaMed)

P65 Development Of Triphenylene-Derived MOFs For Their Use In Green Catalysis (NanosMat & NanoPhotoElectro)

AUTHOR INDEX **106 - 108**

PROGRAM

9.10h – 9.30h **REGISTRATION**

9.30h – 9.40h **WELCOME & OPENING**
Dr. Guillem Aromí, IN²UB Director.

SESSION I Chaired by Dr. Inma Angurell

9.40h – 10.00h **ART1**
Light-Responsive Magnetic Nanorods: Design, Stabilization, and Local Photothermal Ablation Experiments
Dr. Carlos Moya Alvarez
(NanoMagnetics&NanoPharmaMed&NanoPhotoElectro collaboration)

10.00h – 10.20h **O1 High-Resolution 3D Printed Hydrogels in Microfluidic Devices for Biomimetic Angiogenesis Modeling**
Adria Noguera Monteagudo (NanoBio)

10.20h – 10.40h **O2 Micelle Movement And Fiber Vibrations In Bis-Imidazolium Supramolecular Hydrogels**
Daniela Dupkalová (NanoPharmaMed)

10.40 – 11h **O3 The Coupling Of Polarization And Oxygen Vacancy Migration In Ferroelectric $Hf_{0.5}Zr_{0.5}O_2$ Thin Films Enables Electrically Controlled Thermal Memories Above Room Temperature**
Dr. Eric Langenberg Perez (NanoPhotoElectro)

11.00h –11.20h **COFFEE BREAK**

11.20h – 12.15h **POSTER SESSION I**

SESSION II Chaired by Dr. Oriol Arteaga

12.15h – 12.35h **ART2 Impact of Spin Orbit Coupling on Decoherence in Molecular Quantum Bits**, Dr. Júlia Mayans Ayats (NanoMagnetics collaboration: Physics&Chemistry)

12.35h – 12.55h **O4 Unveiling High-Temperature Pigments in 16th–17th Century Bizen Ceramics: A Multiscale Analytical Approach**, Gavriela Logothetou (NanoMet)

12.55h – 13.15h **O5 Study of Active Nematic Dynamics: Transition from 3D to 2D Structures and Self-Assembly Processes**, Marc Vergès Vilarrubia (NanosMat)

13.15h – 13.35h **O6 Cyclometalated Pt(II) Co-Crystals: Luminescence Tuning And Weak Interaction Analysis**, Mar Inés García Del Amo (NanosMat)

13.35h – 14.25h **LUNCH & NETWORKING**

14.25h – 15.20h **POSTER SESSION II**

SESSION III Chaired by Dr. M. Lluïsa Pérez

15.20h – 15.40h **O7**
Characterizing the hard and soft nanoparticle-protein corona with multilayer adsorption, Dr. Giancarlo Franzese (NanoMet)

15.40h – 16.00h **ART3**
Biodegradable, Antioxidant & Antimicrobial Active Food Packaging Films By Acylation of Biomass Cellulose Over Ion-Exchange Resins: Challenges, Facts and Opportunities, Dr. Rodrigo Soto Lopez (NanosMat&NanoEnergy collaboration)

16.00h – 16.20h **O8**
Synthesis and Modification of BiOI-Based Materials For Water Decontamination, Laura Huidobro Rodríguez (NanosMat)

16.20h – 16.40h **COFFEE BREAK**

SESSION IV Chaired by Dr. Arnald Grabulosa

16.40h – 17.00h **O9**
Magnetic Wrinkles For Magnonics, Dr. Regina Galceran Vercher (NanoEnergy)

17.00h – 17.20h **O10**
Understanding Magnetic Hyperthermia Performance Within Physiological Safety Field Limits, Dr. Òscar Iglesias Clotas (NanoMagnetics)

17.20h – 17.40h **O11**
Anchoring Transition of a Smectic Film and Pattern Formation of Focal Conic Domains in Liquid Crystal Flow Cell Geometry, Olga Bantysh (NanosMat)

17.40h – 18.00h **POSTER AWARDS**

18.00h – 18.10h **CLOSING REMARKS**
Dr. Martí Duocastella, IN²UB Deputy Director

ART

ART

ART 1
LIGHT-RESPONSIVE MAGNETIC NANORODS: DESIGN, STABILIZATION AND LOCAL PHOTOTHERMAL ABLATION EXPERIMENTS

Carlos Moya,[1,2*] Jose Alejandro Ruiz Torres,[2,3] Jorge Ara,[2,3] Ana Belén Caballero,[1,2] Mª Antònia Busquets,[2,4] Mª Carmen del Morán,[2,5] Amílcar Labarta,[2,3] Xavier Batlle,[2,3] and Patrick Gamez[1,2]

[1] Departament de Química Inorgànica i Orgànica, Universitat de Barcelona, Martí i Franquès, 1-11, 08028 Barcelona, Spain
[2] Institut de Nanociència i Nanotecnologia (IN²UB), Universitat de Barcelona, 08028 Barcelona, Spain
[3] Departament de Física de la Matèria Condensada, Universitat de Barcelona, Martí i Franquès 1, 08028 Barcelona, Spain,
[4] Departament de Fisicoquímica, Facultat de Farmàcia i Ciències de l'Alimentació, Universitat de Barcelona, Av. Joan XXIII, 27-31, 08028 Barcelona, Spain
[5] Departament de Bioquímica i Fisiologia, Secció de Fisiologia, Facultat de Farmàcia i Ciències de l'Alimentació, Universitat de Barcelona, Av. Joan XXIII, 27-31, 08028 Barcelona, Spain
* email of the presenting author: **carlosmoyaalvarez@ub.edu**

Light-responsive magnetic nanoparticles are promising candidates for localized cancer therapies. Among them, anisotropic iron oxide-based nanostructures offer enhanced cellular penetration, superior magnetic properties, and improved heat generation compared to their spherical counterparts [1],[2]. However, the impact of morphology on their local photothermal efficiency is still not clear. In this 2023 ART project, we focused on the design, and evaluation of magnetite@silica (Fe_3O_4@SiO_2) nanorods with tunable dimensions ranging from 20 to 300 nm as multifunctional nanoheaters for local photothermal ablation *in vitro*. These systems were synthesized through a three-step procedure, starting from a polyethyleneimine-assisted aqueous growth method, followed by a silica coating to improve colloidal stability, and a controlled thermal reduction to Fe_3O_4, preserving the elongated morphology.

Comprehensive characterization confirmed that the composition remained stable after processing and was predominantly composed of Fe_3O_4, surrounded by a uniform silica shell. Besides, Dynamic light scattering measurements confirmed good particle stability in aqueous media, with narrow hydrodynamic size distributions regardless of the particle dimensions. Additionally, UV–Vis spectroscopy revealed a strong dependence of the optical properties on both composition and nanorod dimensions, with enhanced absorption in the near-infrared (NIR) region after phase transformation.

Local photothermal ablation experiments, performed under 808 nm laser irradiation at 0.8 W/cm² using the same particle concentration (1 mg/mL), demonstrated a clear influence of both particle size and composition on heating efficiency. For example, larger 300nm-Fe_3O_4@SiO_2 nanorods produced temperature increases of ~25 °C within 10 minutes, while smaller 100 nm nanorods achieved ~15 °C. Non-magnetic nanorods exhibited only minor heating (~4 °C), confirming the essential role of Fe_3O_4 in light-induced heat generation.

These results highlight the potential of elongated Fe_3O_4 nanoparticles as robust, light-activated nanoheaters, paving the way for future applications in precision oncology strategies that combine magnetic and photothermal treatments.

REFERENCES
[1] C. Moya, *et. al.* Iron Oxide Nanoparticles and their Applications; Villegas, P., Ed.; Nova Science Publishers: 2021; 163–211
[2] X. Batlle, *et. al.* J. Magn. Magn. Mater. 2022, 543, 168594

ART 2
IMPACT OF SPIN ORBIT COUPLING ON DECOHERENCE IN MOLECULAR QUANTUM BITS

J. Mayans[1], J. Torrent[1], A. Escuer[1], A. Figueroa[2], A. Fraile-Rodríguez[2], A. Labarta[2], X. Batlle[2]

[1] Departament de Química Inorgànica i Orgànica, Secció Inorgànica and Institute of Nanoscience and Nanotecnology, Universitat de Barcelona, Barcelona 08028, Spain
[2] Departament de Física de la Matèria Condensada and and Institute of Nanoscience and Nanotecnology, Universitat de Barcelona, Barcelona 08028, Spain
* julia.mayans@ub.edu

The use of electronic spins in magnetic molecules is today one of the driving approaches to build real quantum technologies. Since few years ago, the preferred electronic spin to be used as qubit is the S=½ because it is easily manipulable and controllable. The key parameters to evaluate the qubit performance of a molecular system are the spin-lattice relaxation time (T_1) and the spin-spin relaxation time (T_2), which are closely related. Our goal is to control and quantify one of the parameters that is proposed to highly influence these relaxation times, which is the Spin Orbit Coupling (SOC) in the molecule. It has been demonstrated that SOC increases the spin-phonon relaxation in systems with S > ½, but seems to reduce the relaxation rates for molecules with S = ½, as recently proposed in theoretical calculations.[1] However, such an impact has never been tested experimentally before, as it requires the right combination of techniques: Alter Current magnetometry, Continuous Wave and Pulse-Electronic Paramagnetic Resonance and X-Ray Magnetic Circular Dichroism, that can provide relevant and specific information about the SOC and its effect on the relaxation of the molecule. Figure 1, left, represents the XMCD of some compounds of the family (right).

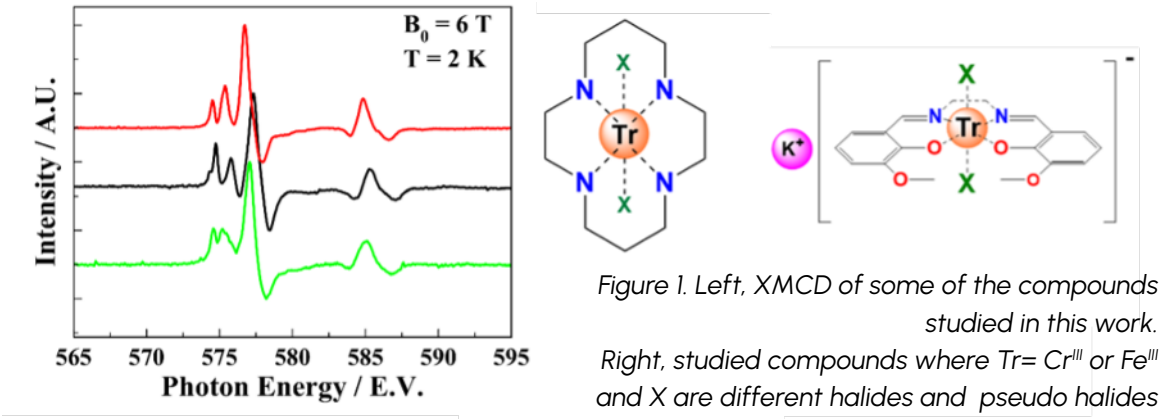

Figure 1. Left, XMCD of some of the compounds studied in this work. Right, studied compounds where Tr= Cr^{III} or Fe^{III} and X are different halides and pseudo halides

REFERENCES
[1] M. Arrio *et Al.*, *Inorg. Chem.*, **2023**, *62*, 18864.
[2] J. Bendix *et Al. J. Phys. Chem.* A. **2012**, *116*, 7842.

ART 3
BIODEGRADABLE, ANTIOXIDANT & ANTIMICROBIAL ACTIVE FOOD PACKAGING FILMS BY ACYLATION OF BIOMASS CELLULOSE OVER ION-EXCHANGE RESINS: CHALLENGES, FACTS AND OPPORTUNITIES

R. Soto[1,*], M. Cuartiella[1], E. Ramirez[1], M. Martínez[2], J. Amorós[3], J. Dosta[1], M. Iborra[1]

[1] Department Of Chemical Engineering & Analytical Chemistry
[2] Department Of Materials Science & Physical Chemistry
[3] Department Of Inorganic & Organic Chemistry
* Corresponding author email: r.soto@ub.edu

INTRODUCTION

An urgent necessity for biomass-based food packaging materials with enhanced biodegradability has become a fact nowadays given the problems triggered in marine ecosystems by petrochemical-based products currently available. Polyethylene (PE), the most widely produced plastic with 10 million ton/year and 34% of total plastics market, represents ~ 42% of the plastic found in the surface sea waters [1]. PE is primarily used as packaging (bags, films, containers, etc.) due to its excellent properties. However, its chemical resilience hinders its decomposition and has generated global concerns on marine ecosystems due to its transfer potential between trophic levels inducing mutagenic and cytotoxic risks [2]. Cellulose alkanoates (CAs) obtained by acetylation of cellulose are a possible solution for film-like packaging applications, being biodegradable and non-toxic. Indeed, some CAs are already used in food packaging [3]. A promising alternative is cellulose acetate propionate (CAP), which can be obtained upon esterification of cellulose with acetic and propionic anhydride (Figure 1c). Promising results for such reaction were obtained with Amberlyst15 in previous research [4], but there is no evidence in the literature about using other ion-exchange resins (IERs). This works aims at shedding light into this fact, by providing a catalyst screening over several IERs with significantly different morphological properties.

MATERIALS & METHODS

Cellulose acylation was performed in 100 mL glass reactors magnetically stirred, immersed in a bath at 55 °C. Anhydrides/cellulose mass ratio of 10, and propionic/acetic anhydrides mass ratio of 1 were used. The catalytic activity of ten different IERs was tested, monitoring the CAP product mass yield and supernatant viscosity (i.e. polymer molecular weight). The CAP solid product separated by crystallization was redissolved in acetone and doped with active ingredients to form the films used in subsequent food rotting prevention efficacy tests.

RESULTS & DISCUSSION

Figure 1 shows the evolution of (a) the CAP formation (exponential increase) and of (b) viscosity (linear increase) for all the IERs evaluated. The resin MN500 was the most productive in terms of mass yield but the corresponding viscosity was far below (about 50%) that obtained with DOW8. The basic resin tested A26-OH exhibited no activity detected. Replication of the runs confirmed their reproducibility with an experimental error below 9%. The results suggest important intraparticle diffusional limitations at play for both gel-type and macroreticular resins, explaining the highest activity and product mass yield obtained over the hypercrosslinked resin MN500 having extra-large size pores. CAP revealing substitution degrees in the order 2.6-2.8 was harvested from each run and used to form active films whose packaging efficiency was evaluated in lab under controlled conditions along with some relevant mechanical properties. Despite not being competitors for polyethylene films, the films formed doped with curcumin exhibited the best behaviour for food packaging and preserve the potential for other type of packaging applications due to other desired properties required for film-like packaging.

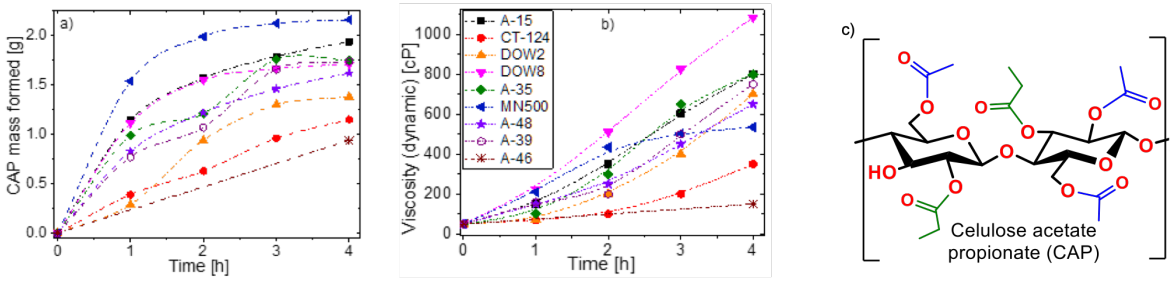

Figure 1. Evolution of CAP formed mass (a) and supernatant viscosity (b) for all the resins evaluated. A26-OH resin not shown (no activity). Dashed lines are a guide to the eye. (c) CAP molecular structure. Blue and green are used to distinguish the moieties from the different acylation agents.

REFERENCES

[1] TG. Erni-Cassola et al. *Journal of Hazardous Materials*, 369 (2019) 691-698.
[2] A. P. C. Araujo et al. *Science of the Total Environment*, 742 (2020) 140217.
[3] D. M. Gouvea et al. *Food Science and Technology*, 63 (2015) 85e91.
[4] G. Fan et al. *Carbohydrate Polymers*, 112 (2014) 203–209.

ORALS

ORALS

O1 NanoBio

HIGH-RESOLUTION 3D PRINTED HYDROGELS IN MICROFLUIDIC DEVICES FOR BIOMIMETIC ANGIOGENESIS MODELING

A. Noguera-Monteagudo[1,*], B. Van Durme[3], Y. Dong[3], S. Van Vlierberghe[3], E. Engel[2], and O. Castaño[1,2]

[1] University of Barcelona, 08028, Barcelona, Spain
[2] Institute for Bioengineering of Catalonia, Spain
[3] Ghent University, Ghent, Belgium.
* adria.noguera@ub.edu

Angiogenesis, the process by which new blood vessels sprout from existing vasculature, plays a fundamental role in tissue regeneration, wound healing, tumor progression, and the integration of biomedical implants. However, replicating this complex process *in vitro* remains a major challenge. Recent technological advances in 3D printing and microfluidics have enabled the development of highly controlled biomimetic platforms for studying angiogenesis [1-2]. Techniques such as two-photon polymerization (2PP) now allow the fabrication of microstructure 3D hydrogels with precise geometries within microfluidic systems, offering improved spatial resolution and environmental control compared to conventional 2D cultures [3].

OBJECTIVES

This study aims to utilize these technologies to fabricate customizable 3D *in vitro* angiogenesis models. By combining 3D printed scaffold, tunable biomaterials, and pro-angiogenic stimuli, the objective is to study how scaffold architecture, material properties, and localized microenvironmental conditions influence vascular network formation and morphogenesis.

MATERIAL AND METHODS

A microfluidic platform designed in AutoCAD was fabricated using PDMS molded from SU8-350 photoresist via standard photolithography. The device includes a central chamber for 3D scaffold integration connected to two lateral channels ending in reservoirs [4]. Scaffolds were designed in Fusion 360 and fabricated via 2PP at 800 nm and 80 mW using a NanoOne Bio printer. By combining 3D printed scaffolds, tunable biomaterials, and pro-angiogenic stimuli, we aim to systematically analyze how scaffold geometry, material stiffness, and local microenvironmental factors affect vascular network growth and structure.

RESULTS

The combination of microfluidics and two-photon polymerization enabled the fabrication of well-defined 3D scaffolds directly within the device, allowing controlled spatial organization of the microenvironment. The printed structures showed high fidelity and supported the formation of vascular-like networks. Preliminary observations indicate that both scaffold geometry and material properties play a critical role in modulating angiogenic responses, highlighting the role of 3D architecture and biomaterial properties in guiding vascular network formation.

CONCLUSIONS AND ACKNOWLEDGMENT

This work demonstrates the potential of combining microfluidics with 3D printing to create biomimetic platforms for angiogenesis studies. The integration of 2PP within microfluidic systems enables precise spatial control and structural complexity, offering a valuable tool for study vascular processes under physiologically relevant conditions.

We gratefully acknowledge the financial support from the Spanish Ministry of Science and Innovation (MICINN) and the Spanish State Research Agency (AEI) through grants RTI2018-097038-B-C22, PID2021-124575OB-I00 and PDC2022-133918-C22, and the the financial support from the European Union's Horizon Europe research & innovation program (EIC-2021-PATHFINDER-OPEN-01-01-101047099 4DBR). Finally, we also appreciate the support of Research Foundation Flanders (FWO) (1SH3W24N).

REFERENCES

[1] E. Akbari, G. B. Spychalski, and J. W. Song, "Microfluidic approaches to the study of angiogenesis and the microcirculation," Microcirculation, vol. 24, no. 5, pp. 1–8, (2017). [2] K. Haase and D. Roger, "Advances in on-chip vascularization," (2017). [3] S. O'Halloran, A. Pandit, A. Heise, A. Kellett, Two-Photon Polymerization: Fundamentals, Materials, and Chemical Modification Strategies. Adv. Sci.2022, 2204072. [4] Adrián López-Canosa, et al., Acta Biomater 2022 Oct 1:151:264-277.

O2 NanoPharmaMed
MICELLE MOVEMENT AND FIBRE VIBRATIONS IN BIS-IMIDAZOLIUM SUPRAMOLECULAR HYDROGELS

Daniela Dupkalová,[1] David B. Amabilino,[2] and Lluïsa Pérez-García[1]

[1] Departament de Farmacologia, Toxicologia i Química Terapèutica, Universitat de Barcelona, Av. Joan XXIII 27-31, Barcelona, 08028, Spain and Institut de Nanociència i Nanotecnologia UB (IN²UB)
[2] Institut de Ciència de Materials de Barcelona (ICMAB-CSIC), Carrer del Til.lers, 08193 Bellaterra, Spain
* **daniela.dupkalova@ub.edu**

The micron-scale movement of biomolecules along supramolecular pathways, evolved in nature, is a remarkable system requiring strong yet reversible interactions between components under the action of a chemical stimulus. Synthetic responsive microscopic systems have been achieved using a variety of stimuli, demonstrating impressive control in relative molecular motion [1]. At a larger scale, our group developed a purely supramolecular system where a molecular 'traveller' moved along a 'path' over several microns when irradiated with visible light [2]. Real-time imaging of the motion in the solvated state using total internal reflection fluorescence microscopy showed that anionic porphyrin molecules move along the fibres of a bis-imidazolium gel upon irradiation.
When recreating the experiment for follow-up research, gels with different structure and morphology were prepared, as the gelation process is very sensitive to parameters including temperature and method of preparation. We have now encountered micelles moving between the gel fibres due to Brownian motion in some of the samples. The size and speed of their movement were further analysed, and the results will be presented.
We also found vibrating fibres in an otherwise immobile network. The vibrations were analysed with respect to different laser intensities used for irradiation. No correlation was found, indicating an intrinsic confined mobility for these fibres in the gel network.

ACKNOWLEDGMENTS
We thank the MICIU-AEI for financing projects PID-2023-146658NB-C32 and PID2021-123873NB-I00, the AGAUR (Generalitat de Catalunya) for a grant to consolidated research groups 2021 SGR 01085 and for a predoctoral scholarship FI Joan Oró. We warmly thank Tania García-Becerra at the Molecular Imaging Platform at the Barcelona Institute of Molecular Biology (CSIC) for assistance with the microscopy.

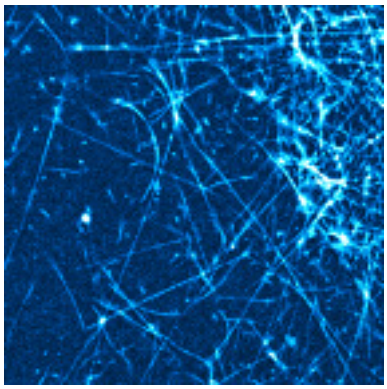

Figure 1: TIRF image of hydrogel sample region where vibrating fibers occurred

REFERENCES
[1] M. Baroncini, S. Silvi, A. Credi, Chemical Reviews, 120, 200–268 (2020).
[2] M. Samperi, B. Bdiri, C.D. Sleet, R. Markus, A.R. Mallia, L. Pérez-García, D.B. Amabilino, Nature Chemistry, 13, 1200-1206 (2021).

O3 NanoPhotoElectro

THE COUPLING OF POLARIZATION AND OXYGEN VACANCY MIGRATION IN FERROELECTRIC $HF_{0.5}ZR_{0.5}O_2$ THIN FILMS ENABLES ELECTRICALLY CONTROLLED THERMAL MEMORIES ABOVE ROOM TEMPERATURE

Dídac Barneo[1,2], Rafael Ramos[3], Hugo Romero[4], Víctor Leborán[4], Noa Varela-Domínguez[3], José A. Pardo[4,5], Francisco Rivadulla[3], **Eric Langenberg**[1,2,*]

[1] Departament de Física de la Matèria Condensada, Universitat de Barcelona, 08028 Barcelona.
[2] Institut de Nanociència i Nanotecnologia (IN²UB), Universitat de Barcelona, 08028 Barcelona.
[3] Centro Singular en Química Biolóxica e Materiais Moleculares (CiQUS), Universidade de Santiago de Compostela, 15782 Santiago de Compostela.
[4] Instituto de Nanociencia y Materiales de Aragón (INMA), CSIC-Universidad de Zaragoza, 50009 Zaragoza.
[5] Departamento de Ciencia y Tecnología de Materiales y Fluidos, Universidad de Zaragoza, 50018 Zaragoza.
* corresponding author: **eric.langenberg@ub.edu**

The finding of materials that allow tuning their thermal conductivity (k) at will using an electric field is key to develop thermal memories that can store and process information using thermal currents. This novel technology has a clear potential to excel in terms of energy consumption, reuse, and recovery, as heat would no longer be a residual waste byproduct, but an input. Here we investigate epitaxial $Hf_{0.5}Zr_{0.5}O_2$ (HZO) ferroelectric thin films as potential candidates, embedded between Au layer and single-crystal yttria-stabilized zirconia (YSZ) substrate.

HZO films were deposited onto 111-oriented YSZ by pulsed laser deposition, and the polar phase confirmed by X-ray diffraction. Au top electrode was ex-situ deposited by sputtering. k was determined by frequency domain thermoreflectance.

The electric-field dependence of k of HZO is found to be hysteretic, resembling the polarization vs electric field hysteresis loops. This dynamic thermal response is incompatible with ferroelectric domain walls being the main phonon scattering contributors as found in other ferroelectrics, since the maximum values of the thermal conductivity would be found at both negative and positive large voltages (single domain scenario). Instead, we ascribe this phenomenon to the coupling between the ferroelectric polarization and the oxygen ion migration, in which the oxygen vacancies are the main phonon scattering sources and the polarization acts an electrically active ion migration barrier that creates the hysteresis. This new mechanism enables two non-volatile thermal states–high (ON) and low (OFF) k states–when the field is removed, with an ON/OFF ratio of 1.6. Both states exhibit high stability over time, though the switching speed is limited by ion mobility in the yttria-stabilized zirconia substrate.

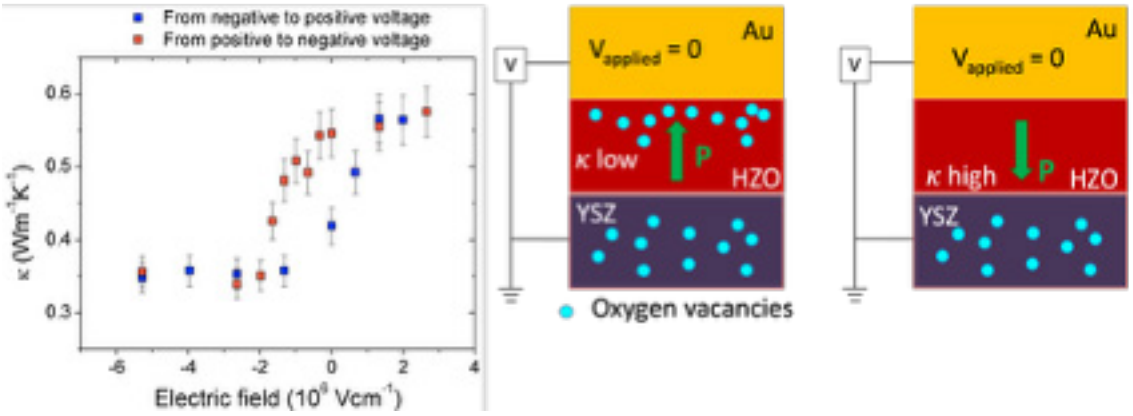

REFERENCES
[1] D. Barneo et al. arXiv:2501.06005. https://doi.org/10.48550/arXiv.2501.06005

O4 NanoMet

UNVEILING HIGH-TEMPERATURE PIGMENTS IN 16th–17th CENTURY BIZEN CERAMICS: A MULTISCALE ANALYTICAL APPROACH

G. Logothetou[1,2,3,*], S. Plana-Ruiz[4], J. Roqué-Rosell[3], E. Tema[5,6], J. Ibáñez-Insa[7], A. Jiménez-Franco[7], M. Stefanova Stankova[6], V. Poulopoulos[2], E. Zymi[1], S. Iwasaki[8], S. Nicolopoulos[9]

[1] Laboratory of Archaeometry, Department of History, Archaeology and Cultural Resources Management, University of the Peloponnese, Greece
[2] Department of Digital Systems, University of the Peloponnese, Greece
[3] Departament de Mineralogia, Petrologia i Geologia Aplicada, Universitat de Barcelona, Spain
[4] Servei de Recursos Científics i Tècnics, Universitat Rovira i Virgili, Spain
[5] Dipartimento di Scienze della Terra, Università degli Studi di Torino, Italy
[6] CIMaN-ALP Palaeomagnetic Laboratory, Peveragno, Italy
[7] Geociències Barcelona (GEO3BCN – CSIC), Spain
[8] Research Institute for the Dynamics of Civilizations, Okayama University, Japan
[9] NanoMEGAS SPRL, Belgium
*g.logothetou@ub.edu

Iron oxide pigments and other minerals play a crucial role in reconstructing the firing technology of ancient ceramics. By understanding how mineral phases transform under different temperatures and redox conditions, it is possible to estimate the firing conditions achieved in the past. This study investigates Bizen Japanese ceramics from the Shikata archaeological site (Okayama, Japan) dated to the 16th to 17th centuries CE to obtain information about their firing conditions. A multiscale analytical approach, combining Petrography, XRF, XRD, and Electron Microscopy and Electron Crystallography techniques, was employed to investigate the pigments responsible for the characteristic hue and colour of the ceramics. Bulk chemical analysis with XRF showed approximately 75 wt% SiO_2, 16 wt% Al_2O_3, 3.5 wt% Fe_2O_3, 0.6 wt% TiO_2, 2 wt% K_2O, and 0.7 wt% CaO. XRD analysis identified the presence of quartz, mullite, plagioclase, and iron oxide phases. However, distinguishing specific iron oxide minerals via XRD was challenging due to a significant amorphous background associated to the development of a silicon-rich glassy matrix and their low peak intensities. The presence of mullite suggests firing temperatures above 950-1100 °C [1]. To confirm these results, multiple advanced electron diffraction applications in the TEM were employed, including precession-assisted 3D ED and 4D-STEM experiments. These characterization techniques allowed us to verify the presence of quartz and mullite and further revealed hematite (Fe_2O_3) nanocrystals embedded within a silicon-rich glassy matrix, along with spinel ($MgAl_2O_4$) and anosovite (Ti_3O_5). Hematite, a pigment that exists in oxidizing kiln conditions, contributes to the characteristic red hue of the ceramics or in parts of them. Spinel formation further indicates firing temperatures around 1100 °C [2], while the presence of anosovite suggests rutile transformation to even higher temperature near 1300 °C [3]. These findings indicate that the firing temperature of the studied ceramics reached up to 1300 °C, corroborating the historical tradition, which holds that Bizen wares were fired at such high temperatures. This study enhances our understanding of the firing technology of Bizen ceramics from the 16th to 17th centuries CE and highlights the importance of the multiscale analytical approach, particularly the use of Transmission Electron Microscopy, for a comprehensive characterization of ancient ceramics.

ACKNOWLEDGMENTS

We warmly acknowledge the Okayama University for providing the Bizen sherds.

REFERENCES

[1] Gliozzo, E. (2020). Ceramic technology. How to reconstruct the firing process. Archaeological and Anthropological Sciences, 12(11), 260. [2] Trindade, M. J., Dias, M. I., Coroado, J., & Rocha, F. (2010). Firing Tests on Clay-Rich Raw Materials from the Algarve Basin (Southern Portugal): Study of Mineral Transformations with Temperature. Clays and Clay Minerals, 58(2), 188–204. [3] Cardarelli, F. (2008). Ceramics, Refractories, and Glasses. In Materials Handbook (Second, pp. 616–617). Springer London.

O5 NanosMat

STUDY OF ACTIVE NEMATIC DYNAMICS: TRANSITION FROM 3D TO 2D STRUCTURES AND SELF-ASSEMBLY PROCESSES.

Marc Vergés[1,2,*] Jordi Ignés[1,2], Francesc Sagués[1,2]

[1] Department of Material Science and Physical Chemistry, Universitat de Barcelona Barcelona, Spain, 08028
[2] Institute of Nanoscience and Nanotechnology, Universitat de Barcelona Barcelona, Spain, 08028
* Presenting author's e-mail: **marc.verges@ub.edu**

Active matter refers to systems that consume energy from their surroundings, converting it into forces and motion, keeping them out of equilibrium and leading to diverse phenomena, from moving crowds to bacterial biofilms. This behaviour drives collective and stochastic dynamics, often linked to biological processes [1]. This study presents an active system with three components: an ATP reservoir, microtubules, and kinesin clusters walking along the microtubules. When brought to an oil-water interface, it forms a bidimensional active nematic material where "active turbulence" emerges due to its stochastic nature [2-3]. Previous studies have presented a methodology for in-situ photopolymerizing fixed 3D hydrogel structures, enabling observation of the photopolymerization process and active material response [4]. This protocol for generating fixed 3D architectures enables the investigation of self-assembly processes driven by external cues. We describe a strategy for engineering an active pump system, wherein a minimal arrangement of obstacles induces directed net flows. Notably, the system is fully reconfigurable, underscoring the versatility and potential of this active material platform for applications in microfluidic technologies. Moreover, we present techniques to transition from fixed 3D structures to mobile 2D structures that are advected by active flows like rafts. This methodology allows us studying how the active fluid organizes and assembles these dispersed objects, providing insights into the spontaneous behaviour of active systems. The 2D structures also serve as a suitable cellular model, offering insights not only into how the material organizes obstacles, but also into how the active material behaves when laterally confined by 2D-like structures. This allows us to study the interaction between two active systems separated by an obstacle, which plays a crucial role in biological organization and may drive advancements in biohybrid machines.

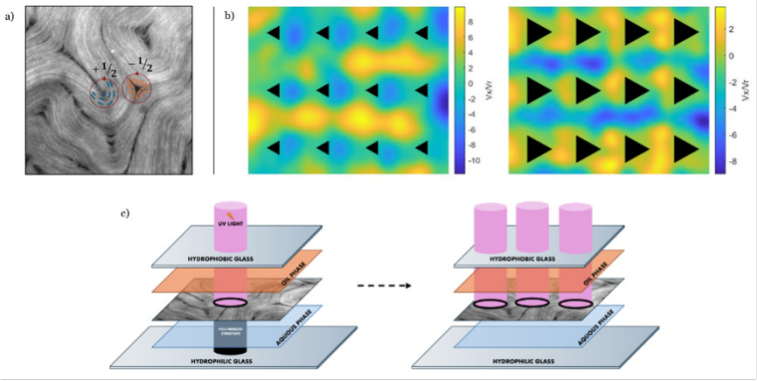

a) Image of an active nematic system showing the topological defects marked as s = +1/2 (blue) and s = –1/2 (orange). b) Time-averaged net flow of the material with embedded objects; we observe a net flow to the right (left panel) and a net flow to the left (right panel) when reversing the orientation of the objects. c) Schematic illustration of the transition from fixed 3D objects to mobile 2D objects generated via photopolymerization.

REFERENCES

[1] Sagués, F., Colloidal Active Matter: Concepts, Experimental Realizations, and Models, 2023, Taylor & Francis, London, UK.
[2] Martínez-Prat, B., Ignés-Mullol, J., Casademunt, J., and Sagués, F., Nature Physics, 2019, 15, 362.
[3] Martínez-Prat, B., et al., Physical Review X, 2021, 11, 031065 (1–16). [4] Vélez-Cerón, I., Guillamat, P., Sagués, F., and Ignés-Mullol, J., Proceedings of the National Academy of Sciences, 2024, 121, e2312494121.
[4] Vélez-Cerón, I., Guillamat, P., Sagués, F., and Ignés-Mullol, J., Proceedings of the National Academy of Sciences, 2024, 121, e2312494121.

O6 NanosMat

CYCLOMETALATED Pt(II) CO-CRYSTALS: LUMINESCENCE TUNING AND WEAK INTERACTION ANALYSIS

M. García[1,2,*], S. Burguera[3], A. Pinto[1,2], A. Lázaro[4], A. Frontera[3], L. Rodríguez[1,2]

[1] Departament de Química Inorgànica i Orgànica, Universitat de Barcelona, Spain
[2] Institut de Nanociència i Nanotecnologia (IN²UB), Universitat de Barcelona, Spain
[3] Departament de Química, Universitat de les Illes Balears, Spain
[4] Institut für Funktionelle Grenzflächen (IFG), Karlsruhe Institute of Technology (KIT), Germany
* mgarcide162@alumnes.ub.edu

Organometallic materials containing ϖ-conjugated entities have gained a special interest in the past few years due to their applications in different fields such as organic light-emitting diodes (OLEDs), organic photovoltaic devices and materials for nonlinear absorption.[1] Cyclometalated compounds derived from platinum present a platinum-carbon bond intramolecularly stabilized by one or several neutral donor atoms. Both the carbon and the neutral donor atom or atoms are located on the same ligand, which acts as a polydentate thus forming a platinacycle where the metal is bound to carbon through a covalent bond while the donor atoms present coordinate bonds.[2-4] These compounds have outstanding luminescent properties since rigidity and the presence of heavy metals generally favour luminescence.[5] In this work several cyclometallated Pt(II) compounds have been synthesised and its luminescent properties have been studied. Finally, this compounds present selectivity for polyaromatic compounds so they can be used as sensors for the detection of contaminants.

In this work it has been studied the critical role of non-covalent interactions between some cyclometalated Pt(II) (1-3) compounds and iodopentafluorobenzene (G). The structural analysis revealed that the Pt(II) center acts as both a halogen bond acceptor and a ϖ-stacking participant, stabilizing the supramolecular assemblies. Moreover, an enhancement in phosphorescence emission was observed for complexes 1·G and 2·G, due to the effect of σ-hole interactions and the double heavy atom effect. Finally, complex 3·G, which lacks σ-hole interactions, exhibited only a slight emission enhancement with a broader spectral band due to its π-stacking arrangement.

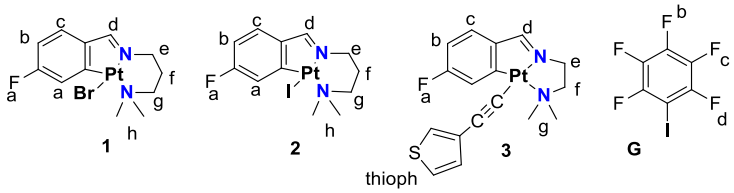

Figure 1. Structures of the cyclometalated Pt(II) compounds synthetized (1-3) and iodopentafluorobenzene (G)

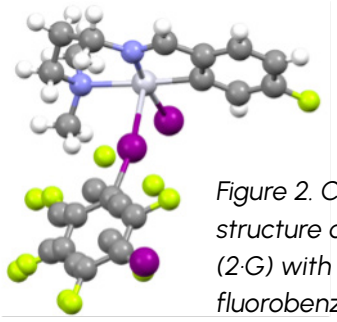

Figure 2. Crystal structure of compound (2·G) with iodopentafluorobenzene

REFERENCES

[1] A. Lázaro, C. Cunha, R. Bosque, J. Pina, J. S. Ward, K. N. Truong, J. C. Lima, M. Crespo, J. S. Seixas de Melo, L. Rodríguez, *New J. Chem.* 2020, 59, 8220-8230

[2] A. Lázaro. Departament de Química Inorgànica, Universitat de Barcelona, 2023, 15-27

[3] M. F. Galimova, S. A. Kondrashova, S. K. Latypov, A. B. Dobrynin, E. M. Zueva, M.M. Petrova, I. E. Kolesnikov, R. R. Musin, E. I. Musina, A. A. Karasik, *Organometallics*, 2023, 42, 2661-2671

[4] S. A. Katkova, D. O. Kozina, K. S. Kisel, M. A. Sandzhieva, D. A. Tarvanen, S. V. Marakarov, V. V. Porsev, S. P. Tunik, M. A. Kinzhalov, *Dalton Trans.* 2023, 52, 4595-4605

[5] A. Lázaro, O. Serra, L. Rodríguez, M. Crespo, M. Font-Badia, *Inorg. Chem.* 2019, 43, 1247-1256

O7 NanoMet

CHARACTERIZING THE HARD AND SOFT NANOPARTICLE-PROTEIN CORONA WITH MULTILAYER ADSORPTION

Alberto Martinez-Serra[1,2,3], Oriol Vilanova[2], Marco P. Monopoli[4], **Giancarlo Franzese**[1,3,*]

[1] Institut de Nanociència i Nanotecnologia (IN²UB), Universitat de Barcelona, Av. Joan XXIII S/N, 08028, Barcelona, Spain
[2] Departament de Bioquímica i Fisiologia, Facultat de Farmàcia i Ciències de l'Alimentació, Universitat de Barcelona, Av. Joan XXIII 27-31, 08028 Barcelona, Spain
[3] Secció de Física Estadística i Interdisciplinària, Departament de Física de la Matèria Condensada, Facultat de Física, Universitat de Barcelona, Martí i Franquès 1, 08028, Barcelona, Spain
[4] Chemistry Department, RCSI (Royal College of Surgeons in Ireland), 123 St Stephen's Green, Dublin 2, Ireland
* Corresponding author: **gfranzese@ub.edu**

Drug delivery across the blood-brain barrier (BBB) via nanoparticles (NPs) is affected by the time-evolution of the biomolecular corona forming around them. This corona comprises proteins that strongly bind to the NP (hard corona) and loosely bound proteins (soft corona) that dynamically exchange with the surrounding solution. While the kinetics of hard corona formation is relatively well understood, thanks to experiments and robust simulation models [1], the experimental characterization and simulation of the soft corona present a more significant challenge. Here, we introduce a novel open-source computational model to simulate its dynamic behavior. We focus on the case of transferrin (Tf) interacting with polystyrene NPs as an illustrative example, demonstrating how this model captures the complexities of the soft corona and offers deeper insights into its structure and behavior. By simulations and experiments, we show that the soft corona is dominated by a glassy evolution that we relate to crowding effects [2]. This work advances our understanding of the soft corona, bridging experimental limitations with improved simulation techniques.

REFERENCES
[1] O. Vilanova, J. Mittag, P. Kelly, S. Milani, K. Dawson, J. Rädler, G. Franzese, ACS Nano, 10, 10842-10850 (2016)
[2] O. Vilanova, A. Martinez-Serra, M.P. Monopoli, and G. Franzese, Front. Nanotechnol. 6:1531039 (2025).

O8 NanosMat
SYNTHESIS AND MODIFICATION OF BiOI-BASED MATERIALS FOR WATER DECONTAMINATION

L. Huidobro[1,2,*], E. Gómez[1,2], A. Serrà[1,2]

[1] Grup d'electrodeposició de Capes Primes i Nanoestructures (GE-CPN), Departament de Ciència de Materials i Química Física, Universitat de Barcelona. Martí i Franqués 1, E-08028, Barcelona
[2] Institut de Nanociència I Nanotecnologia (IN²UB), Universitat de Barcelona. E-08028, Barcelona
* l.huidobro@ub.edu

In this study, BiOI materials were synthetized using both electrochemical and solvothermal methods. The conditions for these synthesis methods were optimized, and the samples were characterized. The effectiveness of these materials in degrading antibiotics was then evaluated under various lighting conditions and in the presence of peroxymonosulfate (PMS). The results demonstrated that BiOI is a promising option for water decontamination due to the synergy between its photocatalytic capabilities and PMS activation, which promotes advanced oxidation processes through radical generation to water decontamination.

To further improve the effectiveness of the synthesized materials, several modifications were implemented. BiOI was subjected to thermal treatment at different temperatures, with 420°C for 4 hours identified as optimal, enhancing degradation effectiveness while maintaining material stability [1]. Furthermore, a composite of BiOI combined with barium ferrites was prepared, which showed improved degradation efficiency, particularly for electrodeposited BiOI [2]. Additionally, thin layers of SnO_2 and TiO_2 were added to the BiOI layers using atomic layer deposition (ALD), a technique that allows precise control over the deposition thickness, optimized at 5 nm. This modification demonstrated good effectiveness in antibiotic degradation under both UV and visible light in combination with PMS. The modified materials also exhibited excellent reusability, stability, and versatility, proving to be effective for the decontamination of water containing various pollutants.

Each modification was systematically evaluated to determine its impact on the overall performance of the bismuth-based materials in water decontamination applications.

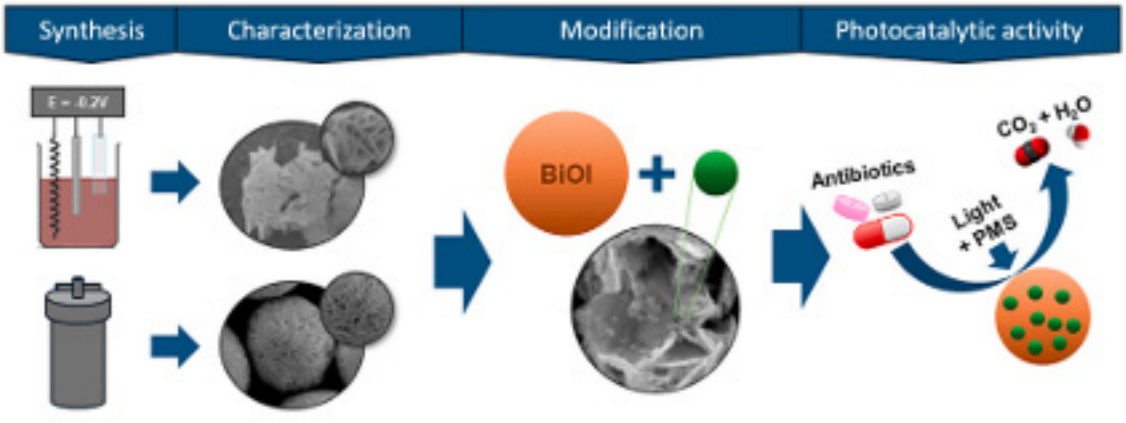

REFERENCES
[1] L. Huidobro et al. Journal of Environmental Chemical Engineering 12 (2024) 112545
[2] L. Huidobro et al. Chemosphere 366 (2024) 143532

O9 NanoEnergy
MAGNETIC WRINKLES FOR MAGNONICS

R. Galceran[1,2,*], J.M. Hernández[2,3], F. Macià[2,3], D. Pesquera[4], G. Catalán[4], B. Casals[1,2]

[1] Dept. Of Applied Physics, University of Barcelona, 08028 Barcelona, Spain
[2] Institute of Nanoscience and Nanotechnology (IN²UB), University of Barcelona, 08028 Barcelona, Spain
[3] Dept. Of Condensed Matter Physics, University of Barcelona, 08028 Barcelona, Spain
[4] Catalan Institute of Nanoscience and Nanotechnology (ICN2), UAB Campus, 08193 Bellaterra, Barcelona, Spain
* rgalceran@ub.edu

Magnonic crystals are engineered magnetic materials designed to control and manipulate spin waves (magnons). Magnons, which are collective excitations of electron spins, hold great promise for data transmission and processing [1] due to their low power consumption and compatibility with conventional CMOS technology. Their propagation can be controlled by engineering artificial periodic structures at the micro-nanoscale in magnetic materials, and are generally fabricated through complex lithographic processes.

When using flexible susbtrates, periodic structures can emerge naturally for certain Systems. These spontaneous surface modulations, or wrinkles, occur as a result of a deformation, accomodating compressive strain. In thin films, these wrinkles can be intentionally induced during the deposition of the thin film on an elastomer substrate under tension [2] (for example to protect the film from future mechanical stresses) and they can induce a change in the magnetic properties due to the strain [3]. Interestingly, the spacing between these wrinkles—ranging from tens of nanometers to micrometers—aligns closely with the typical wavelengths of spin waves in ferromagnetic media.

In this study, we investigate the wrinkles of magnetic thin films grown on flexible polymer substrates, proposing them as an ideal platform for magnonic Systems, thus eliminating the need for expensive lithographic fabrication. We show how these wrinkles influence the magnetic anisotropy, as measured through magneto-optical Kerr microscopy and ferromagnetic resonance techniques. Additionally, we investigate how the wrinkles respond to applied stress, revealing a mechanically bistable behavior in their orientation. This bistability could enable unique forms of tunability in magnonic devices. Finally, micromagnetic simulations allow us to characterize the spin-wave dispersion in these wrinkled films, highlighting their potential for scalable and tunable magnonic applications.

REFERENCES
[1] P. Pirro, Nature Reviews Materials, 6, 1114-113 (2021);
[2] D. Faurie, J. Appl. Phys, 130, 150901 (2021);
[3] F. Zighem, J. Phys.: Condens. Matter, 33, 233002 (2021)

O10 NanoMagnetics
UNDERSTANDING MAGNETIC HYPERTHERMIA PERFORMANCE WITHIN PHYSIOLOGICAL SAFETY FIELD LIMITS

Daniel Faílde[1,2], Victor Ocampo-Zalvide[1], David Serantes[1,3], Òscar Iglesias[4]

[1] Applied Physics Dpt., Univ. de Santiago de Compostela, Spain
[2] Galicia Supercomputing Center (CESGA), Santiago de Compostela, Spain
[3] Instituto de Materiais (iMATUS), Univ. de Santiago de Compostela, Spain.
[4] Dept. de Física de la Matèria Condensada and IN²UB, Universitat de Barcelona, Spain
* oscariglesias@ub.edu

Careful determination of the heating performance of magnetic nanoparticles under AC fields is critical for magnetic hyperthermia applications [1]. However, most interpretations of experimental data are based on the uniaxial anisotropy approximation, which in first instance can be correlated with particle aspect ratio. This is to say, the intrinsic magnetocrystalline anisotropy is discarded, under the assumption that the shape contribution dominates. We show in this work [2] that such premise, generally valid for large field amplitudes, does not hold for describing hyperthermia experiments carried out under small field values. Specifically, given its relevance for in vivo applications, we focus our analysis on the so-called "Brezovich criterion", H·f = 4.85×108A/m· s. By means of a computational model, we show that the intrinsic magnetocrystalline anisotropy plays a critical role in defining the heat output, determining also the role of shape and aspect ratio of the particles on the SLP. Our results indicate that even small deviations from spherical shape have an important impact in optimizing the heating performance (See Fig. 1). The influence of interparticle interactions on the dissipated heat is also evaluated. Our results call, therefore, for an improvement in the theoretical models used to interpret magnetic hyperthermia performance.

We acknowledge the financial support by Spanish MCIU projects PID2019-109514RJ-I00 and PID2021-127397NB-I00, "ERDF A way of making Europe", by the "European Union"; Catalan DURSI (2021SGR0032); Xunta de Galicia for projects ED431F 2022/005 and ED431B 2023/055; AEI for the Ramón y Cajal grant RYC2020-029822-I that supports the work of D. S. We also acknowledge CESGA for computational resources.

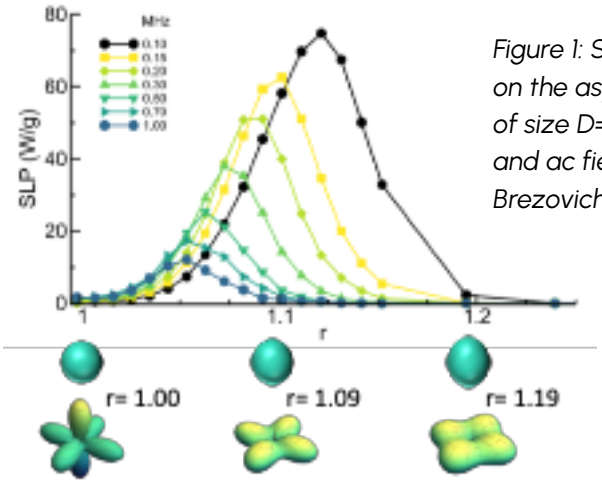

Figure 1: Specific loss power dependence on the aspect ratio (r) of magnetite NP of size D= 25 nm at different frequencies and ac field values complying with the Brezovich criterion.

REFERENCES
[1] H. Gavilán et al., Nanoscale 13, 15631 (2021)
[2] D. Faílde, V. Ocampo-Zalvide, D. Serantes, Ò. Iglesias, Nanoscale 16, 14319 (2024) https://doi.org/ 10.1039/d4nr02045f

O11 NanosMat

ANCHORING TRANSITION OF A SMECTIC FILM AND PATTERN FORMATION OF FOCAL CONIC DOMAINS IN LIQUID CRYSTAL FLOW CELL GEOMETRY

Olga Bantysh[1,*], F. Sagués[1], J. Ignés-Mullol[1]

[1] Department of Materials Science and Physical Chemistry of the University of Barcelona
[2] Institute of Nanoscience and Nanotechnology of the University of Barcelona (IN²UB)
* olga.b.bantysh@ub.edu

Liquid crystals (LC) are anisotropic fluids composed of elongated organic molecules (mesogens) that tend to align along a common director, n, and displaying a number of mesophases. After a phase transition or the application of an externally imposed stimulus, reorganization of molecular order usually leads to the formation of topological defects, either as kinetically trapped metastable objects or as components of free energy-minimizing configurations [1]. Understanding and controlling defects in LCs is important to many technological applications.

The most common LC phases are the nematic (N) and smectic A (SmA). In the first one mesogens preserve only the orientational order characterized by a director field. The SmA phase possesses a density wave resulting in a layered structure, where n is normal to equally spaced smectic layers, thus this phase preserves both orientational and translational order. In the presence of an interface, the spatial symmetry of N LC breaks, and the surface influences the orientation of its director field. This phenomenon is known as anchoring of LC on a surface. The chemical composition and the structure of the surface determine preferred anchoring directions for the LC molecules, both with respect to the surface normal and to an in-plane projection. Changing of the molecular anchoring is named anchoring transition. This phenomenon has been studied mostly in nematic films, and there are only few reports of anchoring transitions in a smectic film formed either between two soft (water and air) [2] or two solid interfaces [3].

In this work we present a new approach to create thin, relatively large and flat films of 8CB LC enclosed between solid (glass) and fluid (water solution) interfaces, where the LC anchors homeotropically and planarly, respectively. Upon cooling, the N-SmA phase transition takes place, accompanied by a drastic reorganization of the director field geometry and formation of focal conic domains (FCDs) [4]. These events are followed by an anchoring transition in which the SmA layer changes from planar to homeotropic at the water interface, leading to the disappearance of the FCDs. By locally removing regions of the hydrophobic silane coating from the glass surface, we create the regions, where FCDs anchor and persist during said anchoring transition. Such a simple way of controlling the spatial arrangement of FCDs may be used in applications based on regularly ordered micro- and nanosystems [5]. Besides, relaxation towards the final pattern of FCDs can be expedited by the local stirring of the aqueous subphase, which we have realized here using an active gel of microtubules and kinesin motors.

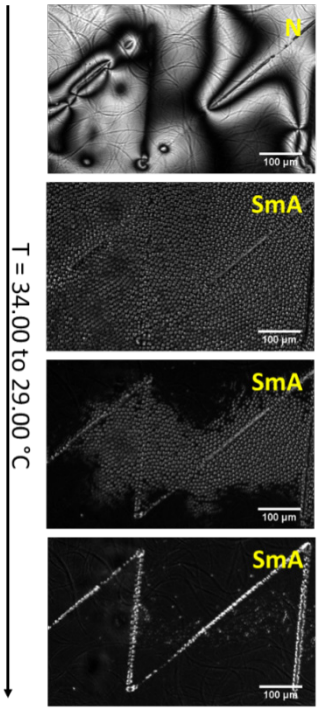

Figure 1. Temperature driven anchoring transition in 8CB LC resting on the top of an active gel inside a flow cell

REFERENCES

[1] Kurik, M.V. and Lavrentovich, O.D. (1988) Soviet Physics—Uspekhi, **31**, 196-224.
[2] Liang, H.-L, et al. (2012) Soft Matter, **8**, 5443-5450.
[3] Zappone, B. et al. (2020) PNAS, **117** (30) 17643-17649.
[4] Gim, MJ., et al. (2017) Nat Commun, **8**, 15453.
[5] Honglawan, A., et al. (2012) PNAS, 110 (1) 34-39.

POSTERS BY RESEARCH AREAS

NanoMet

P1
CRYSTALLINE PHASE-DEPENDENT DIELECTRIC PROPERTIES OF HfO_2: A TEM AND EELS STUDY

B. Vargas [1], P. Nandi [1], S. Estradé [1], L. Yedra [1], D. Nasiou [2], L. Molina-Luna [2], C. Coll[3], D. del Pozo Bueno [1], N. Kaiser [4], L. Alff [4], L. López-Conesa[1], F. Peiró [1]

[1] LENS, Department of Electronics and Biomedical Engineering and Institute of Nanoscience and Nanotechnology (IN²UB), University of Barcelona (UB), Barcelona, Spain.
[2] Department of Materials and Earth Sciences, Advanced Electron Microscopy, Technical University of Darmstadt, Darmstadt, Germany.
[3] Catalan Institute of Nanoscience and Nanotechnology (ICN2), CSIC and BIST, Campus UAB, Bellaterra, Spain.
[4] Department of Materials Science, Advanced Thin Film Technology, Technical University of Darmstadt, Darmstadt, Germany.
* bvargas@ub.edu

Hafnium oxide (HfO_2) is widely used in advanced semiconductor devices due to its high dielectric response [1]. At the nanoscale, its dielectric behavior can differ from the bulk form due to defects and surface effects [2].

This work compares the dielectric function and energy loss function (ELF) of HfO_2 thin films in rhombohedral, monoclinic, and hexagonal phases using Electron Energy Loss Spectroscopy (EELS) and Kramers-Kronig (KK) analysis. Samples were grown on TiN substrates and exposed to an oxygen-rich atmosphere, forming an O-rich nanolayer (HfO_{x+y}).

Notable differences in optical response were observed between phases. Increasing oxygen concentration reduced optical intensity and induced a phase shift from rhombohedral to monoclinic, while the hexagonal phase retained structural features despite optical changes. Density Functional Theory (DFT) simulations aligned well with experiments, emphasizing the role of crystalline phase and oxygen content in modifying optical of HfO_2 and dielectric properties.

METHODOLOGY

The dielectric properties of the samples were studied using EELS data analyzed through Kramers-Kronig calculations, applying the algorithm by Eljarrat and Koch [3]. We used the Hyperspy library in Python to process the spectra and eliminate plural scattering effects through Fourier-Log deconvolution. Density Functional Theory (DFT) simulations were performed using the VASP package, providing a theoretical basis for the optical properties observed experimentally.

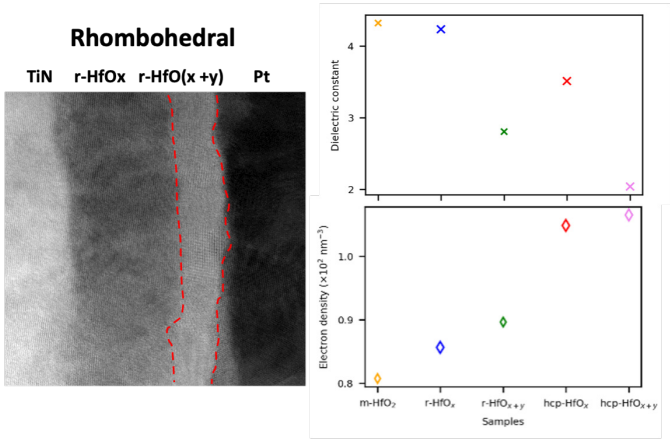

Figure 1. HAADF image of the rhombohedral phase, showing the different layers, along with a visualization of the changes in the dielectric constant and electron density as the oxygen concentration increases for each phase.

RESULTS AND CONCLUSIONS

The results demonstrated clear differences in the dielectric function and ELF between oxygen-rich and non-oxygen-rich regions (HfO_{x+y}) and HfO_x). As oxygen concentration increased, the optical response intensity decreased, affecting the dielectric constant and the density of electrons. For the rhombohedral phase, the increased oxygen concentration induced a phase transition towards the monoclinic phase. In the hexagonal phase, the optical response changed, but the shape of its main features remained the same. These findings highlight the crucial role of oxygen content in influencing the optical and dielectric properties of HfO_2 across different crystalline phases.

ACKNOWLEDGEMENTS

The authors acknowledge the financial support from the MICIIN project PID2022-138543NB-C21, Gencat project 2021SGR00242, and Grant 2024FI-1 00430. Special thanks to the ATFT group at TU Darmstadt for sample preparation.

REFERENCES

[1] E. I. Suvorova, O. V. Uvarov, N. A. Arkharova, A. D. Ibrayeva, V. A. Skuratov, and P. A. Buffat. Structure evolution, bandgap, and dielectric function in La-doped hafnium oxide thin layer subjected to swift Xe ion irradiation. *J Appl Phys*, vol. 128, no. 16, Oct. 2020, doi: 10.1063/5.0025536.
[2] J. Park and M. Yang, 'Determination of complex dielectric functions at HfO2/Si interface by using STEM-VEELS', *Micron*, vol. 40, no. 3, pp. 365–369, Apr. 2009, doi: 10.1016/J.MICRON.2008.10.006.
[3] A. Eljarrat and C. T. Koch. Design and application of a relativistic Kramers–Kronig analysis algorithm. *Ultramicroscopy*, vol. 206, Nov. 2019, doi: 10.1016/j.ultramic.2019.112

NanoBio

P2
DWELL TIME DISPERSION IN DNA TRANSLOCATION THROUGH NANOPORES

Alejandro Colchero[1], Isabel Pastor del Campo[1], Félix Ritort[1]

[1] Small Biosystems Lab, Departament de Fisica de la Matèria Condensada, Facultat de Fisica, Universitat de Barcelona, Carrer Marti i Franques, 1, Barcelona 08028, Spain.
* alejandro.colchero@ub.edu

Nanopores are a widely used technique to study nucleic acids and proteins. They can be utilized in a wide range of applications, from detecting single molecules to DNA sequencing. For the specific case of DNA translocation, when a long molecule like λ-DNA is translocated through nanopores of 10-30 nm size, the DNA molecule can translocate in different folding configurations. The translocation time is dependent on this folding configuration of the molecule, as more folded (compact) configurations have shorter translocation times. Moreover, a broad dispersion is observed for λ-DNA translocation times of molecules having a similar folding configuration. This big dispersion is not yet well understood. In this work, we explore the origin of this dwell time dispersion and show how it cannot be exclusively attributed to the diffusive behavior of the DNA molecules when translocating through the nanopore. Using a simple 1D diffusion model, together with simulations of λ-DNA equilibrium conformations, we demonstrate how the initial 3D conformation of the λ-DNA molecules prior to translocation also affects its translocation time. Therefore, the dwell time dispersion observed in the experimental data is explained by the different initial 3D conformation prior to translocation.

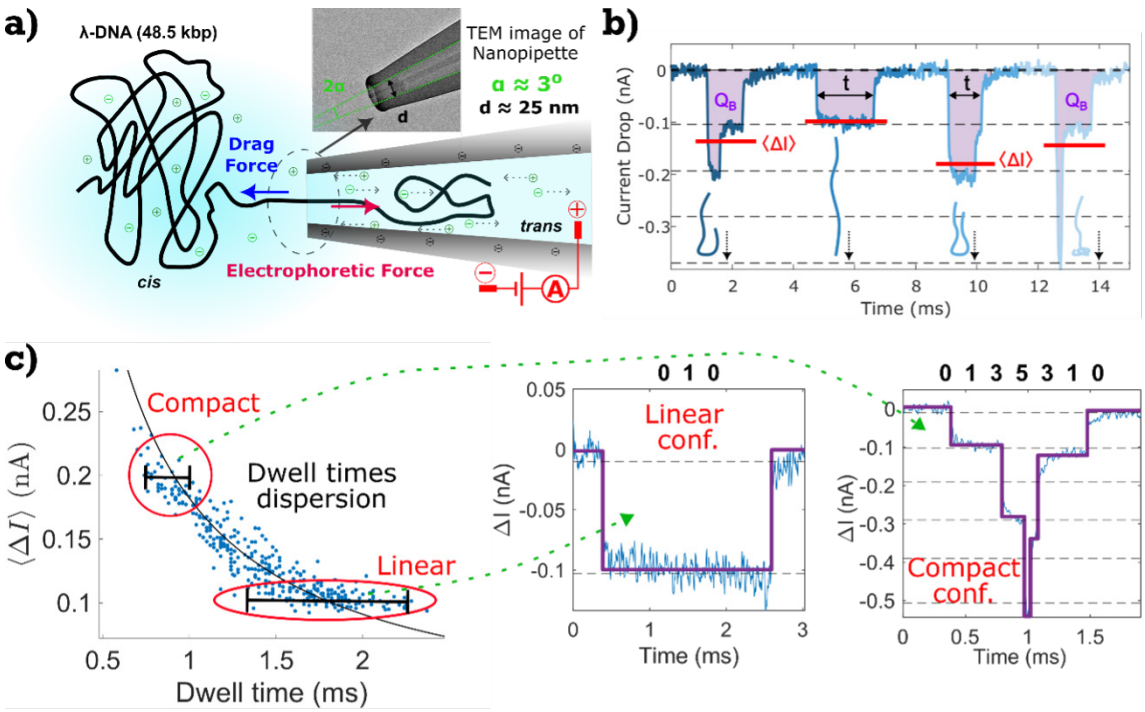

a) Schematic representation of a DNA translocation experiment. b) Signal of λ-DNA translocation event through a nanopipette. c) Dwell time dispersion for different configurations. The scatter plot of dwell time vs. mean current drop of λ-DNA translocation events, shown on the left, shows the dwell time dispersion depending on the configuration. More compact configurations show less dwell time dispersion. An example of a linear and a compact configuration are shown on the right

P3
CANNABIDIOL ON SYNTHETIC NEURONAL MEMBRANES

Adrià Botet-Carreras[1,2], K. Biernacki[3], M. Teresa Montero[1,2], Jordi Borrell[1]; Òscar Domènech[1,2]

[1] Physical Chemistry Section, Faculty of Pharmacy and Food Sciences, University of Barcelona, Barcelona, Spain
[2] Institute of Nanoscience and Nanotechnology IN²UB
[3] Department of Physical Chemistry and Electrochemistry, Faculty of Chemistry, Jagiellonian University
* abotetcarreras@ub.edu

Cannabidiol (CBD) has experienced a notable rise in popularity due to its significant pharmacological benefits and minimal side effects. Some of the therapeutic effects of this molecule include reducing the severity of seizures in epilepsy [1], providing anxiolytic benefits by helping treat social anxiety disorder and insomnia [2], preventing cortical and hippocampal neurodegeneration, and offering anti-inflammatory and antioxidant properties. Additionally, CBD reduces the hyperphosphorylation of Tau protein and protects against neurotoxicity induced by the beta-amyloid peptide [3], among other effects.

MATERIAL & METHODS

CBD and a specific lipidic neuron membrane mimicking mixture including 1-palmitoyl-2-oleoyl-glycero-3-phosphocholine (POPC); 1-palmitoyl-2-oleoyl-sn-glycero-3-phosphoethanolamine(POPE); 1-palmitoyl-2-oleoyl-sn-glycero-3-phospho-L-serine (POPS); Sphingomyelin (SM); Cholesterol at (0.33/0.27/0.08/0.05/0.33 mol to mol) were studied using a 312 DMC Langmuir-Blodgett trough (NIMA Technology Ltd. Coventry, England). Atomic Force Microscopy studies were performed with a Nanoscope IV from Digital Instruments (Santa Barbara, CA). Images and force curves were acquired using V-shaped silicon nitride cantilevers (OMCL TR400PSA, Olympus, Japan) with a nominal spring constant of 80 pN $nm^{-1,}$ in air and in Tapping® mode. Extractions of monolayers on mica were performed at π= 30 mN m^{-1}.

RESULTS AND DISCUSSION

We investigated the interaction between CBD molecules and synthetic lipid bilayers that mimic the neuronal plasma membrane, aiming to understand the impact of CBD on the lipid membrane when administered to patients. Our monolayer experiments showed that as the lateral surface pressure increased, CBD and the lipids in the monolayer exhibited repulsive forces. However, when the mole fraction of CBD was increased, attractive forces between the molecules were observed. Additionally, atomic force microscopy images showed that the height and roughness of lipid bilayers were similar with and without CBD. However, Force Spectroscopy experiments revealed that the presence of CBD altered the lateral packing of the lipid bilayer.

REFERENCES

[1] Jones, N.A.; Hill, A.J.; Smith, I.; Bevan, S.A.; Williams, C.M.; Whalley, B.J.; Stephens, G.J., J. Pharmacol. Exp. Ther., 332 (2010) 569-577.
[2] Zhornitsky, S.; Potvin, S., Pharmaceuticals, 5 (2012) 529-552.
[3] Watt, G.; Karl, T., Front. Pharmacol., 8 (2017) 234828.

P4
NANOSTRUCTURED TOPOGRAPHIES FOR CARDIOMYOCYTE ALIGNMENT USING TWO-PHOTON POLYMERIZATION

P. Ferrando-Huertas[1,2,*], R. E. Yanac-Huertas[1,2], A. Noguera-Monteagudo[1,2], J. Huguet[1,2], R. Rodriguez[1,2], S. Van Vlierberghe[3], J. A. Del Río[2], O. Castaño[1,2]

[1] Electronics and biomedical Engineering, University of Barcelona (UB), Spain
[2] Institute for Bioengineering of Catalonia (IBEC), Spain
[3] Polymer Chemistry & Biomaterials, Ghent University (UGent); Belgium
* **paulaferrando@ub.edu**

Cardiovascular diseases (CVD) are the leading cause of death worldwide. Common treatments include lifestyle changes, medication, and surgery. New trends in regenerative therapies such as stem cells or fibroblast reprogramming aim to mitigate myocardium damage. All these therapies require preclinical testing in *in vitro* models. [1]

Cardiac tissue formed from cardiomyocytes, which are interwoven with collagen, is highly vascularized. Its structure results in directionally dependent electrical and mechanical properties, creating an anisotropic cardiac tissue. The cardiac muscle is characterized by its organization and its ability to propagate electrical signals transduced in the contraction of its fibers. [2,3]

Recent advances in tissue engineering and manufacturing processes have facilitated the development of microfluidic platforms and different approaches used to mimic cell behavior and functionality. One is the 3D microfabrication, which is used to precisely control the micro- and nanoscale scaffold architecture essential for tissue engineering applications. Among these, two-photon polymerization (2PP) presents high resolution and design flexibility. [4,5]

In this work, we focus on the use of 2PP to fabricate micro-scaffolds with controlled surface topographies aimed at promoting cardiomyocyte alignment. Scaffolds with sub-3 µm surface grooves were fabricated via 2PP (780 nm wavelength, 80 mW power), achieving resolutions below 700 nm. These scaffolds were analyzed by scanning electron microscopy (SEM) to validate the printed structures.

Cardiomyocytes were seeded on the scaffolds, and then were fixed, immunostained and confocal imaging was performed to assess cell alignment. The analysis was supported by Fourier transform methods to quantify alignment degree. The results indicate that surface patterns on the scaffolds improve cardiomyocyte alignment *in vitro*.

Unlike isotropic 3D scaffolds, our topographical patterns replicate native cardiac anisotropy, enabling targeted electromechanical coupling studies. This platform enables high-throughput drug testing for CVD therapies and paves the way for patient-specific cardiac patches.

REFERENCES

[1] Hoover-Plow, J., & Gong, Y. (2012). Challenges for heart disease stem cell therapy. Vascular health and risk management, 8, 99–113. https://doi.org/10.2147/VHRM.S25665.

[2] Engelmayr, G. C., Jr, Cheng, M., Bettinger, C. J., Borenstein, J. T., Langer, R., & Freed, L. E. (2008). Accordion-like honeycombs for tissue engineering of cardiac anisotropy. Nature materials, 7(12), 1003–1010. https://doi.org/10.1038/nmat2316.

[3] López-Canosa, A., Perez-Amodio, S., Yanac-Huertas, E., Ordoño, J., Rodriguez-Trujillo, R., Samitier, J., Castaño, O., & Engel, E. (2021). A microphysiological system combining electrospun fibers and electrical stimulation for the maturation of highly anisotropic cardiac tissue. Biofabrication, 13(3), 10.1088/1758-5090/abff12. https://doi.org/10.1088/1758-5090/abff12.

[4] O'Halloran, S., Pandit, A., Heise, A., & Kellett, A. (2023). Two-Photon Polymerization: Fundamentals, Materials, and Chemical Modification Strategies. Ad vanced science (Weinheim, Baden-Wurttemberg, Germany), 10(7), e2204072. https://doi.org/10.1002/advs.20220407234.

[5] Faraji Rad, Z., Prewett, P.D. & Davies, G.J. (2021). High-resolution two-photon polymerization: the most versatile technique for the fabrication of microneedle arrays. Microsyst Nanoeng, 7, 71. https://doi.org/10.1038/s41378-021-00298-3.

P5
PCSK9 INHIBITION BY POLYPURINE REVERSE HOOGSTEEN HAIRPINS

Ester López-Aguilar[1,2,*], Silvia Cecilia Pacheco-Velázquez[3], M-Antonia Busquets[2,4], Joshua Hay[3], Paul A. Mueller[3], Sergio Fazio[3], Carlos J Ciudad[1,2], Véronique Noé[1,2], Nathalie Pamir[3]

[1] Department of Biochemistry and Physiology, School of Pharmacy and Food Sciences, Universitat de Barcelona (UB), 08028 Barcelona, Spain.
[2] Institute of Nanoscience and Nanotechnology, Universitat de Barcelona (IN²UB), 08028 Barcelona, Spain.
[3] Center for Preventive Cardiology, Knight Cardiovascular Institute, Oregon Health & Science University, Portland, OR, USA.
[4] Department of Pharmacy and Pharmaceutical Technology and Physical Chemistry, School of Pharmacy and Food Sciences, University of Barcelona, 08028 Barcelona, Spain.
***ester.lopez@ub.edu**

PCSK9 is a therapeutic target for hypercholesterolemia. Though different strategies to inhibit PCSK9- such as monoclonal antibodies, small molecules, or nucleic acid drugs- are currently available, the demand for safer and inexpensive alternatives remains. In this study, we developed a time-, cost-, and resource- efficient silencing approach using Polypurine Reverse Hoogsteen (PPRH) hairpins to target PCSK9. Two hairpins targeting PCSK9 at exon 9 (HpE9) and exon 12 (HpE12) were designed. Binding affinities, assessed by EMSA were measured, achieving Kd values of 7.86x10-8 M and 7.5 x10-7 M for HpE9 and HpE12, respectively. PPRHs were complexed with the cationic polymer jetPEI forming nanoparticles of 167nm as characterized by Dynamic Light Scattering. Upon transfection into HepG2 cells, both HpE9 and HpE12 significantly suppressed PCSK9 mRNA levels (by 63% and 74%, respectively) and protein expression (by 76% and 87%) within 24 hours. Human PCSK9 overexpressing mice receiving a single injection of HpE12 decreased plasma PCSK9 levels by 50 % by day 3 post-injection and levels returned to baseline by day 15. Total plasma cholesterol levels were reduced by 47% by day 3 and recovered at day 15. Wild-type mice receiving the PPRHs did not exhibit changes in body weight, liver enzymes or pro-inflammatory markers when compared to mice injected with jetPEI alone. These findings support the potential of PPRH-based gene silencing as a novel, affordable, effective and easy to develop therapeutic technology for targeting PCSK9.

Work supported by the National Institutes of Health (NIH) RO1HL132985-02 and Spanish Ministry of Science and Innovation (MICINN) PID2021-122271OB-100.

P6
MICRO AND MANOENGINEERED HEART-ON-A-CHIP FOR *IN VITRO* STUDY AND TREATMENT SCREENING OF CATECHOLAMINERGIC POLYMORPHIC VENTRICULAR TACHYCARDIA

R.E. Yanac-Huertas[1,2,*], P. Ferrando Huertas[1,2], C. Gracia Ruiz[1], J. Huguet Suárez[1,2], A. Noguera Monteagudo[1,2], J. López-Sánchez[1], R. Rodríguez1,[2,3], J.A. Del Río[2], O. Castaño1,[2,3,4]

[1] Electronics and Biomedical Engineering, Universitat de Barcelona (UB), 08028 Barcelona, Spain
[2] Institute for Bioengineering of Catalonia (IBEC), The Barcelona Institute of Science and Technology (BIST), Barcelona, Spain
[3] Institute of Nanoscience and Nanotechnology of the University of Barcelona, IN²UB, Barcelona, Spain
[4] CIBER en Bioingeniería, Biomateriales y Nanomedicina, CIBER-BBN, Madrid, Spain
*eduardo.yanac@ub.edu

Catecholaminergic Polymorphic Ventricular Tachycardia (CPVT) is a rare, inherited arrhythmia linked to mutations in calcium-handling genes like RYR2. Children and adolescents are commonly affected, if untreated, carries a high risk of sudden cardiac death, with up to 31% of patients dying by the age of 30 [1]. The condition involves abnormal Ca^{2+} cycling, causing delayed afterdepolarizations (DADs) and triggered activity, which are difficult to reproduce in existing models. We introduce a heart-on-a-chip platform using HL-1 cardiomyocytes, GCaMP6 Ca^{2+} sensors, interdigitated electrodes and drug treatments to reproduce CPVT dynamics and evaluate anti-arrhythmic drugs in real time.

MATERIALS AND METHODS
HL-1 cells were cultured and stably transfected with GCaMP6 lentivirus for optical Ca^{2+} imaging. The chip platform was nanofabricated using soft lithography with 50 µm gold electrodes (10 nm Ti adhesion layer) on PDMS, enabling subcellular resolution for calcium wave detection for electrocardiogram (ECG) and electrical impedance spectroscopy (EIS). Surfaces were coated with an aligned PLA70/30 aligned nanofiber mesh for cell adherence, compatibility and guidance. Electrical pacing protocols were synchronized with Ca^{2+} imaging and ECG recording (Biopac and Analog Discovery). CPVT-like phenotypes were induced using isoproterenol at 100mM and caffeine at 100µM. Known treatments such as flecainide and verapamil were tested to assess therapeutic responses.

RESULTS
The platform supported spontaneous and paced contractions with stable beat rates and high cell viability. Electrical stimulation protocols revealed a close temporal correlation between Ca^{2+} transients and ECG peaks, demonstrating proper excitation–contraction coupling. Under isoproterenol challenge, we observed simultaneously distinctive arrhythmic Ca^{2+} signals (DAD, irregular transients) as well as ECG waveforms. Drug treatment with flecainide at 10uM restored synchrony in both optical and electrical domains. EIS analysis further indicated shifts in tissue impedance during arrhythmic episodes, identifying a frequency window at 1-10MHz for non-invasive invasive monitoring akin to wearable cardiac devices. A dose-response curve was established for each intervention.

DISCUSSION
This HL-1 based heart-on-a-chip accurately recapitulates the electrophysiological and calcium-handling abnormalities of CPVT. While HL-1 cells exhibit atrial-like action potentials, β-adrenergic stimulation induced ventricular-like Ca handling instability, as seen in CPVT patients. Its integration of real-time optical and electrical modalities allows robust characterization of arrhythmic dynamics and drug responses. While HL-1 cells reflect an atrial phenotype, the platform offers a high-throughput and modular structure for personalized cardiac modeling. Future work will involve CRISPR/Cas9-based mutation modeling and incorporation of hiPSC-derived ventricular cardiomyocytes to enhance clinical relevance.

REFERENCES
[1] Schneider, L., Begovic, M., Zhou, X., Hamdani, N., Akin, I., & El-Battrawy, I. (2025). Catecholaminergic Polymorphic Ventricular Tachycardia: Advancing From Molecular Insights to Preclinical Models. Journal of the American Heart Association, 14(6), e038308.

P7
TRIFAPYS AS LIPID-BASED DELIVERY OF PPRHS TARGETING SURVIVIN IN CANCER AND BRAIN ENDOTHELIAL CELLS

Ana Delgado[1,*], Berta Isanta[2], Carlos Ciudad[1], Maria Antonia Busquets[3], Nuria Llor[2], Rosa Griera[2] and Véronique Noé[1]

[1] Department of Biochemistry & Physiology
[2] Department of Pharmacology, Toxicology and Therapeutic Chemistry
[3] Department of Pharmacy and Pharmaceutical Technology and Physical Chemistry
School of Pharmacy and Food Sciences & IN²UB, University of Barcelona, 08028 Barcelona, Spain
* **anadelgado@ub.edu**

The advancement of gene therapy depends on the development of novel delivery vectors that are simultaneously efficient, biocompatible, and economically viable. In this context, our research introduces a class of synthetic lipid-like vectors—termed TRIFAPYs—synthesized from a 1,3,5-tris[(4-alkyloxy-1-pyridinio) methyl]benzene tribromide core. These structures are functionalized with fatty acid chains of varying lengths, ranging from 4 to 20 carbon atoms (C4 to C20). The transfection potential of TRIFAPYs was assessed using Polypurine Reverse Hoogsteen (PPRH) hairpins as a model gene therapy tool. Binding experiments via gel retardation assays demonstrated a high affinity between the liposomes and PPRHs. Biophysical characterization confirmed the formation of nanoparticles with an average size of ~125 nm, as visualized by Cryo-TEM and dynamic light scattering analysis. Cellular internalization was evaluated through fluorescence microscopy and flow cytometry in prostate cancer cells (PC-3), identifying clathrin-mediated endocytosis as the predominant uptake pathway. Notably, TRIFAPYs bearing C12–C18 fatty acyl chains exhibited high transfection efficiency for the previously validated PPRH (HpsPr-C) targeting the BIRC5 gene across representative cancer cell lines from prostate (PC-3) and breast (SKBR-3). Post-transfection assays against the antiapoptotic target survivin, showed a significant downregulation of mRNA and increased levels of apoptotic markers in PC-3 cells. Additionally, TRIFAPY C12 successfully delivered HpsPr-C into hCMEC/D3 endothelial cells—a representative *in vitro* model of the blood-brain barrier—resulting in reduced cell viability and a high percentage of positively transfected cells, as detected by flow cytometry. The *in vivo* efficacy of the TRIFAPY-mediated delivery system was further validated using the chick chorioallantoic membrane (CAM) model. All together, these findings highlight the potential of TRIFAPY-based delivery vehicles for the effective transfection of therapeutic nucleic acids.

Work supported by the Spanish Ministry of Science and Innovation (MICINN) PID2021-122271OB-100.

NanoPharmaMed

P8
3D SPHEROIDS INDUCED BY SUPERHYDROPHOBICITY AS BOTH *IN VITRO* DIAGNOSTIC AND THERAPEUTIC TOOLS

M.C. Morán[1,2,*], F. Cirisano[2], **M. Ferrari**[2,3,*]

[1] Departament de Bioquímica i Fisiologia, Secció de Fisiologia—Facultat de Farmàcia i Ciències de l'Alimentació, Universitat de Barcelona, Avda. Joan XXIII, 27-31, 08028 Barcelona, Spain
[2] Institut de Nanociència i Nanotecnologia—IN²UB, Universitat de Barcelona, Avda. Diagonal, 645, 08028 Barcelona, Spain
[3] CNR-ICMATE Istituto di Chimica della Materia Condensata e di Tecnologie per l'Energia, via De Marini, 6, 16149 Genova, Italy
* **mcmoranb@ub.edu** and **michele.ferrari@cnr.it**

Cell therapies commonly pursue tissue stimulation by replacing cell numbers or supplying functional def iencies. To this aim, monodispersed cells are usually transplanted for incorporation by local injection, but the limitations of this strategy include poor success associated with cell death, insufficient retention, or cell damage due to shear forces associated with the injection. Spheroids have recently emerged as a model that mimics an *in vivo* environment with more representative cell-to-cell interactions and better intercellular communication [1]. Nevertheless, cost-effective and lab- friendly fabrication and effectively performed recovery are challenges that restrict the broad application of spheroids [2]. In this work, surfaces were modified with environmentally friendly superhydrophobic coatings, and such surfaces were used for the 3D spheroid preparation from different cell lines ranging from tumoral and non-tumoral cell lines [3-5]. The resulting 3D spheroids were characterized in terms of size distribution and circularity as well as cell viability in the 3D environment as a function of cell density. These results demonstrated the capability of these entities as diagnostic tools serving as a more faithful model for *in vitro* studies and drug screening. Recent results under coculture conditions highlight the potential of these surfaces for tailoring 3D cancer models and studying tumor-stroma or tumor-epidermal interactions *in vitro*.
Moreover, the effectiveness of the spheroids to be recovered and grown under 2D culture conditions was also evaluated. The morphology of the migrated cells from the 3D spheroids was characterized at the nano-microscale through 3D profilometry. Results demonstrated improved adhesion and proliferation in the migrated cells of representative skin cell lines, both advanced properties for regenerative applications [4]. When considering macrophage-derived spheroids, changes in polarization and activation of migrated cells exhibited promising properties to be used in immunotherapy [5].

ACKNOWLEDGMENTS This work was conceived in the framework of the Cooperation Agreement between Faculty of Pharmacy and Food Science (UB)—Institute for Chemistry of Condensed Matter and Technologies for Energy (ICMATE-CNR) (Codi GREC 18407, 2018–2026). F.C. and M.F. acknowledge funding by National Recovery and Resilience Plan (NRRP), Mission 4, Component 2, Investment 1.5, project "RAISE - Robotics and AI for Socio-economic Empowerment" (ECS00000035).

REFERENCES

[1] M. C. Decarli, R. Amaral, D.P.D. Santos, L. B. Tofani, E., Katayama, R.A. Rezende et al. Cell Spheroids as a Versatile Research Platform: Formation Mechanisms, High throughput Production, Characterization and Applications. Biofabrication 2021, 13, 032002.
[2] M, Ferrari, F, Cirisano, M. C. Morán, Super Liquid-repellent Surfaces and 3D Spheroids Growth. Front. Biosci. (Landmark Ed) 2022, 27, 144.
[3] M, Ferrari, F, Cirisano, M. C. Morán, Mammalian Cell Spheroids on Mixed Organic–Inorganic Superhydrophobic Coating, Molecules 2022, 27, 1247.
[4] M. C. Morán, F. Cirisano, M. Ferrari, Spheroid Formation and Recovery Using Superhydrophobic Coating for Regenerative Purposes. Pharmaceutics 2023, 15, 2226.
[5] M. C. Morán, F. Cirisano, M. Ferrari, Superhydrophobicity Effects on Spheroid Formation and Polarization of Macrophages . Pharmaceuticals 2024, 17, 1042.
[6] M. C. Morán, F. Cirisano, M. Ferrari, Superhydrophobicity Effects on Spheroid Formation, Architecture and Viability on Coculture Conditions. Pharmaceuticals 2025, submitted

P9
SYNTHESIS OF TPE-BASED AIE FLUORESCENT PROBES AND THEIR APPLICATION IN BIOIMAGING

Ruxin Li[1,2,3,*], Jinhui Wang[3], Lluïsa Pérez-García[1,2,*]

[1] Departament de Farmacologia, Toxicologia i Química Terapèutica, Universitat de Barcelona, Av. Joan XXIII 27-31, Barcelona, 08028 Spain.
[2] Institut de Nanociència i Nanotecnologia IN²UB, Universitat de Barcelona
[3] Institute of Drug Discovery Technology, Ningbo University, Ningbo 315211, China
* liruxin@ub.edu and mlperez@ub.edu

Nitroreductase (NTR), a biomarker for tumor hypoxia, is closely linked to lysosomal dysfunction in diseases. 1 Conventional "turn-off" fluorescent probes suffer from aggregation-caused quenching (ACQ) and false positives, while aggregation-induced emission (AIE)-based probes mitigate these limitations. 2-3 This study designed two TPE-scaffolded probes, TPEDCH-PBN (turn-off) and M-TPE-P (turn-on), to achieve precise NTR detection and lysosome-targeted imaging.

MATERIALS AND METHODS

The TPE-based probes were synthesized, characterized, and optically analyzed. Molecular docking (AutoDock/Vina) elucidated structural interactions between probes and NTR. Cellular imaging in 4T1 cells assessed time-dependent fluorescence (24–72 h) and lysosomal colocalization using Lyso-Tracker Red.

RESULTS AND DISCUSSION

Docking studies revealed a stepwise NTR-probe interaction: (1) TPEDCH-PBN's nitro group formed hydrogen bonds with Lys15/Lys167, critical for catalysis (Fig. 1. left), while its TPE core engaged Pro163/Leu152 via Pi-alkyl bonds. (2) M-TPE-P's nitro group bound Lys14/Lys74 through hydrogen and Pi-cation bonds, with additional hydrogen bonds between its phenol/carbonyl groups and Asn71/Arg207 (Fig. 1. right). TPEDCH-PBN exhibited red fluorescence at 24 h (quenched by 72 h), reflecting NTR activity dynamics. M-TPE-P demonstrated lysosome-specific OFF-ON fluorescence, colocalizing with Lyso-Tracker Red (Pearson coefficient: 0.97). This work pioneers AIE-driven probes for hypoxia imaging and lysosomal targeting, offering a robust design strategy for biomarker detection.

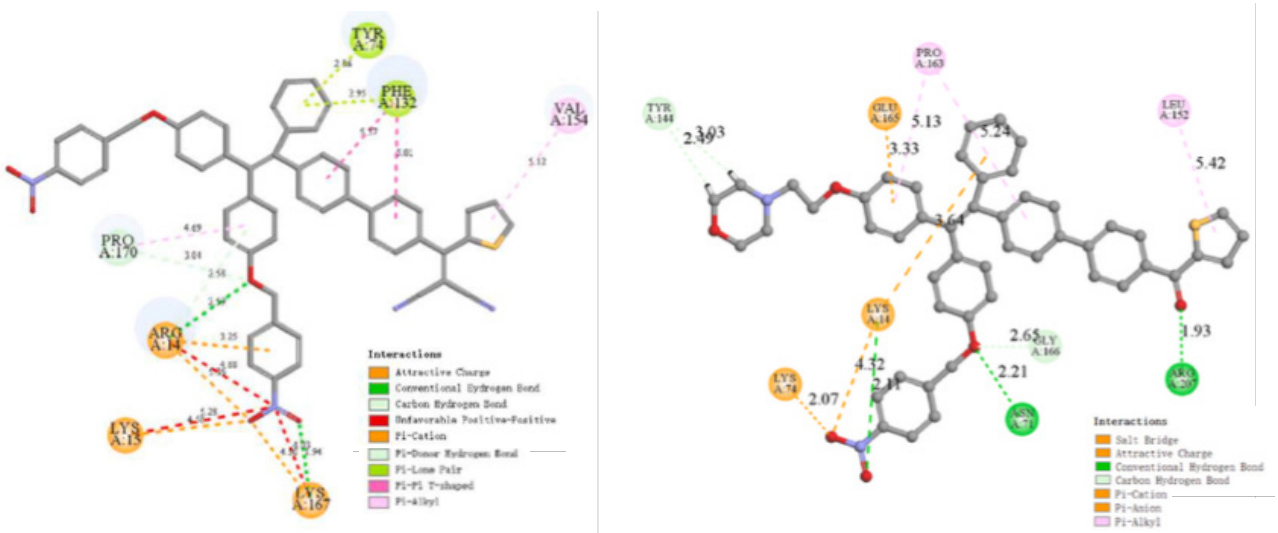

Fig. 1. 2D view of interaction between probe TPEDCH-PBN (left), probe M-TPE-P (right) and NTR active site

REFERENCES

[1] W. R. Wilson and M. P. Hay, Nat Rev Cancer., 2011, 11, 393-410.
[2] Y. Hong, J.W.Y. Lam, B.Z. Tang, Chem. Soc. Rev., 2011, 5361–5388.
[3] R. Hu, N.L.C. Leung, B.Z. Tang, Chem. Soc. Rev., 2014, 43, 4494–4562.

P10
HALLOYSITE BASED NANOMATERIALS FOR POTENTIAL THERANOSTIC APPLICATION

F. Leone[1,*], S. Bagherpour[2,3], R. de Melo Barbosa[4], M. Massaro[1], R. Noto[1], L. Pérez-Garcia[2,3], F.M. Raymo[5], R. Sánchez-Espejo[6], C. Viseras[6,7], S. Riela[8]

[1] Dipartimento di Scienze e Tecnologie Biologiche, Chimiche e Farmaceutiche (STEBICEF), Università di Palermo, Viale delle Scienze, Parco d'Orleans II, Ed. 17, 90128, Palermo, Italy **federica.leone04@unipa.it**
[2] Departament de Farmacologia, Toxicologia i Química Terapèutica, Universitat de Barcelona, Av. Joan XXIII 27-31, Barcelona, 08028, Spain.
[3] Institut de Nanociència i Nanotecnologia IN²UB, Universitat de Barcelona, Barcelona, 08028, Spain
[4] Department of Pharmacy and Pharmaceutical Technology, School of Pharmacy, University of Seville, C/ Professor García González 2, 41012 Sevilla, Spain.
[5] Laboratory for Molecular Photonics, Department of Chemistry, University of Miami, Coral Gables, Florida 33146-0431, United States
[6] Department of Pharmacy and Pharmaceutical Technology, Faculty of Pharmacy, University of Granada, Campus Universitario de Cartuja, 18071 Granada, Spain
[7] Andalusian Institute of Earth Sciences, CSIC-UGR, 18100 Armilla, Granada, Spain
[8] Dipartimento di Scienze Chimiche (DSC), Università di Catania, Viale Andrea Doria 6, 95125 Catania, Italy
* **federica.leone@ub.edu**

Theranostic merges diagnostic and therapeutic functions into a single platform, enhancing both treatment efficiency and disease management. Among diagnostic tools, fluorescence bioimaging stands out for its high sensitivity and non-invasive nature [1]. Various carriers have been developed to improve solubility and boost fluorescence of many organic chromophores at the target site [2]. In this context, halloysite nanotubes (HNTs) gain increasing attention for potential theranostic application. Thanks to their natural biocompatibility and modifiable surface chemistry, HNTs represent a versatile platform for biomedical applications. Over the years, numerous chemical modifications have been applied to the HNTs surface, leading to promising systems for delivering active agents with different therapeutic effects [3]. In this study, we investigate the potential of halloysite-based nanomaterials for theranostic applications, including chemodynamic therapy and biosensing. We present the synthesis and characterization of various HNTs-based systems incorporating different fluorescent probes, focusing on their photophysical properties, morphological features, and the chemical experiments to assess their suitability as theranostic agents.

ACKNOWLEDGEMENT
Avviso 01/2022 – Borse regionali di ricerca in Sicilia A.A 2022/2023 – CUP: G71I22001190006, National Recovery and Resilience Plan (NRRP), funded by the European Union– Next Generation EU-DD 1409 Progetti di Rilevante Interesse Nazionale (PRIN) 2022 PNRR published on 14-09-2022 by the italian MUR, Missione 4 (Istruzione e Ricerca) Component 2, Investment 1.1. Project Title: Small Molecule Anticancer Ligands Library from mediterranean plants (SMALL)– CUP B53D23025910001–Code P2022YJZ5F and Project PID2023-146658NB-C32 was funded by MCIN/AEI/10.13039/501100011033 and by FEDER, EU. We also thank AGAUR (Generalitat de Catalunya) for a grant to consolidated research groups 2021 SGR 01085.

REFERENCES
[1] Peng H-S et al. (2015) Chem. Soc. Rev. 44: 4699- 4722
[2] Massaro M et al. (2022) ACS Appl. Nano Mater. 5: 13729–13736
[3] Massaro M et al. (2022) Colloids Surf. B. Biointerfaces 213: 112385

P11
BIOLOGICAL PROFILING OF ZnO AND TiO_2 NANOPARTICLES: HEMOCOMPATIBILITY AND PHOTOTOXICITY COMPARED

A.S. Maddaleno[1,2,*], L. Bescós[2], E. Teixidó[3], L. Guardia-Escoté[3], M.P. Vinardell[1,2], M. Mitjans[1,2]

[1] Institut de Nanociència i Nanotecnologia (IN²UB), Universitat de Barcelona.
[2] Fisiologia. Departament de Bioquímica i Fisiologia, Facultat de Farmàcia i Ciències de l'Alimentació, Universitat de Barcelona.
[3] Toxicologia, Departament de Farmacologia, Toxicologia i Química Terapèutica, Facultat de Farmàcia i Ciències de l'Alimentació, Universitat de Barcelona.
* Corresponding author's mail: adrianamaddaleno@ub.edu

Cosmetics and other everyday products may include compounds that become phototoxic upon exposure to UV radiation. The use of UV filters has risen notably in recent years, driven by increasing public awareness of skin cancer risks. These agents play a crucial role in protecting the skin from UV-induced damage; however, some can induce phototoxic effects due to their chemical reactivity. Inorganic filters are commonly incorporated into sunscreens, offering several advantages over their organic counterparts—particularly in terms of safety and broader UV protection. [1]. The effectiveness of these filters is closely linked to particle size, with nanoparticles exhibiting higher reactivity than microparticles because of their greater surface area.

In this study, characterization and the haemolytic, coagulant and phototoxic ability of zinc oxide (ZnO) and titanium dioxide (TiO_2) nanoparticles (NPs), commonly used as inorganic UV filters in cosmetics, were evaluated. Hydrodynamic diameter was determined in different media, showing a decrease in the presence of proteins in the media in the two times assayed, overall, in the case of ZnO. Both nanoparticles, show a high polydispersity index. After confirming the non-haemolytic effect by both nanoparticles, coagulation studies were performed. To achieve this, prothrombin time (PT) and activated partial thromboplastin time (aPTT) were studied to evaluate the extrinsic and intrinsic pathways of coagulation, respectively. Plasma was incubated with each of the ZnO and TiO_2 nanoparticles for a period of 30 min at 37 °C under soft rotation before evaluating the effects on coagulation time [2]. Results indicated that as the concentration of the ZnO NPs increases, the coagulation time, both extrinsic and intrinsic pathways, also increases. Contrary, in the case of TiO_2NPs, the concentrations of 0.5 and 1.0 mg/mL decrease the coagulation time, favouring clot formation. In both pathways, TiO_2 NPs induce increase of clotting time inversely proportional to concentration.

Phototoxicity was evaluated in the human keratinocyte cell line HaCaT, following the OECD Test Guideline 432 with slight modifications [3]. Cells were exposed to UVA irradiation at a dose of 4 J/cm². Cell viability was assessed using two colorimetric assays: MTT, which measures the reduction of 2,5-diphenyl-3-(4,5-dimethyl-2-thiazolyl) tetrazolium bromide, and the Neutral Red Uptake (NRU) assay. The phototoxic potential of ZnO and TiO_2 nanoparticles was estimated by calculating the Photoirritation Factor (PIF), defined as the ratio between the IC_{50} (the concentration reducing cell viability by 50%) in non-irradiated versus irradiated conditions. According to the OECD criteria, a PIF < 2 indicates "no phototoxicity", a PIF between 2 and 5 suggests an "equivocal" response, and a PIF > 5 indicates "phototoxicity". For ZnO NPs, the average PIF was 1.5 in the MTT assay and >0.5 in the NRU assay, suggesting no phototoxic risk. In contrast, TiO_2 NPs showed a PIF of 5.1 in MTT and 3.0 in NRU, indicating potential phototoxic effects under the tested conditions.

ZnO and TiO_2 nanoparticles, widely used as inorganic UV filters, showed no haemolytic activity but had different effects on coagulation: ZnO prolonged clotting times, while TiO_2 reduced them at certain concentrations. Phototoxicity assays indicated no risk for ZnO, whereas TiO_2 showed potential phototoxic effects. These results highlight the need for careful safety evaluation of nanoparticulate UV filters in cosmetics.

REFERENCES
[1] Serpone, N. (2021). Sunscreens and their usefulness: have we made any progress in the last two decades? Photochemical and Photobiological Sciences, 20(2), 189–244. https://doi.org/10.1007/s43630-021-00013-1.
[2] Mitjans, M., Marics, L., Bilbao, M., Maddaleno, A.S., Piñero, J.J., Vinardell, M.P. Size Matters? A Comprehensive In Vitro Study of the Impact of Particle Size on the Toxicity of ZnO. Nanomaterials. 2023, 13, 1800. https://doi.org/10.3390/nano13111800. [3] OECD TG 432, 2019. In Vitro 3T3 NRU Phototoxicity Test.

P12
MOLECULAR PHOTOSWITCHING: ENERGY STORAGE AND CONTROLLED RELEASE IN LIGHT-INDUCED TRANS-CIS ISOMERIZATION

Aysha Fasna,[2,*] Zakir Ullah,[2] David B. Amabilino,[3] Monika Gupta and Lluïsa Pérez-García[1]
[1] Departament de Farmacologia, Toxicologia i Química Terapèutica, Universitat de Barcelona, Av. Joan XXIII 27-31, Barcelona, 08028, Spain and Institut de Nanociència i Nanotecnologia UB (IN²UB),
[2] Institut de Ciència de Materials de Barcelona (ICMAB-CSIC), Carrer del Til.lers, 08193 Bellaterra, Spain,
[3] Indian Institute of Technology Ropar, Rupnagar, Punjab 140001, India
* ayshafasna@ub.edu

Photoswitchable molecules, particularly azobenzenes, have emerged as pivotal tools in energy storage and controlled release applications due to their reversible light-induced trans-cis isomerization. This property allows them to store energy in a high-energy state and release it upon returning to the stable trans configuration. Recent advancements have focused on optimizing azobenzene's performance through solvent effects, molecular modifications, and integration into materials like supramolecular gels. This study explores the integration of azobenzene into a bis-imidazolium gel matrix to enhance energy storage efficiency and enable light-responsive drug delivery

OBJECTIVES

The study aims to: (1)Develop photosensitive materials by synthesizing azobenzene derivatives and characterizing their isomerization using UV-Vis spectroscopy (irradiation at 350–550 nm). (2)Analyze solvent effects (ethanol, water, ethanol-water mixtures) on switching kinetics, measuring photostationary states and conversion rates. (3)Integrate azobenzene into bis-imidazolium gels to assess stability and energy release profiles under light triggers. (4)Explore drug delivery potential by testing light-controlled release mechanisms in gel matrices.

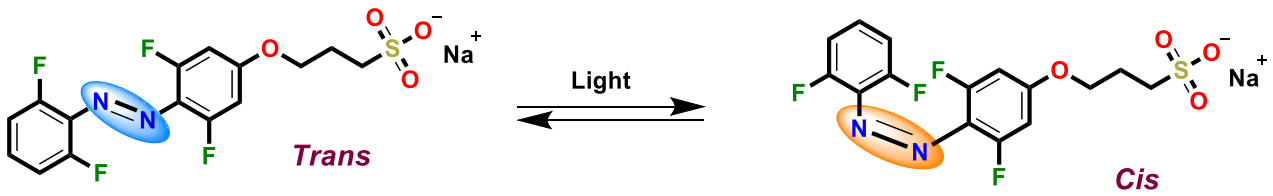

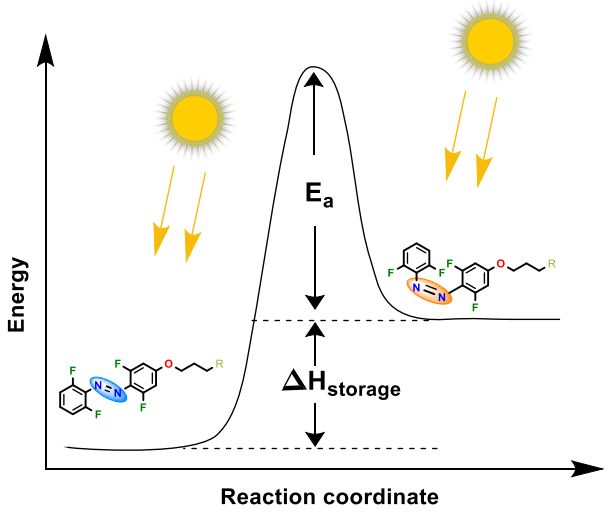

RESULTS AND DISCUSSION

UV-Vis spectroscopy revealed that the efficiency of trans-cis and cis-trans isomerization varies significantly with solvent environment. The highest cis-to-trans conversion rate was observed in an ethanol-water mixture, followed by water and ethanol, highlighting the role of solvent polarity and hydrogen bonding in isomerization kinetics. The photostationary state was achieved fastest in water (33s), compared to ethanol (56s) and the ethanol-water mixture (52s). These findings underscore the importance of solvent optimization for enhancing azobenzene-based energy storage systems.

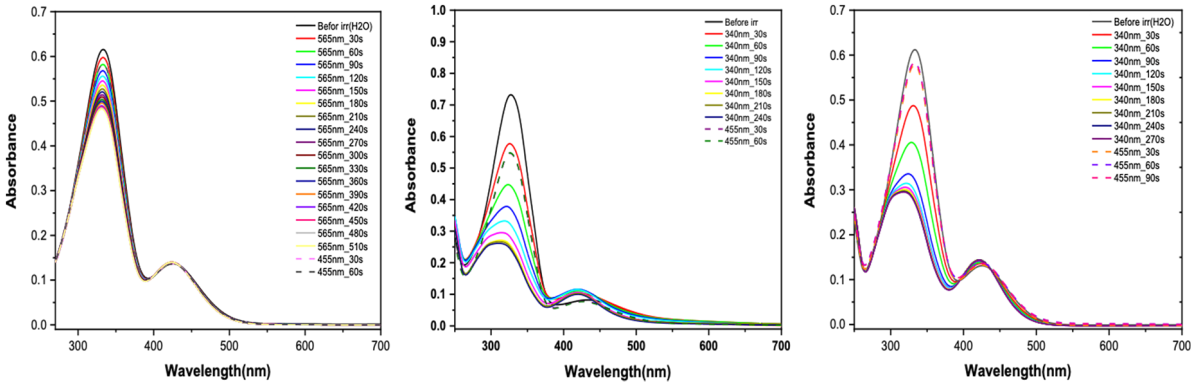

REFERENCES

[1] Samperi, M., et al. (2021). Light-controlled micron-scale molecular motion. Nature Chemistry, 13(12), 1200-1206.
[2] Gupta, M., & KM, A. K. (2024). Sunlight driven E–Z isomerization of liquid crystals based on hexahydroxytriphenylene nano-templates for enhanced solid-state solar thermal energy storage. Journal of Materials Chemistry A.

P13
RESPONSIVE-FUNCTIONALIZED SILICON OXIDE MICROCHIPS AS A SENSING PLATFORM FOR INTRACELLULAR RECOGNITION OF GLUTATHIONE

Saman Bagherpour[1,2,*], Patricia Vázquez[3,4], Marta Duch[5], José Antonio Plaza[5], Teresa Suárez[3], Lluïsa Pérez-García[2]

[1] Departament de Farmacologia, Toxicologia i Química Terapèutica, Universitat de Barcelona, Av. Joan XXIII 27-31, Barcelona, 08028, Spain.

[2] Institut de Nanociència i Nanotecnologia IN²UB, Universitat de Barcelona, Barcelona, 08028, Spain

[3] Centro de Investigaciones Biológicas Margarita Salas, CIB (CSIC), Madrid, 28040, Spain

[4] Departamento de Bioquímica y Biología Molecular, Facultad de Medicina, Universidad Complutense de Madrid, Madrid, 28040, Spain

[5] Instituto de Microelectrónica de Barcelona, IMB-CNM (CSIC), Campus UAB, Cerdanyola del Vallès, Barcelona, 08193, Spain

* saman.bagherpour@ub.edu

Self-assembly monolayers (SAMs) are considered a key tool in the surface design of nanolayers for the bioactive coating of biomedical devices. Recently, microparticles have emerged as promising tools for potential use as intracellular micrometric devices [1]. Advanced microfabrication methods allow the creation of microchips, which offer significant benefits and can be leveraged in the development of innovative biomedical devices [2].

For the first time, we present a sensing platform built on microfabricated silicon oxide microchips, functionalized with either reversible or irreversible fluorescent probes, designed for the intracellular detection of glutathione (GSH) in live cells. This novel method overcomes common challenges faced by traditional fluorescent probes used in biological solutions, particularly in terms of accurate quantification and long-term tracking of GSH.

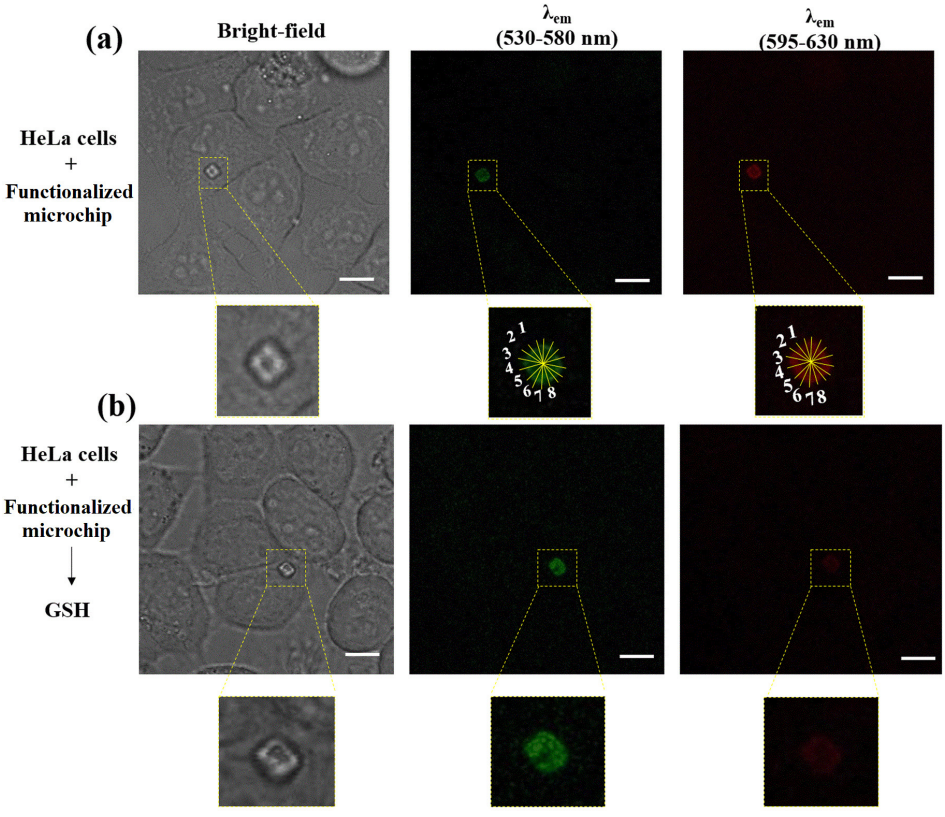

Figure 1. (a) Internalized functionalized microchip in HeLa cells during overnight incubation time (λ_{em} = 530–580 nm and λ_{em} = 595–630 nm). Yellow lines are fluorescence intensity profiles used for the ratiometric signal calculations. (b) HeLa cells incubated with unctionalized microchip overnight followed by incubation with GSH for 4 h.

ACKNOWLEDGMENT

Projects PID2020-115663GB-C3 and PID2023-146658NB-C32 were funded by MCIN/AEI/10.13039/501100011033 and by FEDER, EU. We also thank AGAUR (Generalitat de Catalunya) for a grant to consolidated research groups 2021 SGR 01085.

REFERENCES

[1] Torras, N.; Agusil, J. P.; Vázquez, P.; Duch, M.; Hernández-Pinto, A. M.; Samitier, J.; De La Rosa, E. J.; Esteve, J.; Suárez, T.; Pérez-García, L.; Plaza, J. A. Adv. Mater. 2016, 28, 1449–1454.
[2] Limón, D.; Hornick, J. E.; Cai, K.; Beldjoudi, Y.; Duch, M.; Plaza, J. A.; Pérez-García, L.; Stoddart, J. F. ACS Nano, 2022, 16, 5358–5375.

P14
NANOTECHNOLOGICAL BREAKTHROUGH FOR ALS: MULTIFUNCTIONAL PVEC-PEG-PLGA NANOPARTICLES FOR TARGETED RILUZOLE DELIVERY TO MOTOR NEURON DISEASES

G.Esteruelas[1–3], M.Ettcheto[4–7], I.Haro[3], M.Herrando-Grabulosa[8,9], N.Gaja-Capdevila[8,9], M.J. Gomara[3], X. Navarro[8,9], M.Espina[1,2], A.Camins[4–6], M-L.García[1,2,5], E.Sánchez-López[1–3,5]

[1]Dep.of Pharmacy, Pharmaceutical Technology and Physical Chemistry, Faculty of Pharmacy and Food Sciences, University of Barcelona;
[2]Institute of Nanoscience and Nanotechnology (IN²UB), University of Barcelona;
[3]Unit of Synthesis and Biomedical Applications of Peptides, IQAC-CSIC;
[4]Dep. of Pharmacology and Therapeutic Chemistry, Faculty of Pharmacy and Food Sciences, University of Barcelona;
[5]Biomedical Research Network Center in Neurodegenerative Diseases;
[6]Institute of Neuroscience, Universitat de Barcelona;
[7]Institute of Pere Virgili Health Research;
[8]Group of Neuroplasticity and Regeneration, Dep. of Cell Biology, Universitat Autonoma de Barcelona;
[9]Physiology and Immunology, Institute of Neurosciences, Universitat Autonoma de Barcelona.
* Corresponding author: **gesteruelas@ub.edu**

Amyotrophic lateral sclerosis (ALS) is the most prevalent and devastating motor neuron disorder, characterized by the progressive degeneration of both upper and lower motor neurons, ultimately leading to muscle atrophy, paralysis, and death [1]. Riluzole, despite being approves for ALS treatments, possess limited clinical efficacy due to its poor penetration into the central nervous system (CNS) requiring high systemic dosages, which increases the likelihood of adverse effects [2]. These challenges underscore the critical need for the development of advanced drug delivery systems capable of selectively targeting Riluzole to the CNS while minimizing systemic exposure [3,4].

MATERIALS AND METHODS

We developed a multifunctional nanotechnological platform based on poly(lactic-co-glycolic acid) (PLGA) nanoparticles functionalized with polyethylene glycol (PEG) and the cell-penetrating peptide pVEC to facilitate BBB crossing and enhance targeting to motor neurons. Riluzole was encapsulated using solvent displacement method, and the nanoparticles (pVEC-PEG-PLGA-RLZ NPs) were thoroughly characterized by DLS, TEM, FTIR, DSC, and HPLC. In vitro release kinetics were assessed under sink conditions, and in vivo biodistribution, pharmacokinetics, and CNS localization were evaluated in wild-type and SOD1G93A ALS mouse models via LC-MS/MS and confocal microscopy [3].

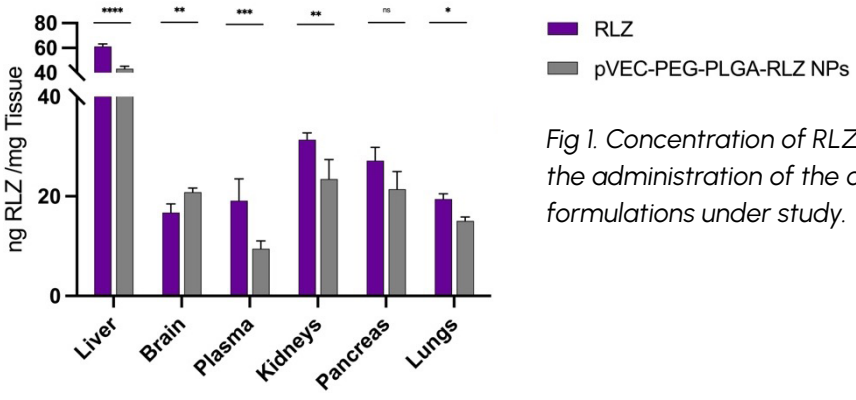

Fig 1. Concentration of RLZ after 1 h of the administration of the optimized formulations under study.

RESULTS

pVEC-PEG-PLGA-RLZ NPs exhibited a mean diameter of 164.0 ± 1.4 nm, low polydispersity (PI = 0.115 ± 0.005), and positive surface charge (+19.2 mV), confirming successful pVEC surface attachment. Encapsulation efficiency exceeded 95%, and Riluzole release followed a sustained profile, releasing 55 % of the drug over 24 h and fitting the Korsmeyer–Peppas model ($r^2 = 0.9911$). In vivo studies demonstrated a 2.3-fold increase in brain Riluzole concentration of pVEC-PEG-PLGA-RLZ NPs against free Riluzole at 1 h post-administration ($p < 0.01$) (Fig 1), with concurrent reductions of 40–60 % in peripheral organs such as liver, pancreas, and kidneys, indicating a high degree of tissue specificity. Importantly, CNS levels of Riluzole remained detectable at 24 h in the NP-treated group, while free Riluzole was nearly undetectable beyond 16 h. Confocal imaging of fluorescently labelled NPs confirmed rapid and selective accumulation in motor neurons of spinal cord, with intracellular localization evident both perinuclearly and in the cytoplasm, and persistence up to 24 h post-injection.

CONCLUSION

This study presents a novel double-functionalized nanoplatform integrating PEGylation and CPP-mediated targeting, along with a biodegradable polymeric platform to optimize Riluzole delivery to spinal motor neurons. pVEC-PEG-PLGA-RLZ NPs significantly enhanced CNS bioavailability and show potential to improve Riluzole therapeutic efficacy. These findings highlight the high translational potential of this strategy for ALS and other neurodegenerative diseases requiring targeted delivery to the central nervous system.

REFERENCES

[1] P. Masrori and P. Van Damme, Amyotrophic Lateral Sclerosis: A Clinical Review, Eur. J. Neurol. 27, 1918 (2020).
[2] R. G. Miller, J. D. Mitchell, M. Lyon, and D. H. Moore, Riluzole for Amyotrophic Lateral Sclerosis (ALS)/Motor Neuron Disease (MND), Cochrane Database Syst. Rev. 3, (2012).
[3] G. Esteruelas et al., Novel Tissue-Specific Multifunctionalized Nanotechnological Platform Encapsulating Riluzole against Motor Neuron Diseases 4, Int. J. Nanomedicine (2025).
[4] L. Ribovski, N. M. Hamelmann, and J. M. J. Paulusse, Polymeric Nanoparticles Properties and Brain Delivery, Pharmaceutics 13, 1 (2021).

P15
SELF-ASSEMBLED PORPHYRIN GELS FOR ENHANCED SINGLET OXYGEN GENERATION FOR PHOTODYNAMIC THERAPY

N. V. Lakshmi Kavya Anguluri[1], Saman Bagherpour[1,2], **Lluïsa Pérez-García**[1,2,*]

[1] Departament de Farmacologia, Toxicologia i Química Terapèutica, Universitat de Barcelona, Spain
[2] Institut de Nanociència i Nanotecnologia UB (IN²UB), Universitat de Barcelona, Spain
* **mlperez@ub.edu**

Singlet oxygen (SO) is a highly reactive oxygen species important for environmental remediation and photodynamic therapy (PDT). Efficient generation of SO has attracted significant attention, driving the development of new materials and methodologies. Supramolecular gels incorporating SO-generating chromophores offer a promising platform for controlled and localized therapeutic applications.

MATERIALS AND METHODS:
Supramolecular gels were prepared by mixing a bis-imidazolium gelator with porphyrin in a water-ethanol solution and allowed to self-assemble at room temperature. Their physicochemical properties, singlet oxygen generation, drug release, rheology and antimicrobial efficacy against E. coli and S. aureus were evaluated using CFU assay.

RESULTS AND DISCUSSION:
The supramolecular gels formed stable, fibrous networks capable of encapsulating porphyrins, confirmed by rheological analysis. Antibacterial tests showed TPPP@Gel achieved 97% and 100% CFU reduction for E. coli and S. aureus, respectively. These findings support the potential of porphyrin-loaded supramolecular gels for effective antimicrobial photodynamic therapy.

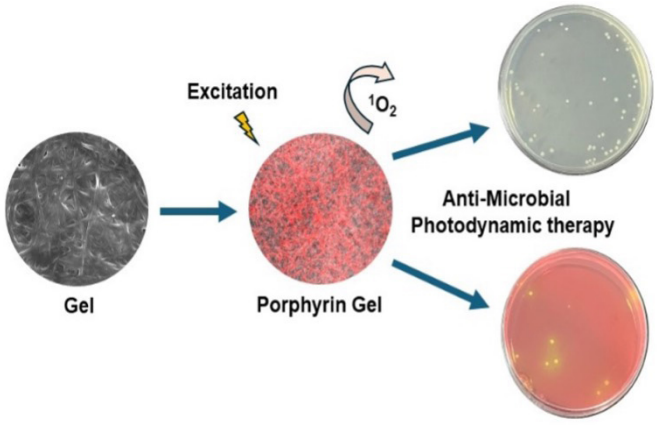

REFERENCES
[1] Samperi, M.; Limón, D.; Amabilino, D. B.; Pérez-García, L. Enhancing Singlet Oxygen Generation by Self-Assembly of a Porphyrin Entrapped in Supramolecular Fibers. Cell Reports Physical Science 2020, 1, 100030.

P16
ADVANCED NANOCARRIER PLATFORMS FOR THE DELIVERY OF BAKUCHIOL, ENCAPSULATION EFFICIENCY AND RELEASE PROFILING

T. Kakabadze[1,*], L.C. Rosales Rivera[1,2], E. Escribano Ferrer[1,3,4,5], G. Morral Ruíz[1,6], M.J. García Celma[1,3,5,6]

[1]Department of Pharmacy and Pharmaceutical Technology and Physical Chemistry, Faculty of Pharmacy and Food Sciences. University of Barcelona (UB), Joan XXIII, 27-31, 08028, Barcelona, Spain. [2] Department of Chemical Engineering, CUCEI, University of Guadalajara, Marcelino García Barragán 1421, 44430, Guadalajara, Mexico [3] Institute of Nanoscience and Nanotechnology (IN²UB), University of Barcelona, Spain. [4] CIBER-OBN, Institute of Health Carlos III, Madrid, Spain [5] Pharmaceutical Nanotechnology Group, Associated Unit to CSIC through the IQAC, Barcelona, Spain [6]CIBER-BBN, Institute of Health Carlos III, Madrid, Spain.
* tkakabka7@alumnes.ub.edu

Bakuchiol (BAK) is a bioactive compound recognised for its antioxidant, antimicrobial, anti-inflammatory, and estrogen-mimetic properties [1]. Despite its promising pharmacological profile, its poor aqueous solubility and chemical instability present significant challenges to design topical formulations incorporating BAK. In addition, to find a suitable receptor solution that ensure sink conditions for BAK release studies is particularly difficult. Microemulsions, which are isotropic and thermodynamically stable systems capable of solubilizing both, hydrophilic and lipophilic substances are promising candidates for use as receptor media [2]. Hexosomes, that are nanostructures composed of reverse hexagonal liquid crystal dispersed in water, can provide protection against chemical degradation and enhance cutaneous absorption of BAK [3]. Accordingly, the present study focuses on the design and characterization of hexosomes as advanced nanocarrier systems for topical delivery of BAK, as well as the development of suitable microemulsions as receptor solutions for in vitro release studies.

MATERIALS AND METHODS

BAK (DKSH), C41V (Nisshin Oillio Group), Poloxamer 407 and Kolliphor®RH40 (BASF), Ethyl acetate (Merck), Isopropyl myristate (Sigma), Labrasol (Gattefossé), and Milli-Q water.

METHODS

Hexosomes were prepared following a previously described method [4]. Non-equilibrium pseudo-ternary phase diagrams were constructed at 37oC to identify microemulsion regions and to select suitable compositions for use as receptor media in drug release studies. Characterization of liquid crystalline structures was performed by cross-polarized light microscopy (CPLM), small-angle X-ray scattering (SAXS) and cryo-TEM. The mean particle size and polydispersity index of both formulations were determined by DLS using a Zetasize nano ZS. In vitro release studies were conducted at 37 °C using the VISION® G2 ELITE 8TM dissolution tester system, employing regenerated cellulose acetate dialysis bags. Microemulsion were used as receptor medium to maintain sink conditions. Quantification of BAK was determined by high-performance liquid chromatography (HPLC).

RESULTS AND DISCUSSION

BAK was successfully incorporated into hexosomes at a concentration of 0.5 wt% and solubilized in microemulsions at concentrations up to 3.5 wt%. Particle size analysis revealed nanostructures with a mean diameter of 131.2 ± 0.2 nm for hexosomes and droplet sizes of 14.14 ± 0.3 nm for microemulsions, with both formulations showing narrow size distributions (PDI < 0.2). The incorporation of BAK into diglycerol monoisostearate-based hexosomes demonstrates the potential of these advanced nanostructured systems to enhance the solubility and stability of poorly water-soluble actives. Moreover, microemulsions were found to be suitable as receptor media for BAK release studies, allowing the accomplishment of sink conditions. Preliminary release assays have been performed, and ongoing research is focused on evaluating the potential use of these nanocarriers as drug delivery systems for the topical administration of other challenging active pharmaceutical ingredients.

REFERENCES

[1] Xin Z, Wua X, Jia T, Xu B, Han Y, Sun M, Jiang S, Li T, Hu W, Deng C, Yang Y. Pharmacological Research 2019, 141: 208-213. [2] Zhai J, Fong C, Tran N, Drummond CJ. ACS Nano 2019; 13: 6178-6206. [3] Zhai J, Fong C, Tran N, Drummond CJ. ACS Nano 2019; 13: 6178-6206. [4] Rodrigo Magana J, Homs M, Esquena J, Freilich I, Kesselman E, Danino D, Rodríguez-Abreu C, Solans C. J Colloid Interface Sci. 2019, 550: 73-80.

P17
ROBUST CALIX[4]ARENE–POLYETHYLENEIMINE FUNCTIONALIZED IRON OXIDE NANOPARTICLES FOR EFFICIENT RECOVERY OF GOLD AND PLATINUM CHLORIDE COMPLEXES

Carlos Moya,[1-3*] Natacha Brion,[4] Joost Brancart,[5] Ludovic Troian-Gautier,[6] Ivan Jabin,[7] Gilles Bruylants[1]

[1]Departament de Química Inorgànica i Orgànica, Universitat de Barcelona, Martí i Franquès, 1-11, 08028 Barcelona, Spain
[2] Engineering of Molecular NanoSystems, Ecole Polytechnique de Bruxelles, Université libre de Bruxelles, Brussels 1050, Belgium
[3] Institut de Nanociència i Nanotecnologia (IN²UB), Universitat de Barcelona, 08028 Barcelona, Spain
[4] Analytical and Environmental Geochemistry (AMGC), Vrije Universiteit Brussel, Pleinlaan 2, 1050 Brussels, Belgium
[5] Physical Chemistry and Polymer Science, Materials and Chemistry Department, Vrije Universiteit Brussel, Pleinlaan 2, 1050 Brussels, Belgium
[6] Institute of Condensed Matter and Nanosciences, Molecules, Solids and Reactivity (IMCN/MOST), Université catholique de Louvain, Place Louis Pasteur 1, 1348 Louvain-la-Neuve, Belgium
[7] Laboratoire de Chimie Organique, Université libre de Bruxelles, Avenue F.D. Roosevelt, 50 B-1050 Brussels, Belgium
*carlosmoyaalvarez@ub.edu

Magnetic removal and recovery of precious metals from wastewater and complex biological media pose significant challenges mostly due to the need for efficient, selective, and stable materials [1]. This work reports a methodology that allows these challenges to be addressed by synthesizing iron oxide nanoparticles (IONPs) coated with a covalent layer of calix[4]arene-tetracarboxylate (X4C4) capable of binding polyethylenimine (PEI) functionalities via electrostatic interactions [2]. In contrast to citrate coating, which was previously utilized as an attachment layer for PEI, the reductive grafting of X4C4-tetra-diazonium salts onto IONPs results in a considerably more stable coating that proves to be an excellent substrate for the adsorption of PEI. This efficiently results in a synergistic interaction that significantly improves the durability of the PEI coating and maintains the particles in a dispersed state. The stability of the resulting IONPs@X4C4@PEI particles is demonstrated by their ability to withstand both acidic and alkaline conditions without significant particle aggregation or loss of magnetic properties. Moreover, these particles exhibit exceptional magnetic reusability, retaining their selectivity and recovery efficiency over multiple separation cycles. The selective affinity of IONPs@X4C4@PEI particles for gold (Au) and platinum (Pt) stems from the specific binding interactions between the complexes formed by these metals in solution and the PEI coating, enabling efficient recovery of these precious metals [3]. This work places these IONPs at the forefront in terms of stability, reusability, and selectivity, which will undoubtedly open new avenues for environmental remediation and purification applications.

REFERENCES
[1] Makvandi, P. et. al. Environ. Chem. Lett. 2021, 19 (1), 583–611.
[2] Moya, C. et. al. Environmental Science: Nano. 2025, 12, 777-790.
[3] Betancur, J. C. et. al. Hydrometallurgy 2019, 189, 105128.

P18
IN VITRO RELEASE AND EX VIVO PERMEATION STUDY OF A LIPID SOLUTION FOR TOPICAL TREATMENT OF PSORIASIS

R. Mohammadi Mey Abadi[1,2], A. Calpena[1,2], M. Mallandrich[1,2]

[1] Department of Pharmacy, Pharmaceutical Technology and Physical-Chemistry, Faculty of Pharmacy University of Barcelona, 08028 Barcelona, Spain.
[2] Institut de Nanociència i Nanotecnologia IN²UB, Universitat de Barcelona, 08028 Barcelona, Spain.
* rmohammo31@alumnes.ub.edu

Psoriasis is a chronic inflammatory skin disease with a global prevalence of 1–3%, characterized by erythematous papules and plaques with well-defined borders and covered with silvery-white scales distributed in localized areas [1]. Today, there are various treatments for this disease. A topical formulation can potentially provide therapeutic effects while minimizing side effects. However, conventional topical formulations often face challenges such as poor solubility, limited skin penetration, and inadequate and uncontrolled release [2]. Baricitinib is a drug that selectively inhibits JAK1/JAK2 tyrosine kinases [3]. In this study, Baricitinib formulation in oily solution (BCT-OS) was used as a strategy for the topical treatment of inflammation and characteristic symptoms of psoriasis. Materials & Methods: Accordingly, the in vitro release study and Ex vivo permeation study were measured using Franz diffusion cells. Results: The results of the release study showed that the drug release from the BCT-OS formulation is indicated by the cumulative amounts of BCT released as a function of time. After 51 h of testing, about 80% of the initial drug was released from the formulation (Figure 1). The results of BCT permeation from ex vivo studies are shown. Only a small amount of the drug was found in the samples extracted from the recipient fluid during the 23.5-hour study, indicating the difficulty of the drug in penetrating the deep layers of the skin. The results showed (Table 1) that the drug flux (Jss) was 0.10 ± 0.02 µg/(h/cm2), the permeability coefficient (Kp) was 0.19 ± 0.03 × 10−4 cm−4/h, and the time required for BCT to appear in the recipient fluid at a constant rate (Tl) was 8.42 ± 0.78 h. The predicted theoretical steady-state plasma concentration (Css) was 0.06 ± 0.01 ng/mL, and the amount of BCT remaining in the skin was 277.62 ± 52.75 µg/g skin/cm2 (Figure 2). The amount of drug in the samples obtained from this study was determined by HPLC-FLD. Discussion: According to the results obtained, it was shown that this formulation is capable of releasing the drug and therefore will not hinder the penetration of the drug through the skin. In other words, the release of the drug will not be a rate-limiting step in the penetration of the drug through the skin. Ex vivo penetration studies showed that BCT-OS can be a topical dermal therapeutic approach without significant systemic side effects.

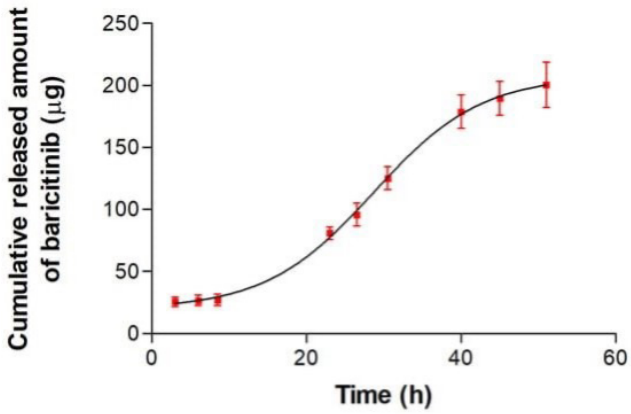

Fig.1

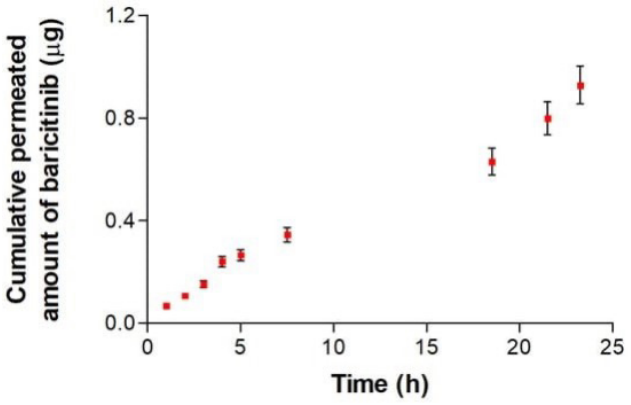

Fig.2

Parameters	Mean ± SD
J_{ss} (μg/(h/cm²))	0.10 ± 0.02
K_p (×10⁴ cm/h)	0.19 ± 0.03
Tl (h)	8.42 ± 0.78
P_2 (h^{-1})	1.40 ± 0.13
P_1 (×10⁴ cm)	0.14 ± 0.02
C_{ss} (ng/mL)	0.06 ± 0.01
Q_{ret} (μg/g skin/cm²)	277.62 ± 52.75

Abbreviations: J_{ss} (flux), K_p (Permeability coefficient), Tl (lag time), P_1 (vehicle/tissue parition coefficient), P_2 (difussion coefficient), C_{ss} (steady-state plasma concentration, and Q_{ret} (amount of drug retained in the tissue)

REFERENCES

[1] Armstrong, A.W.; Read, C. Pathophysiology, Clinical Presentation, and Treatment of Psoriasis: A Review. JAMA 2020, 323, 1945–1960.

[2] Kathe, K.; Kathpalia, H. Film Forming Systems for Topical and Transdermal Drug Delivery. Asian J. Pharm. Sci. 2017, 12, 487–497.

[3] O'Shea, J.J.; Schwartz, D.M.; Villarino, A.V.; Gadina, M.; McInnes, I.B.; Laurence, A. The JAK-STAT Pathway: Impact on Human Disease and Therapeutic Intervention. Annu. Rev. Med. 2015, 66, 311–328.

NanoMagnetics

P19
DESIGN OF AN OPTOMAGNOMECHANICAL CRYSTAL FOR THE INVESTIGATION OF NOVEL QUANTUM STATES OF MATTER

P. Cerrato-Serrano[1,*], A. García-Santiago[1,2], J. M. Hernàndez[1,2], D. Navarro-Urrios[3], M. V. Costache[1,2]

[1]Departament de Física de la Matèria Condensada, Universitat de Barcelona
[2]Institut de Nanociència I Nanotecnologia (IN²UB)
[3]Departament d'Enginyeria Electrònica i Biomèdica, Universitat de Barcelona
*pablo.cerrato@ub.edu

Hybrid systems came up as a way to combine the best aspects of different quantum systems. Spin systems in magnetic materials are a promising way to store and process information as well as a good environment to study magnon quantum states. Photons are known for being good transmitters of quantum information. Therefore, a hybrid system of photons and magnons (collective spin excitations) is of high desirability for applications such as the study of quantum states of matter and information processing and storing.
Optomagnonic systems have been studied in the past with direct coupling between magnons and photons [1]. However, the coupling strength fell short compared to other hybrid systems such as optomechanical (photon and phonon) crystals [2] and magnomechanical (magnon and phonon) systems [3].

We present a design of an optomagnomechanical crystal that takes profit of the large magnon-phonon coupling and the optimized crystal design of optomechanical crystals to achieve a high coupling.
We achieve a high-quality optical cavity, in the range of 105, with high optomechanical coupling of $2\varpi \times 108$ kHz and high magnomechanical coupling of 2.8 MHz. Moreover, due to the coupling mechanism between magnon-phonon and phonon-photon, our cavity is highly tunable and allows for precise measurement of magnon mode by changing the external magnetic field.

Financial support from MCIN / AEI / 10.13039 / 501100011033 under Grants No. PID2023-150721OB-I00 / AEI and CNS2022-135821 (European Union Next Generation EU/PRTR).

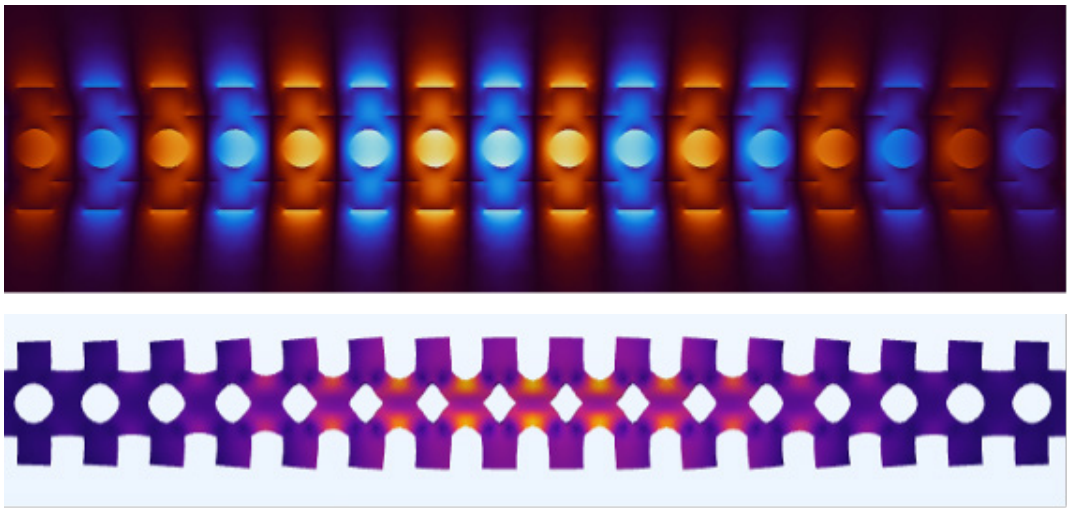

REFERENCES
[1] J. Graf et al., Physical Review Research, 3, 013277 (2021).
[2] Y. Pennec et al., AIP Advances, 1, 041901 (2011).
[3] M. Asano et al., Physical Review B, 108, 064415 (2023).

P20
SYNTHESIZING SMM AND/OR MAGNETOCOOLANT RINGS BY SLIGHT SCHIFF-BASE TUNING

E. Costa-Villén[1,*], J. Mayans[1,2], A. Escuer[1,2]

[1] Departament de Química Inorgànica i Orgànica, Secció Inorgànica, Universitat de Barcelona, Martí i Franquès 1-11, Barcelona-08028, Spain.
[2] Institute of Nanoscience (IN²UB) and Nanotecnology, Universitat de Barcelona, Martí i Franquès 1-11, Barcelona-08028, Spain.
* ecostavillen@ub.edu

Schiff Bases, the N analogue of carbonyl groups (C=O) obtained from the condensation of a primary amine and an aldehyde or a ketone, are promising candidates for synthetizing coordination compounds for different purposes such as luminescence [1], catalysis [2], biological activity [3] and magnetism [4].

Careful selection of the precursors, can modulate multiple properties such as the denticity of the ligand, the charge of the deprotonated ligand, the nature of the donor atoms and of the chelating moieties and/or the nuclearity of the complex giving a platform to design specific ligands for each purpose.

The condensation of carbohydrazide along with ortho-vanillin derivatives, such as ethoxy-vanillin and 5-bromo-vanillin, constitute a family of ligands practically unexplored. Upon the combination of these ligands with the appropriate paramagnetic cations, cyclic complexes with nuclearity $Mn^{III}_2Ln^{III}_2$ or $Mn^{II}_6Ln^{III}_6$ (Ln^{III} = Gd^{III}, Dy^{III}, Tb^{III}, Ho^{III}, Er^{III} and Yb^{III}) have been synthesized and characterized. Magnetic measurements have been analysed to elucidate their magnetic properties.

For the complexes with the highest values of $\chi_M T$ and saturation of the magnetization [$Mn^{II}_6Ln^{III}_6$ (Ln^{III} = Gd^{III}, Dy^{III}, Tb^{III} and Ho^{III})], the magnetic entropy change values ($-\Delta S_m$) were assessed using Maxwell equation5 using the magnetization data measured in the range of 2 – 10 K with magnetic field varying from 0 – 7 T, revealing them, specially $Mn^{II}_6Gd^{III}_6$, as suitable candidates for magnetic refrigeration. Comparison between two complexes of $Mn^{II}_6Gd^{III}_6$ obtained with different experimental conditions has been done focusing in the $-\Delta S_m$ dependence with the mass and the volume.

Also, alternating current (ac) susceptometry measurements were performed focusing specially on the out-of-phase response which evidences if the complex retains the magnetization upon switching the magnetic field. Data from ac susceptometry has been analysed and fitted to obtain the relaxation time (
τ0τ0
) and the relaxation processes involved in giving information about which modifications would be necessary to enhance the SMM behaviour [6].

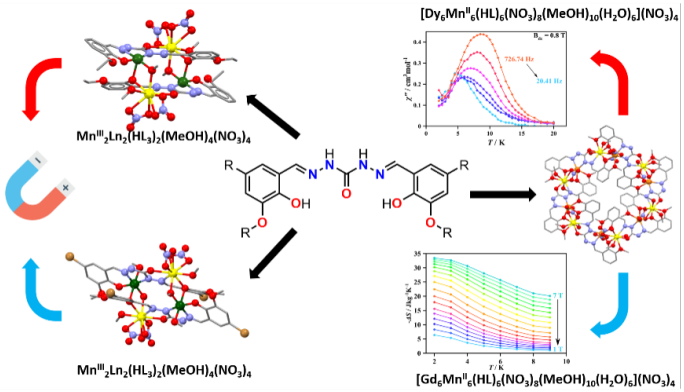

REFERENCES
[1] M. Sengar & A. Kumar Narula. J. Fluoresc. 2019, 29, 111 – 120 [2] X. Liu, C. Manzur, N. Novoa, S. Celedón, D. Carrillo, J.-R. Hamon. Coord.Chem.Rev. 2018, 357, 144 – 172 [3] M.S. Sinicropi et. al. Int. J. Mol. Sci. 2022, 23, 14840 – 14860. [4] E. Costa-Villén, M. Font-Bardia, J. Mayans, A. Escuer Cryst.Growth Des. 2024, 24, 5806 – 5817. [5] Ibrahim, M.; Peng, Y.; Moreno-Pineda, E.; Anson, C.E.; Schnack, J.; Powel, A.K. Small Struct. 2021, 2, 2100052-2100058 [6] R. Sessoli, D. Gatteschi, A. Caneschi, N.A. Movak. Nature 1993, 365, 141–143.

P21
MAGNETIC INDUCED TRANSPARENCY IN CAVITY-MAGNON POLARITONS

A. Lambíes Asensio[1,*], P. Cerrato Serrano[1], A. García-Santiago[1,2], J.M. Hernández[1,2], M. V. Costache[1,2]

[1] Departament de Física de la Matèria Condensada. Universitat de Barcelona.
[2] Institut de Nanociència I Nanotecnologia (IN²UB)
* Corresponding author: alambias18@alumnes.ub.edu

Magnons and phonons are collective excitations of the spin system and the atomic lattice of a material, respectively, interacting via magnetostrictive forces. In high-quality magnets such as Y3Fe5O12 (YIG), strong coupling of these quasiparticles has been observed, revealing phenomena like Magnomechanical Induced Transparency (MMIT). Recently, these effects have garnered significant scientific interest due to their potential applications in low-power information processing and quantum communication technologies.

MMIT is a quantum coherent phenomenon that arises when magnons hybridize with mechanical vibrations (phonons). This interaction leads to destructive interference between excitation pathways, creating a transparency window around the magnon resonant frequency [1].

In this work, we investigate magnon-phonon coupling in a magnetic YIG film grown on a non-magnetic Gd-3Ga5O12 (GGG) substrate. Through phonon pumping, magnetization dynamics generate phonon currents that leak into the substrate, which acts as a phonon cavity, carrying away energy and angular momentum from the ferromagnet [2, 3]. Specifically, we report ferromagnetic resonance (FMR) spectra of these bilayers over various power and magnetic field ranges and analyze their associated parameters (phonon and magnon linewidths, magnetoelastic coupling strength, cooperativity, etc.) to detect and characterize magnetic transparency.

Financial support from Beca de col·laboració amb el departament de Física Quàntica i Astrofísica (FFIS2025.4.FFIS) and MCIN/AEI/10.13039/501100011033 under Grants No. PID2023-150721OB-I00/AEI and CNS2022-135821 (European Union Next Generation EU/PRTR).

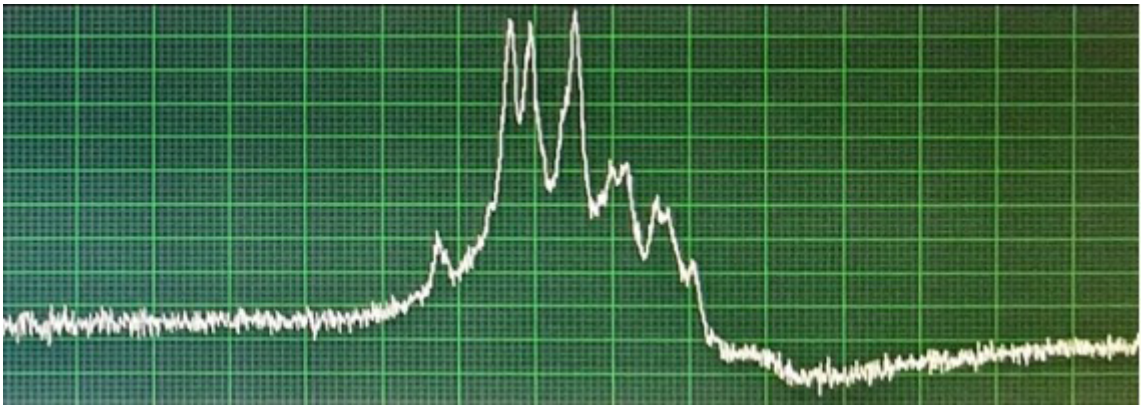

REFERENCES
[1] X. Zhang et al., Science Advances, 2, e1501286 (2016).
[2] S. Streib et al., Phys. Rev. B., 121, 027202 (2018).
[3] R. Schlitz et al., Phys. Rev. B., 106, 014407 (2022).

P22
A TRICLINIC CO(II)–POLYOXOMETALATE COMPLEX $(C_9H_{13}N_2O_2)_2[(CO(H_2O)_5)_2TEMO_6O_{24}]\cdot 2H_2O$: SYNTHESIS, STRUCTURE AND SMM PROPERTIES

Abir Dhaou[1], E. Carolina Sañudo[2,3], Sonia Abid[1]

[1] University of Carthage, Faculty of Sciences of Bizerte, LR13ES08, Laboratory of Chemical Materials, 7021, Bizerte, Tunisia.
[2] Departament de Química Inorgànica i Orgànica, Secció de Química Inorgànica, Universitat de Barcelona, Av.Diagonal 645, 08028 Barcelona, Spain
[3] Institut de Nanociència i Nanotecnología, Universitat de Barcelona (IN²UB), C/Martí i Franques 1-11, Barcelona, 08028, Spain
* Email of the corresponding author: **abir.dhaou@ub.edu**

Polyoxometalates (POMs) are an important class of metal-oxygen cluster anions known for their structural diversity, redox activity, and magnetic properties [1]. The incorporation of transition metals such as cobalt(II) into POM frameworks offers opportunities to engineer novel molecular architectures with unique electronic and magnetic behavior. Particularly, the emergence of Single-Molecule Magnets (SMMs) within POM–metal hybrid systems open new avenues in the development of nanoscale materials for quantum computing and high-density data storage [2,3].

A novel organic–inorganic hybrid compound, $(C_9H_{13}N_2O_2)_2[(Co(H_2O)_5)_2TeMo_6O_{24}]\cdot 2H_2O$, was synthesized via slow evaporation at room temperature. Single-crystal X-ray diffraction reveals that it crystallizes in the triclinic system, space group P-1, with unit cell parameters: a = 10.0989(8) Å, b = 10.2496(8) Å, c = 13.3266(9) Å, α = 80.501(4)°, β = 80.956(4)°, γ = 62.086(3)°. The structure features a discrete polyoxometalate anion $[TeMo_6O_{24}]^{6-}$, which is directly coordinated to two $[Co(H_2O)_5]^{2+}$ units, forming a robust 0D molecular framework stabilized by hydrogen bonding with the organic cations $C_9H_{13}N_2O_2^+$. The compound was fully characterized by FT-IR, Raman, UV–Vis, and luminescence spectroscopy, confirming the hybrid architecture and electronic interactions. Remarkably, magnetic studies reveal Single-Molecule Magnet (SMM) behavior, with a clear frequency-dependent out-of-phase signal (χ") observed in AC susceptibility. Fitting the magnetic relaxation data to the Arrhenius law yielded an effective energy barrier Ueff = 11.1 K and a relaxation time $\tau_0 = 2.25 \times 10^{-5}$ s, indicating slow relaxation of the magnetization via an Orbach process. These results are consistent with a negative axial zero-field splitting parameter D = –15.77 cm^{-1}, derived from PHI-model simulations of magnetization vs. temperature and field data. The magnetic behavior, coupled with the structural versatility of the polyoxometalate and Co(II) centers, highlights the potential of this compound in molecular spintronic devices, data storage, and quantum information processing.

KEYWORDS
Single Molecule Magnet (SMM), Polyoxometalate, Magnetic relaxation, Crystal structure, optical properties.

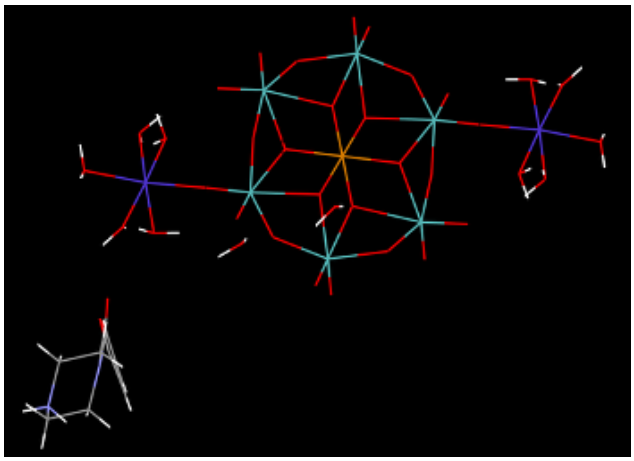

REFERENCES
[1] Y. Li, J. Zhang, Y. Wang, "Recent advances of polyoxometalate-based materials applied for energy storage and conversion," Coord. Chem. Rev., 2024, 500, 214345.
[2] S. Wang, L. Chen, "Recent advances in polyoxometalate-based single-molecule magnets," Coord. Chem. Rev., 2023, 492, 215205.
[3] X. Liu, H. Zhao, "Field-induced mononuclear cobalt(ii) single-molecule magnet (SMM) based on a π-conjugated ligand," Dalton Trans., 2022, 51, 12345–12352.

P23
RAYLEGIH-JEANS CONDENSATION OF MAGNONS IN AN OPTOMAGNOMECHANICAL SYSTEM.

D. González[1,*], P. Cerrato[1], A. García-Santiago[1,2], J. M. Hernàndez[1,2], D. Navarro[1,2], M. V. Costache[1,2]

[1] Department de Física de la Matèria Condensada, Universitat de Barcelona
[2] Institut de Nanociència I Nanotecnologia (IN²UB)
* Corresponding author: dgonzadi18@alumnes.ub.edu

Over the past two decades, the dynamics of parametrically pumped magnons in thin Yttrium-Iron-Garnet (YIG) films have been extensively explored at room temperature [1-3]. Since the discovery of a singularity in the population of the lowest-energy state in 2006 [1], significant efforts have been made to understand the fundamental properties of this unintuitive system. This led to the development of a stochastic Landau-Lifshitz-Gilbert (LLG) equation with non-Markovian damping [4], classifying this effect as a classical phenomenon, Rayleigh-Jeans Condensation (RJC), analogous to the quantum Bose-Einstein Condensation (BEC).

MATERIALS AND METHODS

We simulate magnon dynamics using the LLG equation within MuMax3 [5].

RESULTS AND DISCUSSION

In this study, we investigate RJC within an optomagnomechanical system, characterized by strong couplings between specific magnon, phonon, and photon modes [6]. Our simulations confirm the onset of RJC above a critical oscillating magnetic field. Subsequently, we introduce an additional coupling term to model the strong interaction with a particular mechanical mode, analyzing the dynamics of its population and revealing a rich phase diagram. Furthermore, we explore the potential applications of this condensate in optomagnomechanical systems for quantum information processing.

FINANCIAL SUPORT

Beca Col·laboració 2024.7.FFIS.2 (P1)- Beca Màster + Departament de Física Quàntica i Astrofísica and MCIN/AEI/10.13039/501100011033 under Grants No. PID2023-150721OB-I00/AEI and CNS2022-135821 (European Union Next Generation EU/PRTR).

REFERENCES

[1] [1] S. O. Demokritov et al., Nature, 443, 430-433 (2006).
[2] S. M. Rezende, PRB, 79, 174411 (2009).
[3] P. Nowik-Boltyk et al., Sci. Rep., 2, 482 (2012).
[4] A. Rückriegel et al., PRL, 115, 157203 (2015).
[5] F. Engelhardt et al., PRA, 18, 044059 (2022).
[6] A. Vansteenkiste et al., AIP Advances, 4, 107133 (2014).

P24
THE ROLE OF TERAHERTZ VIBRATIONS IN THE SPIN RELAXATION OF CERIUM-BASED METAL-ORGANIC FRAMEWORKS[1]

Joan Torrent[1], Júlia Mayans[1,2]

[1] Departament de Química Inorgànica i Orgànica, Secció de Química Inorgànica, Universitat de Barcelona, Martí i Franquès 1-11, Barcelona-08028, Spain.
[2] Institut de Nanociència i Nanotecnología (IN²UB), Universitat de Barcelona, Barcelona 08028. Spain.
* **joan.torrent@ub.edu**

The field of molecular magnetism has seen a fast evolution in the past decade, spanning from the study of the nature of slow spin relaxation to the realization of proof-of-concept quantum information processors based on molecular devices[2,3]. This work is focused on the former aspect, since the nature of spin relaxation is not yet fully deconvoluted. This work delves into the role of ultra-low frequency vibrations in the spin relaxation of Cerium ions in designed Metal-Organic Frameworks (MOFs) (Fig. 1a), which is one of the less studied lanthanides in the series. A correlation between alternate current magnetic susceptibility measurements at multiple applied dc fields (Fig. 1b), ultra-low frequency Raman spectroscopy (Fig. 1c), and theoretical calculations elucidates the role of these low-energy phonon modes in promoting spin relaxation in these Cerium-based systems.

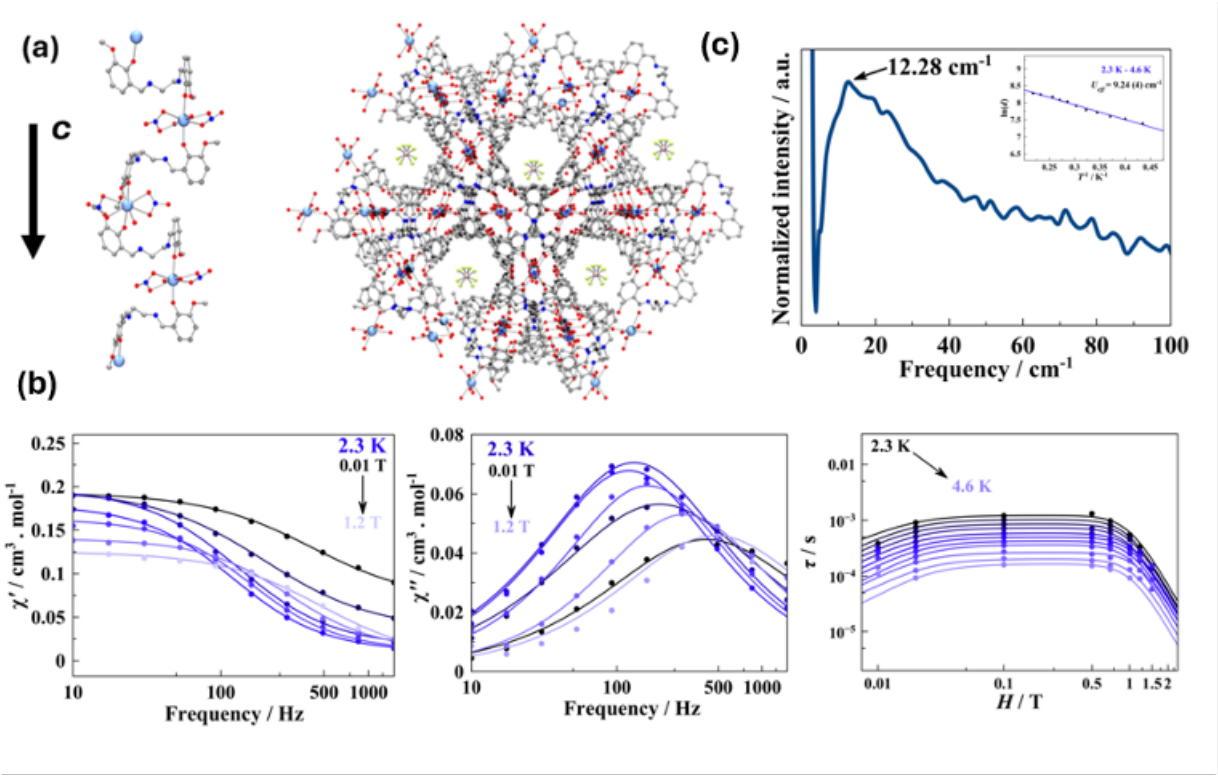

Figure 1: (a) Structure of the studied frameworks. (b) In-phase (Left) and out-of-phase (Right) magnetic susceptibility components recorded at a fixed temperature and variable dc fields, field-dependence of the relaxation time. (c) Ultra-low frequency Raman spectrum.

REFERENCES
[1] Inorg. Chem., 2025, 64, 8, 3735-3746.
[2] Chem. Soc. Rev., 2018, 47, 501-513.
[3] J. Am. Chem. Soc., 2024, 146, 1, 1053-1061.

P25
2D MATERIALS: METALLIC/MOLECULAR HETEROSTRUCTURES FOR SPINTRONICS APPLICATIONS

Hassaan Sajid[1,*], Eva Carolina Sañudo[2], Jérôme Loreau[3]

[1] Institute of Nanoscience and Nanotechnology, University of Barcelona
[2] Department of Inorganic and Organic Chemistry, University of Barcelona, Spain
[3] Department of Chemistry, Katholieke Universiteit Leuven, Belgium
* hsajidsa77@alumnes.ub.edu

In recent years 2D materials have captured significant interest of researchers across the globe especially for spintronics applications due to their unique magnetic and electronic properties. In this study, we tried to establish the possibility of mechanical exfoliation of lanthanide-based metal-organic frameworks (MOFs) into mono- or few- layer nanosheets using Scotch tape method – aiming to provide an alternative to traditional sonication assisted exfoliation route. Gd- and Tb-based MOFs of type-I (metal to ligand ratio 1:2) were synthesized using microwave-assisted method under controlled conditions (125°C for 10 minutes in a 1:1 acetonitrile:methanol solvent system). Pure Gd-MOF and Tb-MOF along with their 50:50 mixed compositions i.e. Gd-La-MOF and TbLa-MOF were grown by leaving the reaction mixture undisturbed for 10-15 days. Powder X-Ray Diffraction (PXRD) confirmed the structure of the MOFs. Exfoliation was performed on silicon substrate through repeated 3-times (3x), 4-times (4x) and 5-times (5x). Scanning electron microscopy (SEM) and atomic force microscopy (AFM) were performed to characterize the exfoliated flakes to investigate its area, aspect ratio and thickness (height profile). It was expected to have a consistent decrease in flake thickness with increasing exfoliation steps while maintaining a stable aspect ratio, consistent with crystal's cleavage planes (monoclinic, space group P21/c). Initial results show a consistent aspect ratio across all exfoliated samples confirming the fragmentation along the crystallographic planes in all the flakes. However the variations in area and the thickness are more pronounced raising questions about whether the flake thickness depends solely on the number of exfoliation steps or there are some other parameters as well. In general, the findings support the viability of the mechanical exfoliation for preparing high quality 2D MOF nanosheets for spintronics device applications.

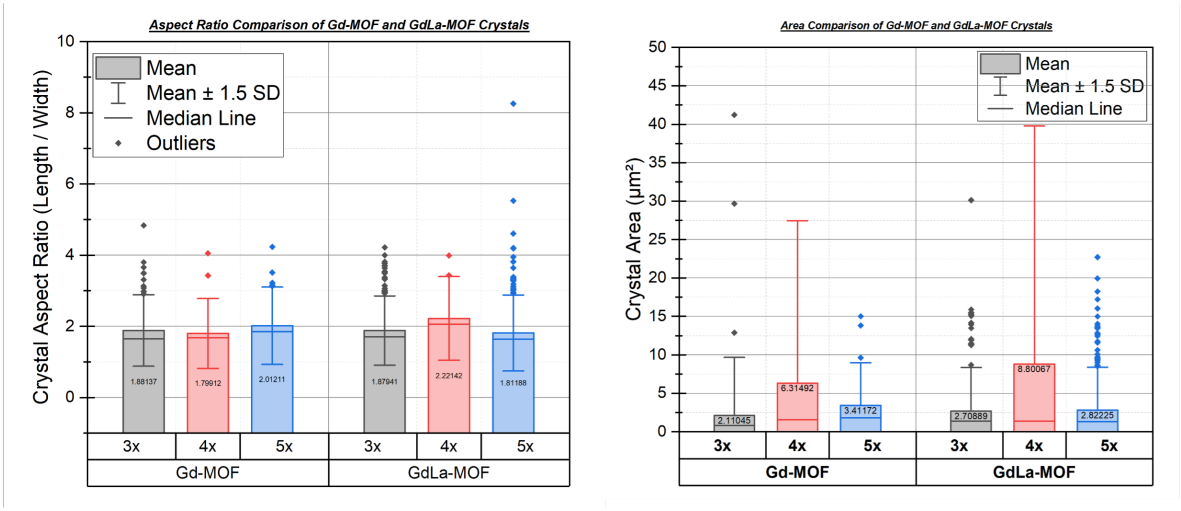

Figure 1 Comparison of (left) crystal aspect ratio (length/width) and (right) crystal area (µm²) for Gd-MOF and GdLa-MOF flakes exfoliated 3x, 4x, and 5x using the Scotch-tape method. Bars represent the mean values with error bars indicating ±1.5 standard deviations; median values are shown as solid lines within each bar. Outliers are marked individually. The aspect ratio remains relatively consistent across exfoliation steps, while greater variability is observed in crystal areas, suggesting additional factors may influence flake fragmentation beyond exfoliation frequency.

P26
ORBITAL CURRENTS GENERATED BY SURFACE ACOUSTIC WAVES IN FM/NM BILAYERS

J. Òdena[1], M. Rovirola[1,2], A. Castellví-Picanyol[1], B. Casals[2,3], J.M. Hernàndez[1,2], A. Hernández-Mínguez[4], P. Perna[5], S. Vélez[5], F. Macià1,[2]

[1] Dept. of Condensed Matter Physics, University of Barcelona, 08028 Barcelona, Spain
[2] Institute of Nanoscience and Nanotechnology (IN²UB), University of Barcelona, 8020 Barcelona, Spain
[3] Dept. of Applied Physics, University of Barcelona, 08028 Barcelona, Spain
[4] Paul-Drude-Institut für Festkörperelektronik, Leibniz-Institut im Forschungsverbund Berlin e.V., 10117 Berlin, Germany
[5] Instituto Nicolás Cabrera, Universidad Autónoma de Madrid, E-28049 Madrid, Spain
* jodena@ub.edu

Surface acoustic waves (SAWs) can be coupled efficiently to magnetostrictive ferromagnetic materials (FM) and are known to drive large angle magnetization precession [1,2]. The resulting magnetization oscillation may pump spin and orbital currents into adjacent nonmagnetic (NM) materials, which eventually can be converted into detectable charge currents from inverse spin and orbit Hall effects. However, pumping mechanisms can have diverse origins such as spin or orbital pumping, magnetorotation, and phonon angular momentum transfer—all of them with different symmetries with respect to the angle between SAW and magnetization. Typically, the detection of spin currents is done through inverse spin Hall effect (ISHE) in large spin orbit coupling (SOC) materials such as Pt, Ta and W. Nevertheless, these materials can be toxic, hard to find and are associated with environmentally harmful techniques. More recently, the orbital angular momentum has taken protagonism as it is predicted to have a comparable or even larger effect than its spin counterpart and may occur in cleaner and less expensive materials.

Here, we explore different pumping mechanisms in bilayer systems made of FM/NM through acoustically driven magnetization waves. The studied hybrid devices consist of a piezoelectric substrate where Interdigital Transducers (IDTs) are placed facing each other to generate and detect SAWs transmission. The FM/NM bilayers are deposited in different structures in the acoustic path in between facing IDTs (see Figure 1 (d)) and both transversal or longitudinal voltages can be detected in presence of SAW. We compare nickel and cobalt as FM and chromium and aluminium as NM.
We demonstrate that SAW may induce orbital currents that are detected in the NM layer. Figure below shows a large inverse orbital Hall effect in the chromium compared with a tiny effect in aluminium. We study further amplitude asymmetries as a function of the angle between SAW and magnetization to quantify both the orbital pumping from FM and the orbital Hall conductivity in the NM metals.

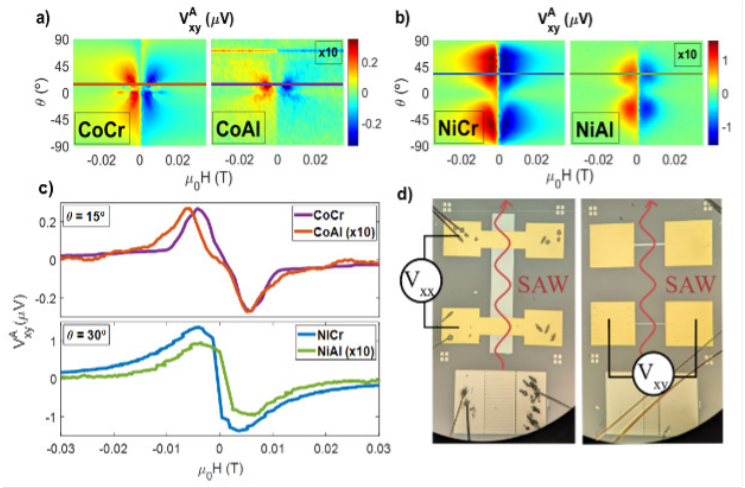

Figure. Measures of the angular dependence of the antisymmetric part of the transversal voltage (V_{xy}^A) for a) Cobalt/Chromium, Cobalt/Aluminium and b) Nickel/Chromium, Nickel/Aluminium bilayers in the presence of 1.3 GHz SAWs. c) Measures of the field dependence of the V_{xy}^A for the Cobalt bilayers at θ=15° and the Nickel bilayers at θ=30° d) Experimental set-up for longitudinal (V_{xx}) and transversal (V_{xy}) voltage detection.

REFERENCES
[1] B. Casals et al., Phys. Rev. Lett. 124, 137202, (2020), [2] M. Rovirola et al., Phys. Rev. Research 6, 023285 (2024)

P27
DESIGN OF HYDROGEN-BONDED SUPRAMOLECULAR SWITCHABLE MAGNETIC MATERIALS

D. Aguilà[1], R. Díaz-Torres[1], H. H. Nielsen[2], P. Vilariño[1], J. F. Nüsing[3], O. Roubeau[4], G. Aromí[1]

[1] Universitat de Barcelona, Barcelona (Spain)
[2] Aarhus University, Aarhus (Denmark)
[3] Johannes Gutenberg University Mainz, Mainz (Germany)
[4] Universidad de Zaragoza, Zaragoza (Spain)
* david.aguila@ub.edu

Spin-Crossover (SCO) molecular materials are fascinating switchable compounds with significant potential for the development of novel technological devices. While their synthesis primary relies on coordination chemistry, weak non-covalent interactions, such as hydrogen bonds, can be further exploited to construct more complex supramolecular architectures. To explore the development of those H-bonded SCO systems, we have designed ligands that incorporate a pyrazolyl-pyridyl chelating unit along with additional hydrogen bond donor and/or acceptor groups.[1,2] The resulting mononuclear Fe(II) SCO complexes can be then used as building blocks to generate new supramolecular entities via hydrogen bonding. In particular, their combination with tetrahedral anions promotes the formation of supramolecular tetrahedral cages, modifying at the same time the switchable magnetic behavior (Figure). Furthermore, this flexible synthetic approach can be extended to other 3d ions to tune the magnetic response of the cage, or to introduce other tetrahedral anionic guests with desirable physical properties such as luminescent units, thus paving the way for a new generation of multifunctional materials.

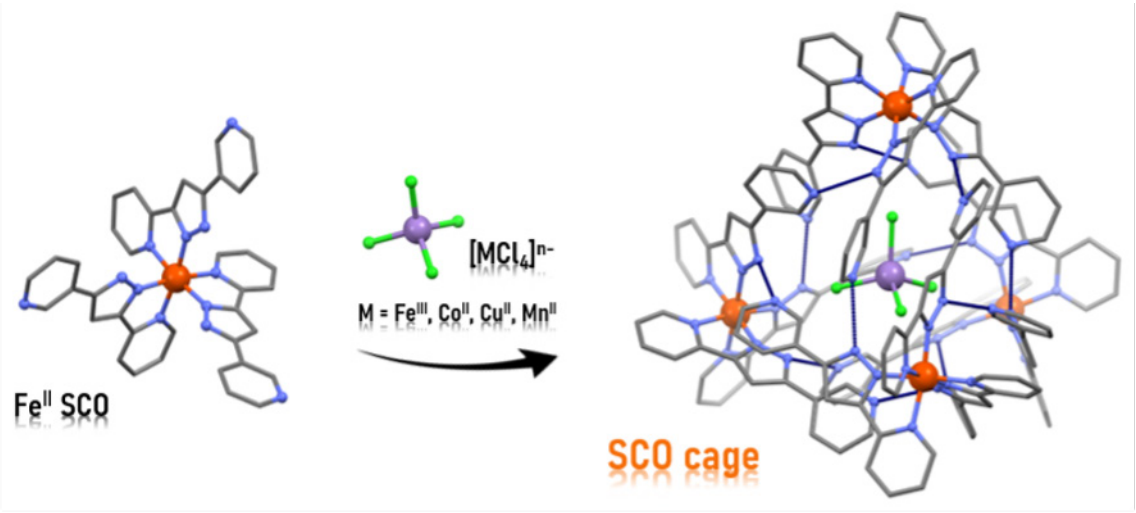

REFERENCES
[1] G. A. Craig, O. Roubeau, G. Aromí. Coord. Chem. Rev. 2014, 269, 13.
[2] H. H. Nielsen, P. Vilariño, G. Rodríguez, F. Trepard, O. Roubeau, G. Aromí, D. Aguilà. Dalton Trans. 2024, 53, 9792.

P28
EXPLORING STRUCTURAL DIVERSITY IN LANTHANIDE-BASED METAL-ORGANIC FRAMEWORKS FOR ADVANCED FUNCTIONAL APPLICATIONS

Chaima Arfa[1,*], E. Carolina Sañudo[2,3]

[1] University of Carthage, Faculty of Sciences of Bizerte, LR13ES08, Laboratory of Chemical Materials, 7021, Bizerte, Tunisia.
[2] Departament de Química Inorgànica i Orgànica, Secció de Química Inorgànica, Universitat de Barcelona, Av.Diagonal 645, 08028 Barcelona, Spain
[3] Institut de Nanociència i Nanotecnología, Universitat de Barcelona (IN²UB), C/Martí i Franques 1-11, Barcelona, 08028, Spain
* email of the corresponding author: **arfaarfachaima@ub.edu**

Organometallic materials, particularly metal-organic frameworks (MOFs), have garnered increasing attention due to their unique crystalline architecture and tunable properties, making them ideal for a wide range of applications. These materials feature well-organized networks, where metal ions are connected by organic ligands, resulting in an open and adaptable structure. In this study, we present a new series of lanthanide-based MOFs, synthesized using benzoic acid (PhCOOH) as the sole carboxylate ligand. The compounds were synthesized with a constant metal ratio of 4:9 between La^{3+} and Gd^{3+} ions, or using Ce^{3+} exclusively for the monometallic structures. Four crystalline structures were isolated, including two cerium-based ones, $[Ce_4(PhCOO)_{12}(MeOH)(MeCN)(H_2O)]_n$ and two heterometallic lanthanide ones, $[La_{0.99}Gd_{0.01}(PhCOO)_3{}_n(MeOH)(H_2O)]$ and $[La_{0.6}Gd_{0.4}(PhCOO)_3]_n$. All compounds were obtained using a combination of MeOH and MeCN solvents, while the cerium complex can also be prepared using methanol only. All materials exhibit a characteristic hexagonal crystalline morphology. Further analyses using infrared spectroscopy (IR) and electron paramagnetic resonance (EPR) were performed to assess the coordination modes, crystal morphology, and magnetic behavior of the materials. These results demonstrate not only the robustness of the crystalline structure but also the ability to modulate the metal composition while maintaining a homogeneous and ordered architecture, using a single aromatic ligand. Future investigations will focus on evaluating the catalytic properties of these MOFs, exploring their potential in specific chemical reactions.

KEYWORDS
Organometallic materials, New series of lanthanide-based MOFs, hexagonal crystalline, catalytic properties.

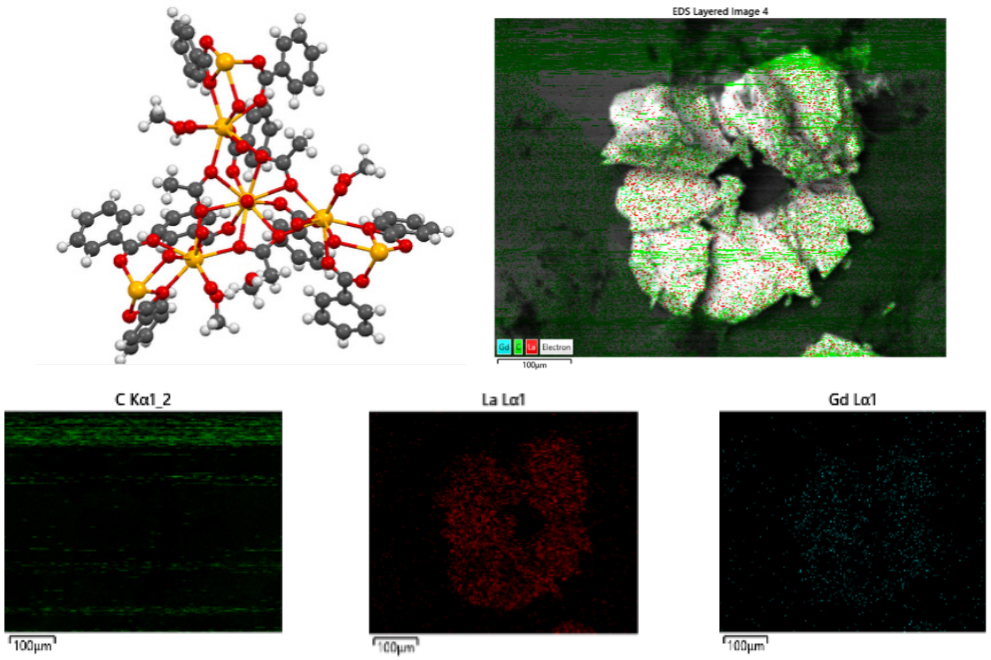

P29
STROBOSCOPIC KERR IMAGING OF MAGNETOACUSTIC WAVES IN FERROMAGNETIC THIN FILMS

A. Castellví-Picanyol[1,*], Q. Badosa[1], J. Òdena[1] , M. Rovirola[1], R. Galceran[2], A. Hernández-Mínguez[4], J. M.Hernàndez[1,2] ,F. Macià[1,2] ,B. Casals[2,3]

[1] Dept. of Condensed Matter Physics, University of Barcelona, 08028 Barcelona, Spain
[2] Institute of Nanoscience and Nanotechnology (IN²UB), University of Barcelona, 08028 Barcelona, Spain
[3] Dept. of Applied Physics, University of Barcelona, 08028 Barcelona, Spain
[4] Paul-Drude-Institut für Festkörperelektronik, Leibniz-Institut im Forschungsverbund Berlin e.V., 10117 Berlin, Germany
* annacastellvi@ub.edu

Spin waves play a crucial role in spintronics as they enable low-power information transport without charge currents. Their controlled excitation and propagation are essential for applications in non-volatile memory, magnetic logic, and wave-based computing. However, existing imaging techniques, such as microfocus Brillouin light scattering and scanning transmission X-ray microscopy, face limitations in temporal resolution or require synchrotron radiation. Time-resolved wide-field MOKE microscopy offers a powerful alternative [1], providing direct, real-time visualization of magnetoacoustic interactions with high spatial and temporal resolution. Surface acoustic waves (SAWs) efficiently couple with magnetostrictive ferromagnetic materials, inducing large-angle magnetization precession [2]. This interaction enables the excitation of spin waves, which can be imaged using magneto-optical Kerr effect (MOKE) microscopy.
In this work, we employ a stroboscopic Kerr imaging technique to visualize magnetoacoustic waves in thin ferromagnetic layers with micrometer spatial resolution. The results of our experiments provide time-resolved images of magnetoacoustic waves, allowing the study of their behavior as a function of the applied magnetic field and propagation angle. These waves are generated by SAWs, excited via interdigital transducers (IDTs) on a piezoelectric substrate, and interact with thin ferromagnetic layers such as nickel and cobalt, inducing magnetization oscillations. A picosecond-pulsed laser illuminates the sample, and the reflected signal is captured using a MOKE microscope.

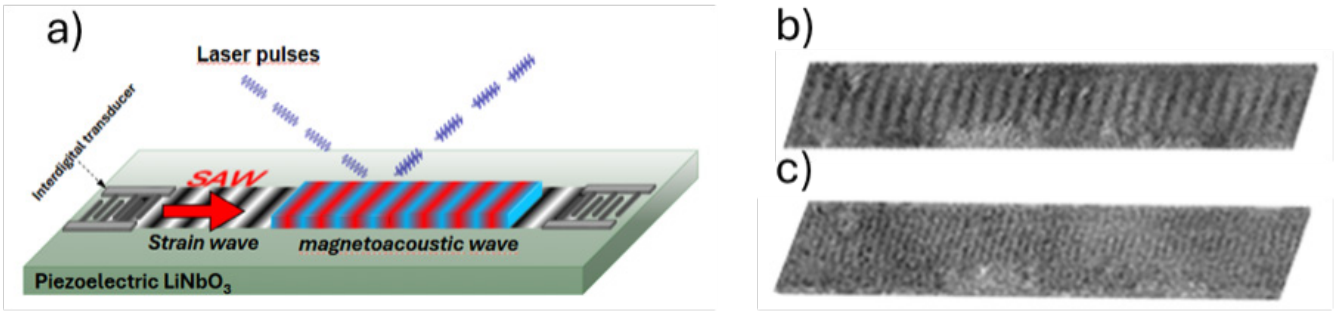

Figure. Set-up showing the generation and propagation of surface acoustic waves (SAWs), the resulting magnetoacoustic wave, and the detection via stroboscopic light. Stroboscopic images of magnetoacoustic waves at (a) 124 MHz and (b) 248 MHz.

REFERENCES
[1] T. Ogasawara Phys. Rev. Appl., 2023, 20 , 024010
[2] B. Casals, Phys. Rev. Lett., 2020, 124, 137202

P30
VERSATILE SUPRAMOLECULAR ARCHITECTURES AS HOST/GUEST SYSTEMS

J. Martínez Morató[1,*], L. A. Barrios[1], G. Aromí[1], V. Novikov[1], O. Roubeau[2]

[1] Departament de Química Inorgànica i Orgànica i IN²UB, Universitat de Barcelona, Diagonal 645, 08028 Barcelona, Espanya.
[2] Instituto de Nanociencia y Materiales de Aragón (INMA), CSIC y Universidad de Zaragoza, Plaza San Francisco s/n, 50009 Zaragoza, España.
* **jordimartinez@ub.edu**

The family of ligands featuring a pyrazolyl-pyridine coordination pocket has been used to develop various supramolecular architectures acting as host/guest systems. One of these systems, known as jellyfish, forms a more flexible structure capable of encapsulating several halides. This system consists of a dimer of two mononuclear $[FeL_3]^{2+}$ units firmly held together by π-π stacking of the uncoordinated arms of the ligands L [1]. Furthermore, it has been observed that increasing the aromatic rings of the system by replacing the pyridine group for a quinoline leads to the formation of the jellyfish supramolecular structure [2]. We are currently using asymmetric ligands to coordinate with Fe^{II} and study the spin crossover properties of the system. In addition, by synthesising a larger ligand with a more extensive cavity, we have also been able to obtain a jellyfish structure which allow to encapsulate two BF_4- and a solvent molecule.

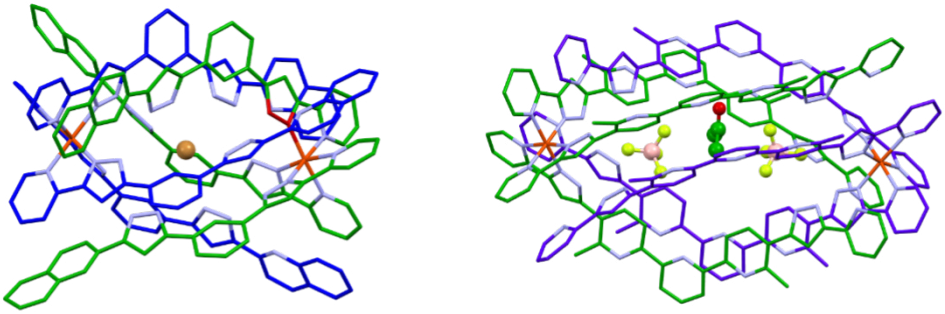

REFERENCES
[1] Chem.Commun., 2017, 53, 569. [2] Chem. Sci., 2024, 15, 9047.

P31
ANTIFERROMAGNETISM AT THE NANOSCALE

J. Ara,[1,2,*] C. Moya,[2,3] M. García del Muro,[1,2] A. I. Figueroa, [1,2] M. X. Aribó [1,2] Ò. Iglesias,[1,2] A. Kleibert,[4] A. Labarta,[1,2] A. F. Rodríguez,[1,2] and X. Batlle[1,2]

[1] Departament de Física de la Matèria Condensada, Universitat de Barcelona, Martí i Franquès 1, 08028 Barcelona, Spain
[2] Institut de Nanociència i Nanotecnologia (IN²UB), Universitat de Barcelona, 08028 Barcelona, Spain
[3] Departament de Química Inorgànica i Orgànica, C/Martí i Franquès 1-11, 1era planta, 08028 Barcelona, Spain
[4] Swiss Light Source, Paul Scherrer Institut, Villigen, PSI CH-5232, Switzerland
*e-mail of presenting author: jaraesca7@alumnes.ub.edu

Antiferromagnetic nanoparticles (NPs) have drawn significant attention due to their unique magnetic ordering and potential multifunctionality, which are leveraged in fields such as electronics, catalysis, and biomedicine. From a fundamental perspective, a comprehensive understanding of the weak ferrimagnetism that can emerge at the nanoscale remains elusive. [2-4].

This work elucidates this phenomenology by performing a model case study in three samples of Nickel Oxide (NiO), with mean particle sizes of 6, 20, and 34 nm, prepared by a two-step synthesis. Structural analysis confirms the high crystalline quality of the particles up to the outermost layers, regardless of their size. Antiferromagnetic properties are size-dependent: 6 nm NP show a weak superimposed superparamagnetic behavior, while 34 nm NP display antiferromagnetic features closely resembling those of bulk counterparts and 20 nm NP corresponds to an intermediate behavior. This is attributed to uncompensated spins associated with surface and structural modifications, particularly in smaller particles.

Using synchrotron-based X-ray photoemission electron microscopy combined with X-ray magnetic linear dichroism, a quantitative, unambiguous 3D determination of the antiferromagnetic Néel axis was obtained for a subset of individual, single-phase, 34 nm NiO NPs. The observed Néel axes are robust against thermal fluctuations at room temperature and are stochastically distributed along the 12 possible easy directions considering the most plausible crystal facets resting on the substrate, as identified through structural characterization. Contrary to seminal theoretical predictions suggesting a multi-sublattice spin arrangement of NiO NPs within this size range [2], our findings show no evidence of a breakdown in the two-sublattice model and are entirely consistent with single-domain states. These findings provide significant insights into antiferromagnetism in three-dimensional nanostructures and open new possibilities for applications requiring precise control over the reading and writing of information based on specific states of the antiferromagnetic Néel axis.

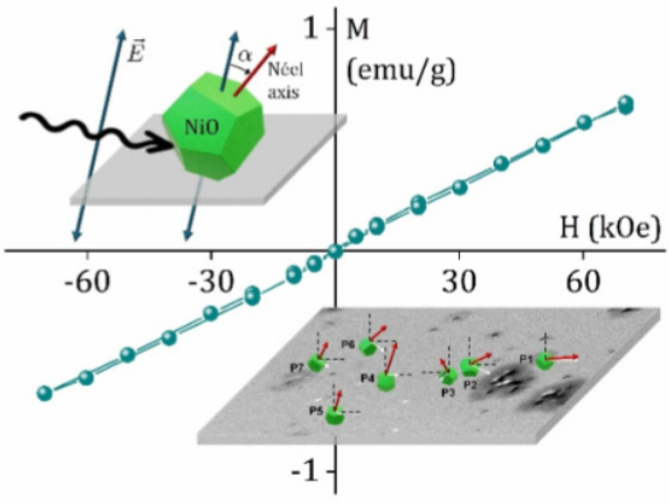

Figure 1. Magnetization curve at room temperature and distribution of Néel axes in a subset of single 34 nm NiO NP

REFERENCES

[1] C. Moya, J. Ara, A. Labarta, X. Batlle; Magnetism, 2024, 4(3), 252–280.
[2] R. H. Kodama, S. A. Makhlouf, A. E. Berkowitz; Phys. Rev. Lett., 1997, 79(7), 1393–1396.
[3] X. Batlle, C. Moya, M. Escoda-Torrella, Ò. Iglesias, A. Fraile Rodríguez, A. Labarta; J. Magn. Magn. Mater., 2022, 543, 168594.
[4] A. I. Figueroa, C. Moya, M. X. Aribó, J. Ara, M. G. del Muro, A. Kleibert, S. Valencia, A. Labarta, X. Batlle, A. F. Rodríguez; Low Temp. Phys., 2024, 50(10), 852–861.

P32
SPIN DYNAMICS IN Ag(II) MOLECULAR SYSTEMS

J. Serra[1,*], A. Escuer[1], J. Mayans[1]

[1] Departament de Química Inorgànica i Orgànica i Institut de Nanociència i Nanotecnologia, Universitat de Barcelona - Barcelona (Spain)
* jserracast@ub.edu

During the last decades, magnetic molecules have been proposed for a wide range of technological applications, such as magnetic memories, quantum computing and spintronics [1]. Specifically, in the field of quantum computing, paramagnetic coordination complexes that exhibit slow relaxation of magnetization have been suggested as a qubits, taking advantage of the high versatility provided by the chemical design of different molecular systems by employing multiple ligands and metallic cations of the d/f blocks. This versatility gives the possibility to tune and optimize the key parameters for a proper qubit performance in future applications. Recently, the magnetic properties of coordination complexes with S=1/2 have been studied[2,3], exhibiting values of spin-lattice relaxation time (T_1) and phase memory time (T_m) considerably high. These molecular systems differ from the classical single molecule magnets by the fact there are not excited spin levels that can foster the magnetic relaxation and the most important decoherence source is the interaction between the nuclear and electronic spins. In this line, we present the study of the magnetic behavior of different Ag(II) complexes derived from macrocyclic or pyridinic ligands (Figure 1, a) with an analysis of the spin dynamics studied by means of AC susceptibility and EPR measurements (Figure 1, b) [4].

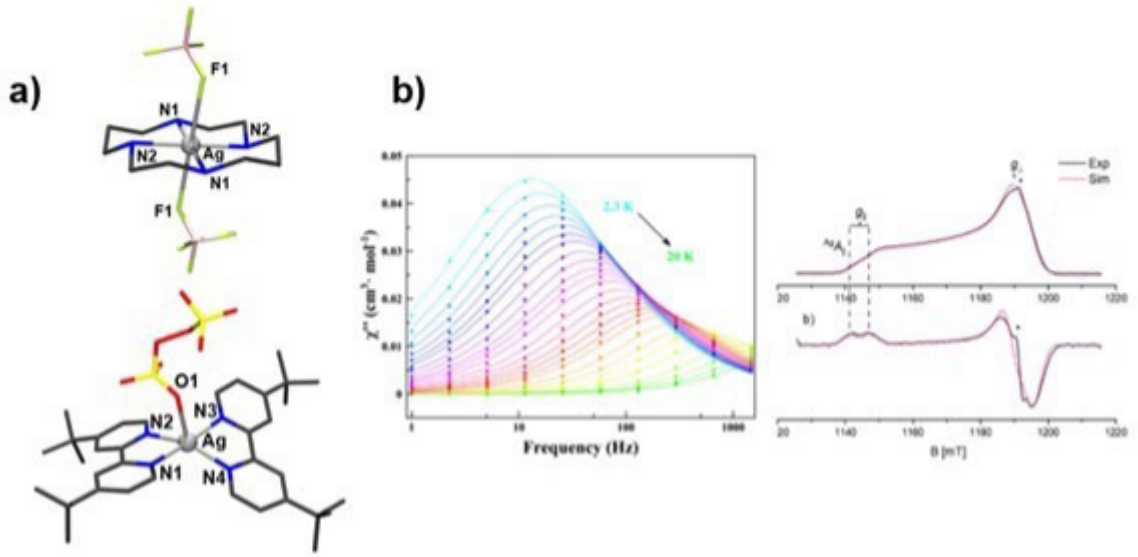

Figure 1. a) Example of the studied Ag(II) coordination complexes. b) Left, example of the frequency dependence of the out-of-phase susceptibility as a function of the temperature of the studied compounds. Right, example of the CW-EPR spectrum (bottom) and the ESE detected EPR spectrum (top) of the studied compounds.

REFERENCES
[1] M. Atzori, R. Sessoli, J. Am. Chem. Soc. 2019, 141, 11339-11352.
[2] T. Ishizaki, T. Ozeki, Dalton Trans 2023, 52, 4678-4683.
[3] L. Tesi, E. Lucaccini, I. Cimatti, et al. Chem. Sci. 2016, 7, 2074-2083.
[4] J. Serra, M. Font-Bardia, A. Escuer, J. Mayans Inorganic Chemistry. 2023, 62, 18804-18808.

P33
BIOCATALYSIS AND PHOTOTHERMAL EFFICIENCY USING SEMICONDUCTING NANOPARTICLES

J. Ruiz-Torres[1,*], C. Moya[1,2], A. Fraile Rodríguez[1,2], A. Labarta[1,2] and X. Batlle[1,2]

[1] Departament de Física de la Matèria Condensada, Martí i Franquès 1, 08028 Barcelona, Spain,
[2] Institut de Nanociència i Nanotecnologia, Universitat de Barcelona, 08028 Barcelona, Spain
*e-mail of presenting author: jruiz-torres@ub.edu

Bismuth sulfide (Bi_2S_3) nanoparticles have attracted significant interest due to their unique electronic properties, which are highly sensitive to morphological and compositional changes. As an n-type semiconductor with a direct bandgap of 1.3 eV in the near-infrared (NIR) region, Bi_2S_3 is suitable for various applications, including thermal ablation, water remediation and photocatalysis [1]. They can act as a photothermal agent in photothermal therapy (PTT) by increasing its temperature while absorbing NIR light [2], and they can absorb light in the visible range to act as photocatalysts to decompose waste water products [3]. However, while the former benefits from defects in the crystalline structure to enhance non-radiative recombination to produce heat, these defects are detrimental to the latter, since the excited charge carriers recombine instead of reaching the surface to react with the adsorbed target. Therefore, a nanosystem that can be effective in these two seemingly opposing applications is of great interest from both fundamental and practical perspectives. In this work, we synthesized stoichiometric Bi_2S_3 nanorods using a previously reported method [4]. For photocatalysis, powder samples in conjunction with methylene blue (MB), due to the characteristic absorbance peaks of that standard dye, were illuminated with a visible light lamp, finding that adding H_2O_2 to a Bi_2S_3+MB solution degrades MB up to 73%, while no degradation occurs without H_2O_2. For photothermal ablation performance, samples were transferred from an organic solvent to water by coating them using dimercaptosuccinic acid (DMSA) through a ligand exchange process. Samples show good stability in water, with DLS measurements showing average diameters below 200 nm, low polydispersity, and a negative ζ-potential. These samples were irradiated with an 808 nm laser to study their photothermal efficiency, with a promising temperature increase of about 20°C.

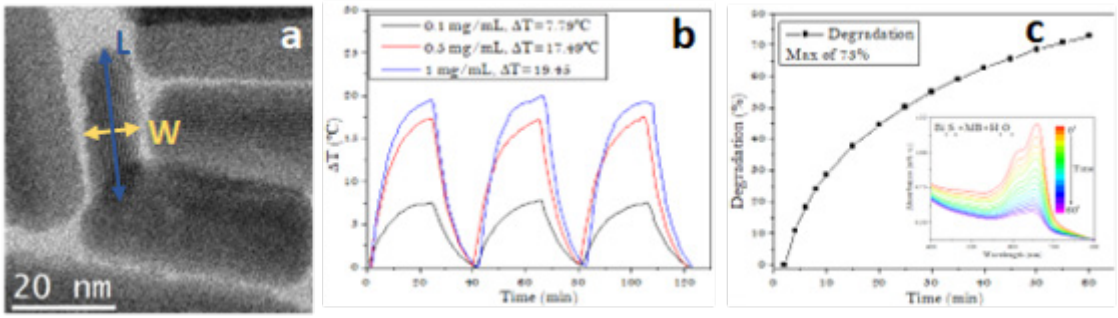

Figure 1. a) HRTEM image of Bi_2S_3 nanorods; b) Three cycles of photothermal efficiency measurements of Bi_2S_3@DMSA with increasing Bi concentration: 0.1 (black), 0.5 (red), and 1mg/mL (blue); and c) Methylene blue degradatoin measured as the percentage decrease of the characteristic 664 nm absorbance peak using powdered Bi_2S_3 photocatalyst in the presence of H_2O_2, at pH7

REFERENCES
[1] Ajiboye, T. O.; Onwudiwe, D. C. Results in Chemistry, 3, 100151 (2021), [2] Cheng, Y, et. al., Angew. Chem. Int. Ed., 57, 246 –251 (2018), [3] Devee D, R. Et. Al., Chem. Phy. Imp., 8, 100605 (2024), [4] Escoda-Torroella, M., et. al., Phys. Chem. Chem. Phys., 25, 3900-3911 (2023).

P34
DEEP LEARNING FOR MAGNETITZATION DYNAMICS

J. Buch-Palasi[1] , J. M. Hernàndez[1,2], M. V. Constache[1,2]

[1] Departament de de Física de la Matèria Condensada, Universitat de Barcelona
[2] Institut de Nanociència i Nanotecnologia (IN²UB)
* jbuchpal22@alumnes.ub.edu

Building block of magnetic memories and sensors are magnetic thin films materials. To calculate the magnetization dynamics of thin magnetic film, the Landau-Lifshitz-Gilbert (LLG) equation is solved numerically. The typical way for solving LLG equations is to first discretize it in space by finite elements or finite differences and than to solve numerically the resulting system in time, and requires a considerable computational effort. To ease this process, by reducing the computational load or assisting in characterizing field measurements, machine learning can be of utility also in the field of magnetism [1-3].

In this work, two deep convolutional neural networks with different dimensionalities (Figure 1) are employed to model ferromagnetic resonance in magnetic thin films. The training data were generated through time integration of the Landau-Lifshitz-Gilbert (LLG) equation and processed through the networks in a supervised learning framework. The models enable the estimation of key ferromagnetic parameters — such as the damping constant, saturation magnetization, inhomogeneous linewidth and anisotropic field — without relying on conventional methods like Kittel or Gilbert fitting.

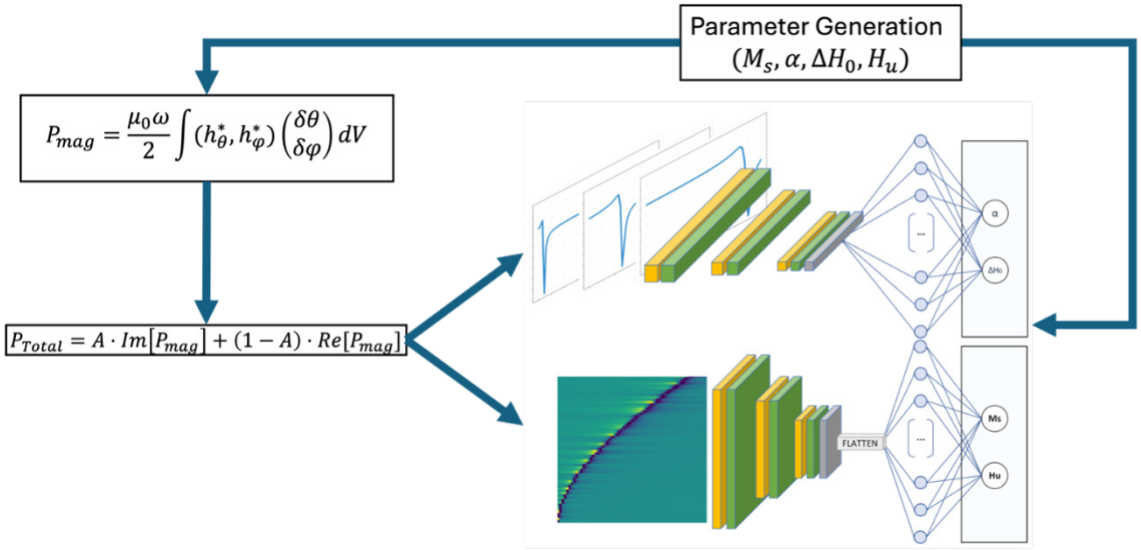

REFERENCES
[1] A. Kovacs et al., J. Magn. Magn. Mater. 491, 165548 (2019)
[2] S. Pollok et al., "Magnetic Field Prediction Using Generative Adversarial Networks" (2022).
[3] S. Pollok, and R. Bjørk, Europhysics News (2022).

P35
HOW LIGAND SURROUNDINGS AFFECT THE COHERENCE OF AN ELECTRON SPIN QUBIT

J. Serrano-Guarinos[1,2,*], Y. Neylubina[3], O. Roubeau[4,5], F. Luis[4,5], D. Aguilà[1,2], G. Aromí[1,2]

[1] Departament de Química Inorgànica i Orgánica, Universitat de Barcelona, Barcelona, Spain.
[2] Institute of Nanoscience and Nanotechnology of the University of Barcelona (IN²UB), Barcelona, Spain
[3] Nesmeyanov Institute of Organoelement Compounds, Russian Academy of Sciences, Moscow, Russia.
[4] Instituto de Ciencia de Materiales de Aragón (ICMA), CSIC, Universidad de Zaragoza, Zaragoza, Spain
[5] Departamento de Física de la Materia Condensada, Universidad de Zaragoza, Zaragoza, Spain
* jose.serranog@ub.edu

Lanthanide(III) ions have been proposed as carriers for electronic spin qubits since last decade. [] It has already been shown that the heterometallic [ErCeEr] trinuclear coordination compound is a promising platform to implement the three-qubit quantum error correction code protecting against pure dephasing.[1] Apart from their promising use as qugates, different [LnLn'Ln] compounds serve as platforms to research unique phenomena arising from the combination of different lanthanides in the same molecule.[2,3]

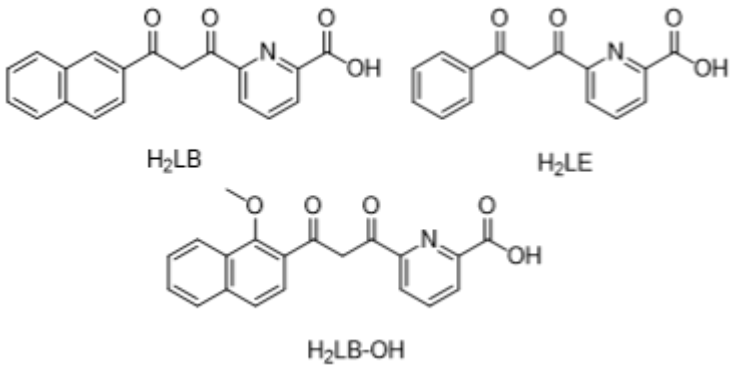

Figure 1. Variations on the asymmetric chelating ligand.
A new methodology to prepare [LnLn'Ln] compounds has been achieved, improving yields and crystallization times by several orders of magnitude. The flexibility of the ligand platform has been studied by changing the pi-stacking unit of the asymmetric ligand, resulting in 2 variations from the original complex that share the same general architecture.

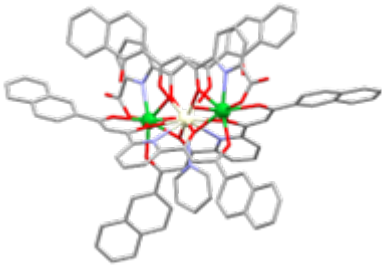

Figure 2. Single crystal XRD structure of [CeLu2(LA)2(LB-OH)2(py)(H2O)](NO3).
Using [LuCeLu] as a platform, we investigate how ligand environment affects the phase coherence of a Ce (S = 1/2) electron spin qubit by solution CW and pulsed EPR techniques.

REFERENCES
[1] E. Macaluso, M. Rubín, D. Aguilà, A. Chiesa, L. A. Barrios, J. I. Martínez, P. J. Alonso, O. Roubeau, F. Luis, G. Aromí, S. Carretta, Chem. Sci. 2020, 11, 10337.
[2] D. Maniaki, A. Sickinger, L. A. Barrios Moreno, D. Aguilà, O. Roubeau, N. S. Settineri, Y. Guyot, F. Riobé, O. Maury, L. A. Galán, G. Aromí, Inorg. Chem. 2023, 62, 3106.
[3] D. Maniaki, A. Sickinger, L. A. Barrios, D. Aguilà, O. Roubeau, Y. Guyot, F. Riobé, O. Maury, L. A. Galán, G. Aromí, Chem. Sci. 2024, 15, 18295.

P36
TUNABLE FUNCTIONALIZATION OF HOST-GUEST SUPRAMOLECULAR ASSEMBLIES VIA SELECTIVE METAL ION EMPLOYMENT

K. Sotirakopoulos[1], L. Barrios[1], G. Aromi[1], V. Novikov[1], O. Rubeau[2]
[1] Departament de Química Inorgànica i Orgànica and IN²UB, Universitat de Barcelona, Diagonal 645, 08028 Barcelona, Spain.
[2] Instituto de Nanociencia y Materiales de Aragón (INMA), CSIC and Universidad de Zaragoza, Plaza San Francisco s/n, 50009 Zaragoza, Spain.
* **ksotirakopoulos@ub.edu**

Dinuclear triple-stranded metallohelicates comprise versatile scaffolds for the synthesis of molecular nanoscale materials with technological applications and tunable functionalization through the encapsulation of different coordination complexes. For instance, the various guests that have been encapsulated in $[Fe^{II}_2L_3]$ helicates can greatly affect the Spin-Transition Temperature for each of the FeII ions [1, 2], while the [CrIII(ox)3]3- complex exhibits an unprecedented Single-Ion Magnet behavior upon its encapsulation [3]. Moreover, the electronic density of the various guests that have been encapsulated in $[Co^{II}_2L_3]$ helicates affects the relaxation rates of their magnetization through Spin-Orbit Coupling (SOC) [4]. In this work, we report the synthesis and characterization of the complexes: $[Al(anilate)_3]@[Fe_2L_3](BF_4)$ (1), $[Al(anilate)3]@[Zn_2L_3](BF_4)$ (2), $[Fe(ClCNAn)_3]@[Ni_2L_3](BF_4)$ (3), $[Cr(ClCNAn)_3]@[Ni_2L_3](BF_4)$ (4), $[Fe(ClCNAn)_3]@[Co_2L_3]Cl$ (5), $[Al(ClCNAn)_3]@[Co_2L_3]Cl$ (6), $[Fe(ClCNAn)_3]@[Zn_2L_3](BF_4)$ (7) and $[Al(ClCNAn)_3]@[Zn_2L_3](BF_4)$ (8). Complexes (1) and (2) constitute the diamagnetic analogues of the published $[Fe(anilate)_3]@[Fe_2L_3](BF_4)$ structure, either regarding the encapsulated guest or the full helicate respectively. In the cases of (3) and (4), the use of the asymmetric $ClCNAn^{2-}$ ligand can potentially lead to 2-qubit systems comprised by inequivalent and individually addressable qubits. Moreover, the encapsulation of the electron-rich $[M(ClCNAn)_3]^{3-}$ ($M = Fe^{III}$, Al^{III}) complex in (5) and (6) could lead to the enchancment of SOC and therefore improve the relaxation rates. Meanwhile, complexes (7) and (8) are structurally similar to (1) and (2) with the only notable difference between them being that their guests bear the $ClCNAn^{2-}$ instead of the $(anilate)^{2-}$ ligand. Finally, the luminescent properties of the $ClCNAn^{2-}$ ligand could lead to multifunctional materials which are sensitive to external stimuli.

REFERENCES
[1] L. A. Barrios, R. Diego, M. Darawsheh, J. Martinez, O. Roubeau, G. Aromi, Chem. Commun. 2022, 58, 5375–5378.
[2] L. A. Barrios, S. J. Teat, O. Roubeau, G. Aromi, Chem. Commun. 2023, 59, 10628–10631.
[3] M. Darawsheh, L. A. Barrios, O. Roubeau, S. J. Teat, G. Aromi, Angew. Chem. Int. Ed. 2018, 57, 13509 –13513.
[4] L. A. Barrios, N. Capo, H. Boulehjour, D. Reta, I. Tejedor, O. Roubeau, G. Aromi Dalton Trans., 2024, 53, 7611-7618.

P37
CHIROPTICAL RESPONSE THROUGH MULTIPOLAR PLASMONIC MODES IN TWISTED TRISKELION STACKS

Rodríguez-Álvarez, J.[1,2,*], Vila-Comamala, J.3, **Mora-Blanco, D.**[1,2], García-Martín, A.[4], Guerrero, A.[5], Borrisé, X.[6], Pérez-Murano, F.[5], David, C.[3], Blanco, A.[7], Pecharromán, C.[7], Batlle, X.[1,2], Fraile Rodríguez, A. [1,2], and Labarta, A.[1,2]

[1] Departament de Física de la Matèria Condensada, Universitat de Barcelona, 08028 Barcelona, Spain
[2] Institut de Nanociència i Nanotecnologia (IN²UB), Barcelona, 08028, Spain
[3] Paul Scherrer Institute, Forschungsstrasse MMM, Villigen 5232, Switzerland.
[4] Instituto de Micro y Nanotecnología IMN-CNM, CSIC, CEI UAM+CSIC, Isaac Newton 8, E28760 Tres Cantos, Madrid, Spain
[5] Institut de Microelectronica de Barcelona (IMB-CNM, CSIC), Bellaterra, 08193, Spain
[6] Catalan Institute of Nanoscience and Nanotechnology (ICN2), CSIC and BIST, Campus UAB, Bellaterra, 08193 Barcelona, Spain.
[7] Instituto de Ciencia de Materiales de Madrid (ICMM), CSIC, Calle Sor Juana Inés de la Cruz 3, Madrid, E28049 Spain
* **dmorabla16@alumnes.ub.edu**

We present a systematic investigation of the optical response to circularly polarized illumination in twisted stacked plasmonic nanostructures, based on previous work by our group [1]. The system consists in two identical, parallel gold triskelia, centrally aligned and rotated at a certain angle relative to each other, as shown in Fig. 1. Sample fabrication was accomplished through a novel multilevel high-resolution electron beam lithography. This stack holds two plasmonic modes of multipolar character in the near-infrared range, showing a strong dependence of their excitation intensities on the handedness of the circularly polarized incident light. This translates into a large circular dichroism which can be modulated by adjusting the twist angle of the stack. Fourier-transform infrared (FTIR) spectroscopy and numerical simulations were employed to characterize the spectral features of the modes. Remarkably, in contrast to previous results in other stacked nanostructures, the system's response exhibits a behavior analogous to that of two interacting dipoles only at small angles. The complexity of those resonances and their nature is studied as the twist angle changes. Finally, simulations for a triangular array of such stacked elements show a sharp mode arising from the hybridization of a surface lattice resonance with the low-energy mode of the stack. This hybridized mode demonstrates the capability to be selectively switched on and off through the light polarization handedness.

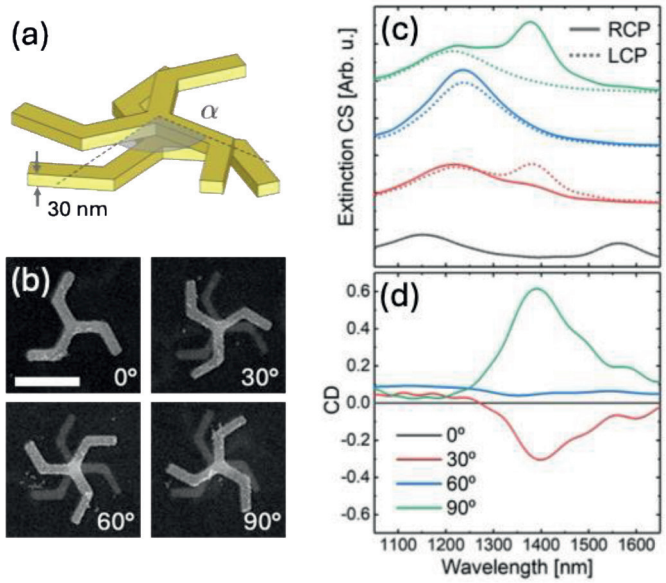

Figure 1. (a) Schematic depiction of the stack indicating the twist angle α. The vertical separation between layers is 20 nm. (b) SEM top-view images of selected fabricated nanostructures. Scale bar is 400 nm. (c) and (d) present the extinction and circular dichroism spectra of the system.

REFERENCES
[1] Rodríguez-Álvarez, J., et al., Scientific reports, 2022, 12, 1-10.
[2] Rodríguez-Álvarez, J., et al., Nanophotonics, 2025, Under Revision

P38
MOLECULAR FLEXIBILITY-DRIVEN SPIN-CROSSOVER MODULATION IN A SINGLE-CRYSTAL FE(II) COMPLEX

R. Díaz-Torres[1,2], O. Martínez[1], O. Roubeau[3], G. Aromí[1,2], D. Aguilà[1,2]

[1] Departament de Química Inorgànica i Orgànica, Universitat de Barcelona, Spain
[2] Institute of Nanoscience and Nanotechnology, University of Barcelona (IN²UB), Spain
[3] Instituto de Ciencia de Materiales de Aragón (ICMA), CSIC and Universidad de Zaragoza, Zaragoza, Spain
* rauldiaz@ub.edu

Spin-crossover (SCO) phenomena in coordination complexes represent a significant area of research due to their potential applications in molecular devices and sensors. These phenomena, influenced by external stimuli such as temperature, pressure, and light, depend on various factors such as the nature of the metal center, the type of ligands, the crystal field strength, or the solvent molecules in the crystal lattice. Studies employing Single-Crystal to Single-Crystal (SC to SC) transformations are essential in understanding the structural aspects and dynamic behavior of spin-crossover complexes. Unfortunately, such studies are relatively scarce due to challenges in obtaining high-quality single crystals suitable for SC to SC experiments.

In this study, a SC to SC investigation of the temperature-dependent behavior of the compound $[Fe(H_2L)_2(NCS)_2]\cdot DCM$ (H_2L = 2-(3-(pyridin-2-yl)-1H-pyrazol-5-yl)phenol, DCM = dichloromethane) is conducted. Initially, the solvated form $[Fe(H_2L)_2(NCS)_2]\cdot DCM$ (1), exhibits a HS state at low temperatures. Upon heating and subsequent solvent removal, denoted as $[Fe(H_2L)_2(NCS)_2]$ (1ds), the complex undergoes SCO. Notably, this SCO is characterized by a remarkable volumetric change of 20 % as evidenced by distinctly shortened Fe-N bond distances (d_{av}Fe-N = 1.85 Å). Interestingly, as the temperature rises further, complex 1ds undergoes a structural transformation wherein one of the NCS anions is uncoordinated and replaced by a water molecule, $[Fe(H_2L)_2(NCS)(H_2O)]NCS$ (1').

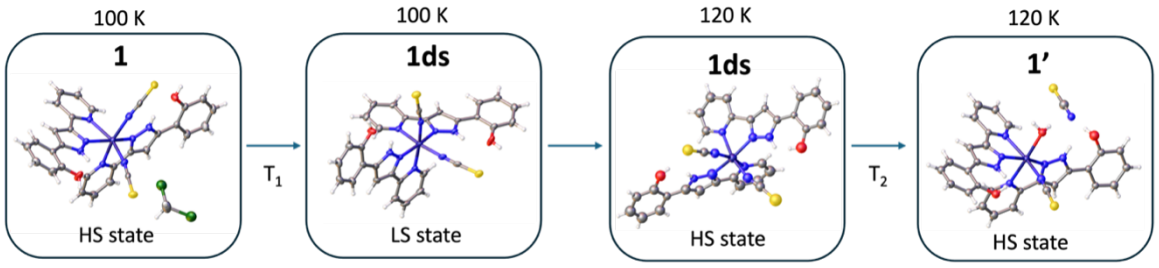

Figure 1. Structures of 1, 1ds (100K and 120K) and 1'.

REFERENCES
[1] X.-Q. Chen, Y.-D. Cai, Y.-S. Ye, M.-L. Tong, X. Bao, Inorg. Chem. Front., 2019, 6, 2194. [2] S. Xue, Y. Guo, Y. Garcia, CrystEngComm, 2021, 23, 7899.

P39
ELECTRIC CONTROL OF SWITCHING FIELDS IN FM THIN FILMS USING SURFACE ACOUSTIC WAVES

Quim Badosa[1], Marc Rovirola[1,2], Anna Castellví Picanyol[1], Júlia Òdena[1], Joan Manel Hernàndez[1,2], Alberto Hernández-Mínguez[4], Blai Casals[2,3] and Ferran Macià[1]

[1] Dept. of Condensed Matter Physics, University of Barcelona, 08028 Barcelona, Spain
[2] Institut of Nanoscience and Nanotechnology (IN²UB), University of Barcelona, 8020 Barcelona, Spain
[3] Departament de Física Aplicada, Facultat de Física, Universitat de Barcelona, 08028 Barcelona, Spain
[4] Paul-Drude-Institut für Festkörperelektronik, Leibniz-Institut im Forschungsverbund Berlin e.V., 10117 Berlin, Germany
* **quimbadosa@ub.edu**

Surface acoustic waves (SAWs) provide a dynamic and energy-efficient means to control magnetization in ferromagnetic thin films through the magnetoelastic effect. By inducing periodic and time varying strain, SAWs can modulate magnetic properties in materials without the need for external magnetic fields. Recent studies have demonstrated SAW-driven magnetization effects in magnetostrictive materials including precessional magnetization switching [1], SAW-activated magnetic domain motion [2] and large angle magnetoacoustic waves [3]. However, a comprehensive understanding of their impact on coercive field reduction remains incomplete.

Here, we explore the influence of SAWs on the switching process of different ferromagnetic systems (Nickel and Cobalt), revealing a significant reduction in the coercive field, reaching up to 75% for certain conditions. This effect was attributed to the strain-induced modulation of magnetic anisotropy, which causes both precessional switching of the magnetic moment and variations in domain wall propagation. To disentangle these effects, we performed experiments on ferromagnetic samples deposited on the acoustic path of a SAW channel (see Figure (a)) and measured simultaneously the magnetoresistance, as a measure of the overall magnetic moment, and the MOKE as an indicator of the magnetic domain configuration. We repeated experiments in samples with different geometries to determine the contribution of both domain wall propagation and magnetic oscillations. In this contribution we present results obtained in Nickel and Cobalt thin films by varying both frequency, angle and amplitude of the applied SAWs. Our findings highlight the potential of SAW-assisted magnetization control for low-power spintronic applications and tunable magnetic devices.

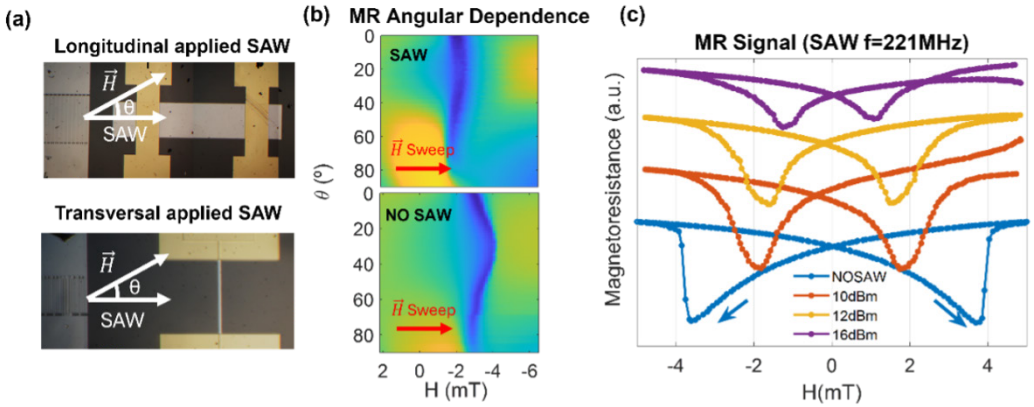

(a) Microscopic image of IDTs, FM material and Au contacts for longitudinal resistance (top) and transversal resistance (bottom) of the sample with respect to the applied SAW. The transversal configuration is made with a FM path smaller than the used SAW wavelength. (b) Angular dependence of the magnetoresistance (MR) signal when a sweep of the magnetic field is carried out from 2 to -6 mT and the angle between the SAW and the magnetic field is rotated from 0o to 90o. Comparison between MR signal when 221MHz-16dBm SAW is applied (top) and without SAW (bottom). (c) MR signal obtained with and without SAW for different amplitudes and same frequency at θ ≈ 45o. Starting at 6mT, arrows indicate the direction of the signal over time.

REFERENCES
[1] Precessional Magnetization Switching by a Surface Acoustic Wave. Phys. Rev. B 93, 134430 (2016)
[2] Generation and Imaging of Magnetoacoustic Waves over Millimeter Distances. Phys. Rev. Lett. 124, 137202 (2020)
[3] Surface acoustic wave effect on magnetic domain wall dynamics. Phys. Rev. B 108, 104420 (2023)

P40
STUDY OF THE SPIN DYNAMICS OF A NEW FAMILY OF SCHIFF BASE HETEROMETALLIC MN(V)-4F COMPLEXES

S. Caballero[1,*], J. Mayans[1], A. Escuer[1]

[1] Departament de Química Inorgànica i Orgànica, Institue of Nanoscience and Nanotechnology, Universitat de Barcelona, Barcelona, 08028, Spain
* scaballerogutierrez@ub.edu

Paramagnetic coordination complexes have been extensively explored for various technological applications, including magnetic memory devices, quantum computing, and spintronics [1]. Magnetic molecular complexes exhibiting slow relaxation of magnetization have emerged as promising candidates for such applications. This is due to the remarkable versatility of coordination chemistry, which allows for the use of diverse ligands and metal cations from either or both the d- and f-block elements [2, 3]. While numerous examples of dinuclear 3d-4f complexes can be found in the literature, no studies on the spin dynamics of Mn(V)-Ln(III) complexes have been reported to date, despite the fact that the Mn(V) cation is relatively common, as it is sometimes used in nitrogen transfer catalytic reactions [4]. Following this premise, a series of novel 3d-4f Schiff base coordination complexes, in which the 3d metal is a high-valent Mn(V) cation stabilized by a nitride ligand, have been synthesized and its crystal structure obtained by single crystal X-Ray diffraction. They have also been magnetically characterized via SQUID magnetometry and continuous wave EPR spectroscopy. The results show that some of them exhibit slow relaxation of magnetization.

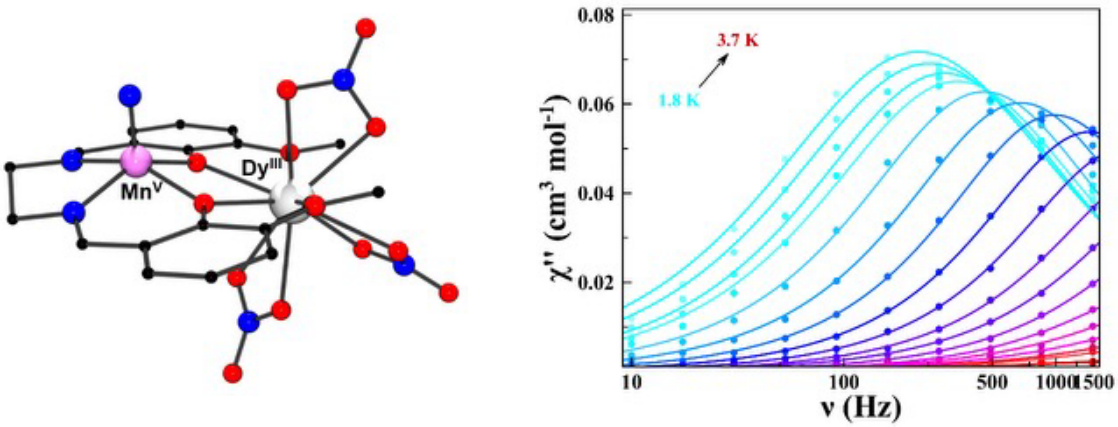

Fig. 1: Crystal structure of the Mn(V)-Dy(III) complex (left). Out-of-phase magnetic susceptibility vs frequency (right) of the Mn(V)-Ce(III) complex. Solid lines represent the best-fit.

REFERENCES
[1] G. Aromí, D. Aguilà, P. Gàmez et al. Chem. Soc. Rev. 2012, 41, 537-546,
[2] M. Atzori, E. Garlatti, G. Allodi et al. Inorganic Chemistry, 2021, 60, 11273-11286,
[3] R. Hussain, G. Allodi, A. Chiesa et al. J. Am. Chem. Soc. 2018, 140, 9814-9818,
[4] N. Svenstrup, A. Bogevig, R. Hazell, K. Jorgensen, J. Chem. Soc. Perkin Trans., 1999, 11, 1559-1566

NanoPhotoElectro

P41
DEVELOPMENT OF ZIF-8 THIN FILM SENSORS FOR THE DETECTION OF VOLATILE ORGANIC COMPUNDS

Sergi González-Martínez[1,2,3], Anna Estany-Macià[1,2], Guillem Domènech-Gil1,[2,*], Ignasi Fort-Grandas[1,2,3], Albert Romano-Rodriguez[1,2], Daniel Sainz-García[2,3], Mauricio Moreno-Sereno[1,2]

[1] Dept Electronic and Biomedical Engineering, Universitat de Barcelona, Barcelona, Spain.
[2] Institute of Nanoscience and Nanotechnology (IN²UB), Universitat de Barcelona, Barcelona, Spain.
[3] Dept Inorganic and Organic Chemistry, Universitat de Barcelona, Barcelona, Spain.
* Present address: Dept Thematic Studies and Environmental Change, TEMA M, Linköping Universitet, Linköping, Sweden. Email: **sergigonzalez@ub.edu**

Volatile organic compunds such as ethanol, acetaldehyde, and formaldehyde in their gaseous forms present significant health and environmental problems. Ethanol, despite it is much less harmful, it is highly flammable and can be dangerous in high concentrations. In contrast, acetaldehyde and formaldehyde are toxic and, especifically, acetaldehyde is generated from the combustion processes. Formaldehyde is the most hazardous and is carcinogenic. Even at low concentrations, formaldehyde exposure can lead to respiratory issues. Given their safety issues, there is a clear necessity for detection systems that are not only highly sensitive and selective, but also energy-efficient. In this regard, the present study concerns the gas detection system development based on metal-organic frameworks (MOFs) due to their unique characteristics.

A particular subclass of MOFs, known as zeolitic imidazolate frameworks (ZIFs), is composed of zinc ions and imidazole-based ligands.[1] ZIFs are explored for various applications such as gas storage, [2] separation, [3] catalysis, [4] and chemical sensing, [5] because of their uniformly sized micropores and excellent structural stability. Among them, ZIF-8 stands out as one of the most extensively studied types. It consists of zinc and 2-methylimidazole (Hmim). While ZIF-8 has commonly been applied in powder form for sorption and catalysis, it also shows promise as a gas sensor when it is deposited as a thin film on a substrate. In this case, its refractive index changes upon gas adsorption, making it suitable for optical sensing techniques [6].

In this work, various synthesis conditions were explored to coat silica substrates with ZIF-8 for their use to detect low concentrations ethanol, acetaldehyde, and formaldehyde diluted in air. The obtained materials were characterized using Powder X-ray Diffraction (Figure 1), Scanning Electron Microscopy (Figure 2), and profilometry to assess their structure, morphology, and film thickness. The change of the optical parameters of these materials when exposed to these fases will be reported and will be discussed as function of the synthesis conditions.

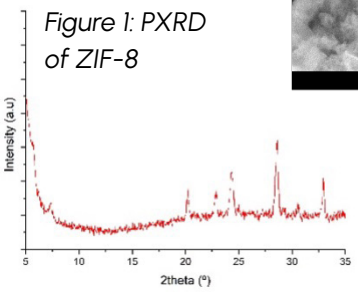

Figure 1: PXRD of ZIF-8

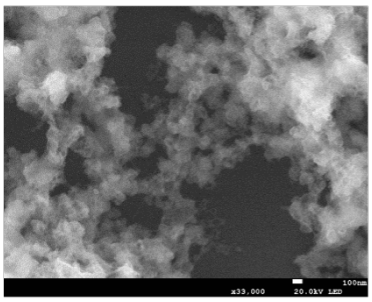

Figure 2: SEM image at 100nm of ZIF-8

REFERENCES
[1] A. Phan, C. J. Doonan, F. J. Uribe-Romo, C. B. Knobler, M. O'keeffe, O. M. Yaghi, Acc. Chem. Res., 2010, 43, 58–67 [2] L. J. Murray, M. Dincâ, J. R. Long, Chem. Soc. Rev., 2009, 38, 1294–1314. [3] M. C. McCarthy, V. Varela-Guerrero, G. V. Barnett, H. K. Jeong, Langmuir, 2010, 26, 14636–14641. [4] H. L. Jiang, B. Liu, T. Akita, M. Haruta, H. Sakurai, Q. Xu, J. Am. Chem. Soc., 2009, 131, 11302–11303. [5] G. Lu, J. T. Hupp, J. Am. Chem. Soc., 2010, 132, 7832-7833. [6] A. E. Macià, I. F. Grandas, N. Joshi, W. E. Svendsen, M. Dimaki, A. R. Rodríguez, M. M. Sereno, Sensors, 2024, 12, 4381.

P42
INKJET-PRINTED $CSCU_2I_3$ PEROVSKITE PHOTODETECTORS: SYNTHESIS, OPTICAL CHARACTERIZATION AND DEVICE PERFORMANCE

J.D. Forero[1,2*], J. Khan1,[2], K. Lobo[1,2], J. Marí-Guaita1,[2], G. Vescio[1,2], F. Palacio[1,2], B. Garrido[1,2], S. Hernandez[1,2], A. Cirera[1,2]

[1] MIND, Department of Electronics and Biomedical Engineering, Universitat de Barcelona, Martí i Franquès 1, E-08028, Barcelona, Spain.

[2] Institute of Nanoscience and Nanotechnology (IN²UB), Universitat de Barcelona, Av. Joan XXIII S/N, E-08028, Barcelona, Spain.

*e-mail: **jdiagofo@ub.edu**

Lead-free halide perovskites have attracted a lot of attention due to the need for effective and sustainable optoelectronic materials. Because of its exceptional optoelectronic qualities, high stability, and non-toxic makeup, $CsCu_2I_3$, a one-dimensional copper-based halide perovskite, has become one of these promising materials. Because of its extensive absorption in the ultraviolet (UV) spectrum and excellent quantum confinement, $CsCu_2I_3$ is a good candidate for use in photodetectors. Its self-trapped exciton (STE) emission mechanism guarantees a significant Stokes shift, which is essential for UV detection, and a high photoluminescence quantum yield in the visible region. [1], [2] In this study, the inkjet printing technique was used to convert $CsCu_2I_3$ into thin films. CsI and CuI were dissolved in 0.5 M solution of dimethyl sulfoxide (DMSO) at a 1:2 molar ratio to create a stable precursor ink. To define our photoresistors, films were printed onto ozone-treated ITO-patterned glass substrates with interdigitated electrodes which presents 50 µm distance between interdigitates. whereas to determine the absorption edge and study the grain morphology, fused silica substrates were used, also applying an ozone treatment. To create consistent and high-quality films, a fixed drop-volume of 10 pl was ejected through a 21-µm diameter nozzle Dimatix cartridge in a Fujifilm Dimatix printer and the inkjet printing factors including drop spacing and platen temperature were adjusted. To improve the printed films' stability and crystallinity, they were vacuum-annealed at 100 °C for 30 minutes. Optical and electrical characteristics of the fabricated photoresistors were assessed. Absorbance measurements of the thin film showed an absorption edge, with wavelengths shorter than 325 nm being efficiently absorbed (see Fig. 1). Our photoresistors' notable UV photodetection capabilities were validated by electrical measurements, from which the responsivity was determined through the 275 – 600 nm wavelength range (see Fig. 2). These obtained results are in good agreement with the ones in literature in terms of tendency although the magnitude of them is lower. [2]

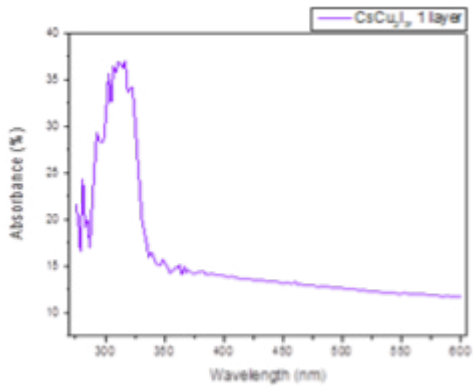

Figure 1. Absorbance-wavelenght spectra of $CsCu_2I_3$ thin film in a range from 275 to 600 nm

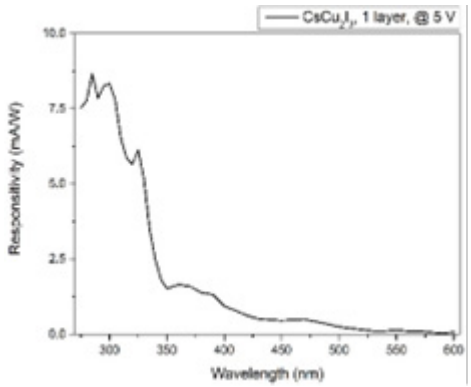

Figure 1. Responsivity-wavelenght graph of $CsCu_2I_3$ thin film in a range from 275 to 600 nm

REFERENCES

[1] B. Zhang et al., Front. Optoelectron. 14, 459-472 (2021) [2] Y. He et al., J. Appl. Phys. 135, 155301 (2024)

P43
NOVEL GAS SENSORS BASED ON (MGCONICUZN)O HIGH-ENTROPY OXIDE

Iván Vergés Gazulla[1], **Paolo Pellegrino**[2], Guillem Domenech Gil1,[2], Albert Romano Rodriguez[1]

[1] IN²UB i Departament d' Enginyeria Electrònica i Biomèdica, Universitat de Barcelona.
[2] Department of Thematic Studies and Environmental Change, TEMA M, Linköping Universitet, Sverige.
* email of the corresponding author: **pellegrino@ub.edu**

(MgCoNiCuZn)O has been synthesized since 2015 belonging to the so-called High Entropy Oxides. This new class of materials can present a stable single phase, despite the variety of crystalline structures of the individual binary oxides which are composing it. We are interested in exploring the performance of this material as a gas sensor. This multicomponent oxide is thought to behave as an improved gas sensor due to the large variety of sites at the surface for absorption of gas molecules and the strong thermal endurance at high temperatures and under extreme conditions such as resilience to harsh gas species.

MATERIAL AND METHODS

Starting from a homogenous mixing of the single oxide components in the form of nanopowders, the resulting mixture was annealed at 1000°C for several hours and then rapidly cooled to stabilize the material into the desired structure. X-ray diffraction confirmed its rock-salt crystal-line structure, allowing to discard the presence of secondary phases. Additionally, the lattice parameters are in quite good agreement with the ones reported in literature. Elemental mapping by Energy Dispersive X-Ray Spectroscopy confirms the homogeneous distribution of all the metallic components in the resulting powder, with an average grain size of few micrometers, while from optical transmission measurements we estimated a direct optical bandgap of 1.4 eV. The fabricated powder was dispersed onto an inter-digitated metallic pattern engraved on a silica slab, mounted on a TO8 support together with a micro-heater and a temperature sensor. The resulting sensor is shown in Figure 1.

RESULTS AND DISCUSSION

We explored the gas sensing behavior of the fabricated structures when exposed to humidity, CH4, and SO2, in a wide range of temperatures and gas concentrations. The temperature behavior of the device resistance and the rectifying characteristics of the electrical contacts point to the semiconducting character of the active synthetized material. The tracking of the relative response of the sensor as a function of temperature enables to single out the optimal operation temperature. A value of 140°C was attained, which corresponds to a maximum response of 60% towards a humidity pulse of 80%. A complete analysis of the interaction and recovery time allows to get insight on the detection mechanisms. The demonstration of the chemoresistive character of such novel material paves the way to further studies and applications in the field of the chemical resistive sensors.

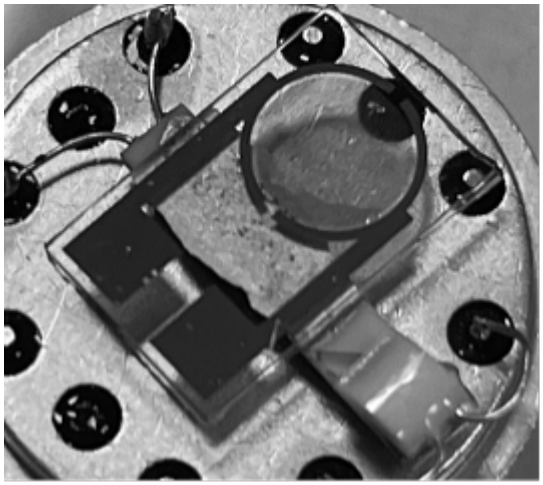

Figure 1. Picture of a fabricated gas sensor

P44
INFLUENCE OF PULSED CURRENT DRIVING ON THE LIFETIME AND EFFICIENCY OF $CsPbBr_3$-BASED PeLEDs

F. Palacio,[1,2] S. Hernández,[1,2] G. Vescio,[1,2] R. Sánchez,[3] I. Mora,[3] B. Garrido,[1,2] A. Cirera[1,2]

[1] MIND, Department of Electronics and Biomedical Engineering, Universitat de Barcelona, Martí i Franquès 1, E-08028, Barcelona, Spain
[2] Institute of Nanoscience and Nanotechnology (IN²UB), Universitat de Barcelona, Av. Diagonal 645, E-08028, Barcelona, Spain
[3] Institute of Advanced Materials (INAM), Universitat Jaume I, Av. de Vicent Sos Baynat, s/n, 12071 Castelló de la Plana, Spain
* email: **francisco.palacio@ub.edu**

Halide perovskite light-emitting diodes (PeLEDs), particularly those based on $CsPbBr_3$, have attracted significant interest due to their high efficiency and ease of fabrication. However, device stability remains a major barrier for practical applications. Recent studies have shown that using pulsed voltage excitation can mitigate degradation effects such as ion migration and interfacial charge accumulation, leading to extended operational lifetimes [1,2]. These approaches, however, rely on voltage modulation, which offers limited control over the total injected charge.

The aim of this work is to explore a current-controlled pulsed driving scheme as an alternative method to enhance stability and performance in PeLEDs. This strategy enables precise control of the injected charge and direct correlation with degradation dynamics. We evaluate the electro-optical behaviour of research-grade CsPbBr3-based LEDs under square-wave current excitation (0–0.2 mA), across frequencies ranging from 20 Hz to 100 kHz and duty cycles from 10% to 100%. Real-time monitoring of electrical and optical responses was carried out, including single-pulse analysis and current-voltage (I–V) characterization before and after stress.

Our results show that pulsed current driving at intermediate frequencies (1–5 kHz) improves a 30% (5 kHz) and 45% (1 kHz) device lifetime compared to continuous DC operation. After normalizing the t50 parameter (time to reach 50% of the initial emission intensity) to the total injected charge, these pulsed conditions outperform the DC reference, while low-frequency excitation (<100 Hz) leads to faster degradation. The I–V curves after ageing reveal minimal deterioration in contact quality, indicating robust operation. These findings highlight the potential of current-pulse engineering to optimize both the efficiency and reliability of CsPbBr3 PeLEDs, providing valuable insights for the design of more stable perovskite optoelectronic devices.

REFERENCES
[1] F. Zhang et al., Nat. Commun. 11, 4143 (2020).
[2] H. Xu et al., Adv. Mater. 35, 2300556 (2023).
[3] D. A. dos Santos et al., Phys. Rev. B 75 (2007) 075307.

P45
DEPTH SENSIBLE INSTRUMENT FOR MUELLER MATRIX IMAGING

I.Pardo[1,*], E. Pascual[1], O. Arteaga[1]
[1] PLAT group, Dep. Física Aplicada, IN²UB, Universitat de Barcelona
* iago.pardo@ub.edu

We introduce an optical imaging system that combines Spatial Frequency Domain Imaging (SFDI) with Mueller Matrix polarimetry to achieve depth-resolved, polarization-sensitive characterization of turbid media. This system enables the acquisition of Mueller matrices at multiple spatial frequencies, probing different optical depths within the sample.

Mueller Matrix imaging provides a comprehensive description of the polarization properties of light after interaction with a sample, encoding information on anisotropy, birefringence, depolarization, and structural orientation [1] . When combined with SFDI, which projects sinusoidal patterns of varying spatial frequencies onto the sample, it becomes possible to selectively modulate photon penetration depth [2]. Low spatial frequencies probe deeper layers due to broader photon diffusion, while high frequencies restrict the light–tissue interaction to more superficial structures.

This approach allows for the separation of polarization phenomena that may originate at different depths, revealing layered structures or subtle changes in tissue organization not detectable by conventional polarization imaging.

This method opens new possibilities in some fields such as biomedical optics, especially for non-invasive assessment of layered biological tissues such as skin, where birefringent and depolarizing behaviors can vary significantly with depth [3].

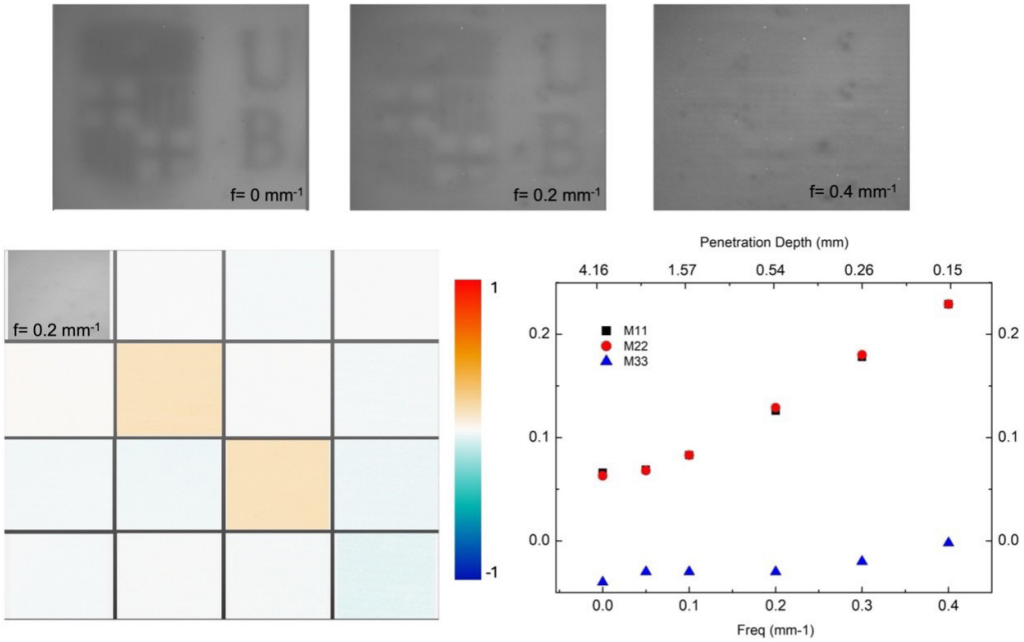

Figure 1. Measurement of a tissue-mimicking phantom using different spatial frequencies and analysis of Mueller Matrix elements as a function of penetration depth

REFERENCES
[1] Chipman, R. A., Lam, W. S. T., & Young, G. P. (2018). Polarized Light and Optical Systems. CRC Press.
[2] Cuccia, D. J., Bevilacqua, F., Durkin, A. J., & Tromberg, B. J. (2009). Quantitation and mapping of tissue optical properties using modulated imaging. Journal of Biomedical Optics, 14(2), 024012.
[3] Pierangelo, A., et al. (2012). Ex vivo characterization of human colon cancer by Mueller polarimetric imaging. Optics Express, 19(2), 1582–1593.

P46
EFFECT OF RELATIVE HUMIDITY AND TEMPERATURE ON THE CHEMORESISITIVE GAS SENSING OF $Ni_3(HHTP)_2$ MOF

I. Fort-Grandas,[1,2,3] G. Domènech-Gil,[1,2] P. Pellegrino,[1,2] M. Moreno-Sereno,[1,2] D. Sainz,[2,3] A. Vidal-Ferran,[3,4] and **A. Romano-Rodríguez**[1,2]

[1] Dept Electronic and Biomedical Engineering, Universitat de Barcelona (UB), 08028 Barcelona, Spain
[2] Inst Nanoscience Nanotechnology (IN²UB), Universitat de Barcelona (UB), 08028 Barcelona, Spain
[3] Dept Inorganic and Organic Chemistry, Universitat de Barcelona (UB), 08028 Barcelona, Spain
[4] Catalan Institute for Research and Advanced Studies (ICREA), 08010 Barcelona, Spain
* email of the corresponding author: **albert.romano@ub.edu**

Current monitoring systems of Greenhouse Gases (GHGs) are bulky and energetically expensive, thus being restricted to a few fixed locations. However, the need arises to develop gas sensing devices that could be placed in large numbers and many locations. For instance, by introducing gas sensors in autonomous data collection and transmission systems, data on specific target gas levels would be acquired, allowing the development of more precise climate change models via the Internet of things (IoT). To fulfil that purpose, the sensing devices must be designed to fit the following criteria: miniaturized, cost-effective, energy efficient and selective. Within the wide arrange of sensor types, room temperature chemiresistive devices stand out due to their low-energy consumption and miniaturized characteristics.

Metal-organic Frameworks (MOFs) show great promise as active materials for gas sensing devices. Their nanostructured, high surface area and high-porosity nature make them a fitting choice for gas related applications, and a subfamily of the MOFs present room-temperature conductivity values ideal for chemiresistive studies. There are various types of conductive MOFs depending on their conduction mechanisms. Amongst them, 2D MOFs with extended conjugation and though-plane conduction have been measured to be highly conductive.[1] More specifically, by the use of triphenylene derivative ligands, such as 2,3,6,7,10,11-hexahydroxytriphenylene (HHTP), electrically conductive MOFs have been obtained using coordination metals like Ni, Co, Cu or Zn. In this work, we study $Ni_3(HHTP)_2$ for the chemoresistive gas sensing of CH_4, CO_2 and NH_3 gases. We report the effect that both temperature and humidity have on the electrical conductivity properties of the material as well as their effect on the chemoresistive response of the MOF.

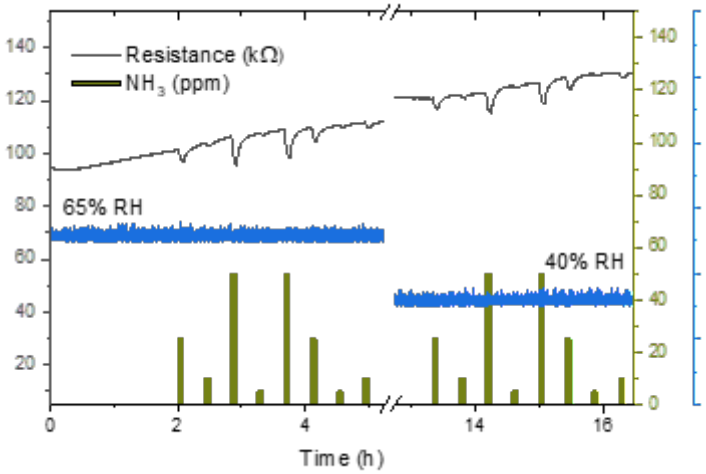

Figure 1 Resistance variation of $Ni_3(HHTP)_2$ MOF to NH_3 pulses at different relative humidity (RH) values

REFERENCES
[1] N. Contreras-Pereda, S. Pané, et al. Coordination Chemistry Reviews 2022, 460, 214459.

P47
FULL STOKES IMAGING USING WAVELENGTH-DEPENDENT RETARDATION IN A POLARIZATION CAMERA

Subiao Bian[1], and **Oriol Arteaga**[1,*]
[1] Dep. Física Aplicada, PLAT Group, IN²UB, Universitat de Barcelona, Barcelona 08028, Spain
Date: April 25, 2025
Corresponding Author: Oriol Arteaga,
* **oarteaga@ub.edu**

Polarization imaging plays a crucial role in numerous fields, such as remote sensing, imaging systems, and augmented reality, by providing additional information that is often not captured by conventional intensity-based cameras. However, achieving complete polarization information in real time remains a significant challenge [1]. This work introduces a novel method for achieving full polarization vision using a commercial polarization camera that only provides projection intensity from four linear polarization states (0°, 45°,90°, 135°). The proposed technique integrates a homogeneous dispersive retarder placed before a commercial color polarization sensor to leverage wavelength-dependent retardation, allowing the differentiation of polarization states across the sensor's color channels as schematically shown in Fig. 1.

The proposed technique incorporates a homogeneous dispersive retarder placed before the camera's color polarization sensor, leveraging wavelength-dependent retardation to differentiate polarization states across the sensor's color channels, as illustrated in Fig. 1. This modification enables the camera to access 12 distinct intensity channels corresponding to varying analyzing states, all captured in a single shot. These channels provide sufficient data to perform matrix inversion and calculate the complete Stokes vector in real time. In fact, from using only two color channels, the Stokes vector can be reconstructed. For these channels, the corresponding eight measured intensities can be expressed as:

$$\mathbf{I} = \begin{bmatrix} I^1_{0^\circ} \\ I^1_{90^\circ} \\ I^1_{45^\circ} \\ I^1_{135^\circ} \\ I^2_{0^\circ} \\ I^2_{90^\circ} \\ I^2_{45^\circ} \\ I^2_{135^\circ} \end{bmatrix} = \begin{bmatrix} 1 & C^2_{2\theta}+S^2_{2\theta}C_{\delta_1} & C_{2\theta}S_{2\theta}(1-C_{\delta_1}) & -S_{2\theta}S_{\delta_1} \\ 1 & -C^2_{2\theta}-S^2_{2\theta}C_{\delta_1} & -C_{2\theta}S_{2\theta}(1-C_{\delta_1}) & S_{2\theta}S_{\delta_1} \\ 1 & C_{2\theta}S_{2\theta}(1-C_{\delta_1}) & S^2_{2\theta}+C^2_{2\theta}C_{\delta_1} & C_{2\theta}S_{\delta_1} \\ 1 & -C_{2\theta}S_{2\theta}(1-C_{\delta_1}) & -S^2_{2\theta}-C^2_{2\theta}C_{\delta_1} & -C_{2\theta}S_{\delta_1} \\ 1 & C^2_{2\theta}+S^2_{2\theta}C_{\delta_2} & C_{2\theta}S_{2\theta}(1-C_{\delta_2}) & -S_{2\theta}S_{\delta_2} \\ 1 & -C^2_{2\theta}-S^2_{2\theta}C_{\delta_2} & -C_{2\theta}S_{2\theta}(1-C_{\delta_2}) & S_{2\theta}S_{\delta_2} \\ 1 & C_{2\theta}S_{2\theta}(1-C_{\delta_2}) & S^2_{2\theta}+C^2_{2\theta}C_{\delta_2} & C_{2\theta}S_{\delta_2} \\ 1 & -C_{2\theta}S_{2\theta}(1-C_{\delta_2}) & -S^2_{2\theta}-C^2_{2\theta}C_{\delta_2} & -C_{2\theta}S_{\delta_2} \end{bmatrix} \cdot \begin{bmatrix} S_0 \\ S_1 \\ S_2 \\ S_3 \end{bmatrix} = \mathbf{W}\mathbf{S}_{in}, \qquad (1)$$

where we have employed the short notation SX ≡ sin(X) and CX ≡ cos(X). θ is the azimuth angle of the retarder and δ_1 and δ_2 are its retardations for the two considered colors. The incoming Stokes vector, Sin, can be directly calculated by left multiplying the intensity vector I by the pseudo-inverse of W.

Assuming weak wavelength dependence of polarization for incoming light, this approach enables the real time, simultaneous measurement of the complete Stokes vector, which fully characterizes the polarization state of incident light. A real-time illustration of our system is presented in Fig. 2, which shows the measurement of the last Stokes parameter, S_3, while varying the stress applied to a glass microscope slide (BK7 glass) by pressing it with fingers. A laptop screen generating a horizontal linear polarization state serves as the background. In Fig. 2(a), the researchers' fingers are merely holding the glass in place with no pressure, and the S3 parameter of the polarized light passing through the glass matches that of the background. However, when pressure is applied to the edge of the glass slide, stress is immediately induced, leading to birefringence due to the photoelastic effect. Figures 2(b) and 2(c) clearly illustrate the distribution of the circular polarization component resulting from this stress-induced birefringence.

This method offers a simple, versatile, and practical solution to capture complete polarization information. Its significance lies in its potential for a wide range of applications, from improving remote sensing accuracy to enhancing visual systems in augmented reality, with implications for more precise environmental monitoring, material analysis, and visual rendering.

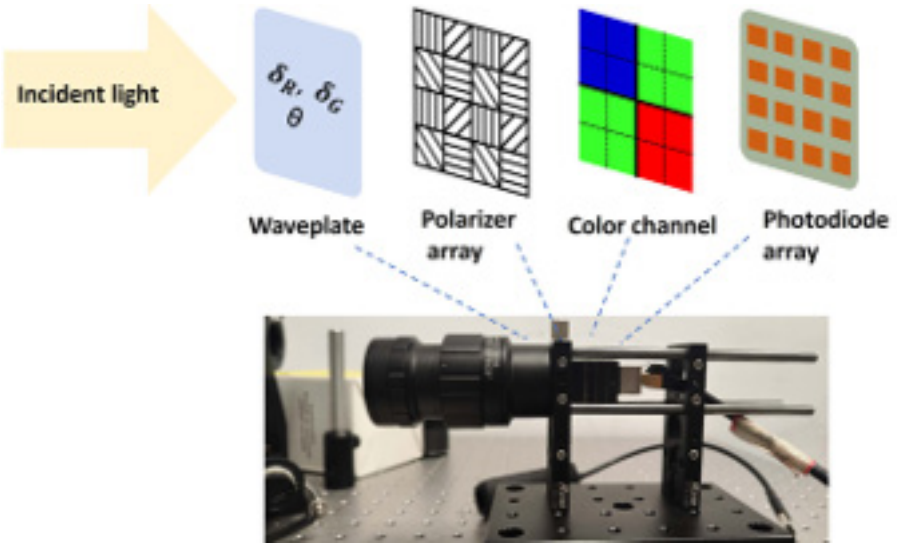

Figure 1. Photo of the full-Stokes polarization camera setup with objective lens

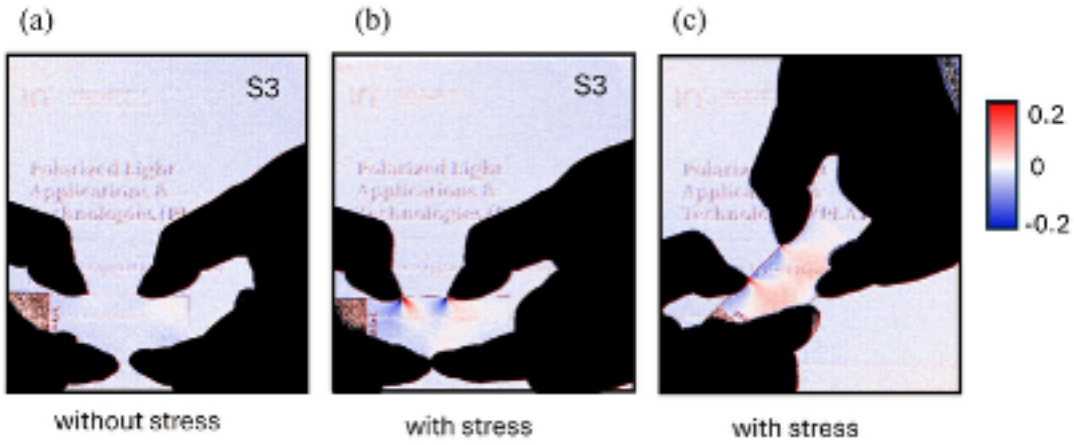

Figure 2. Different frames showing the S3 Stokes parameter imaging of a microscope glass substrate under finger applied pressure. The scale is adjusted to ±0.2, instead of the usual ±1, to enhance the visibility of the effect. The full Stokes video is available as supporting material

REFERENCES
[1] Rubin, N. A., D'Aversa, G., Chevalier, P., Shi, Z., Chen, W. T., Capasso, F. Matrix Fourier optics enables a compact full-Stokes polarization camera. Science, 365(6448) (2019).

NanosMat

P48
C-BRIDGED DIPHOSPHANES WITH A SUBSTITUTED BACKBONE

J. Eusamio[1,2,*], A. Grabulosa[1,2]
[1] Universitat de Barcelona, Departament de Química Inorgànica i Orgànica, Secció de Química Inorgànica
[2] Institut de Nanociència i Nanotecnologia de la Universitat de Barcelona (IN²UB)
* javier.eusamio@ub.edu

Methylene-bridged diphosphanes have demonstrated significant utility in homogeneous catalysis, exhibiting robust performance in both achiral and enantioselective applications. Furthermore, these ligands have been widely employed in coordination chemistry, with dppm serving as a prominent example.[1]
However, the substitution of the methylene bridge presents a notable synthetic challenge, with only a limited number of successful examples reported in the literature, each typically requiring elaborate synthetic methodologies. This represents a critical limitation, as the introduction of substituents at the bridge position could provide a powerful means to modulate the steric and electronic properties of diphosphanes.
To address this challenge, our research has focused on the development of novel diphosphane ligands tailored for applications in coordination chemistry and catalysis. Initial investigations explored fluorene-bridged diphosphanes, where variation of the phosphorus substituents led either to the formation of the intended diphosphane or, unexpectedly, to the isolation of the first structurally characterized phosphanyl-phosphorane.[2] Subsequently, we successfully incorporated a more constrained cyclopropyl bridge into a diphosphane framework, employing an unconventional vinylphosphine as a key synthetic precursor.[3,4]
In this work, we present the synthesis of these diphosphanes, their coordination behavior with rhodium(I) moieties to afford both 16- and 18-electron complexes, and preliminary results on catalysis.

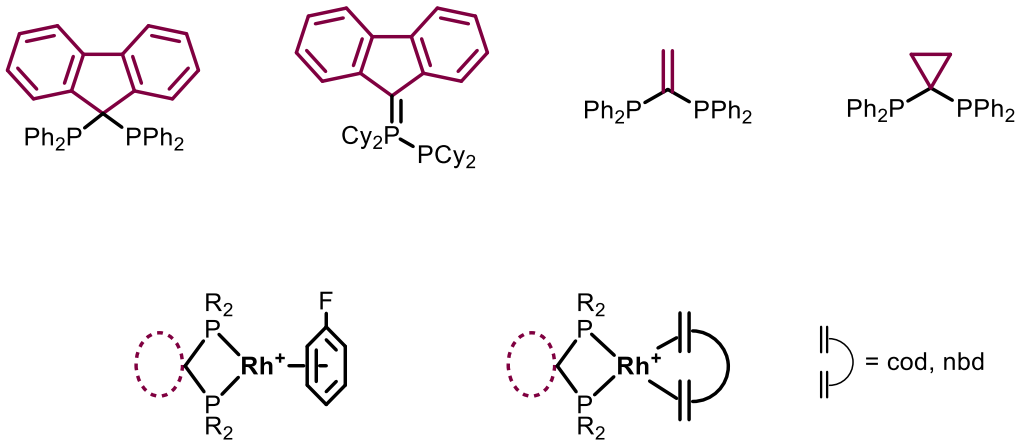

REFERENCES
[1] R. J. Newland, J. M. Lynam, S. M. Mansell, Chem. Commun. 2018, 54 (43), 5482-5485.
[2] J. Eusamio, N. Saumell, A. Vidal-Ferran, A. Grabulosa, Inorg. Chem. 2024, 63 (30), 13820-13824.
[3] M. O. Shulyupin, E. A. Chirkov, M. A. Kazankova, I. P. Beletskaya, Synlett 2005, 2005 (04), 658-660.
[4] H. Schmidbaur, T. Pollok, Helv. Chim. Acta 1984, 67, 2175-2177.

P49
SYSTEMATIC INVESTIGATION OF DEPOSITION AND THERMAL TREATMENT PARAMETERS FOR MO_2C THIN-FILM HER CATALYSTS.

Shubhadeep Majumdar[1,2,*], Stefanos Chaitoglou[1,2], Ghulam Farid[1,2], Yang Ma[1,2], Enric Bertran-Serra[1,2], Roger Amade Rovira[1,2]

[1] Department of Applied Physics, University of Barcelona, C/Martí i Franquès, 1, 08028 Barcelona, Catalunya, Spain
[2] ENPHOCAMAT Group, Institute of Nanoscience and Nanotechnology (IN²UB), University of Barcelona, C/ Martí i Franquès, 1, 08028 Barcelona, Catalunya, Spain
* Corresponding Author email: **shmajumm110@alumnes.ub.edu**

Platinum is the best material for electrocatalytic hydrogen evolution through water splitting, but its high cost and scarcity make scalability a real challenge. Molybdenum carbide (Mo_2C) is known to be a promising candidate for catalysing HER,2,3. The present study focuses on optimizing deposition parameters for enhanced electrocatalytic performance. The investigated parameters are sputtering power, sputtering power source (Pulsed DC Sputtering, RF Magnetron Sputtering) and effect of thermal annealing parameters of the Mo_2C thin films (gas composition, ex-situ/in-situ annealing, annealing temperature).

Mo_2C films of 100nm thickness were deposited on graphite paper in an environment of 1Pa of Ar at room temperature using 25W, 50W, 100W, 150W and 200W of power using pulsed DC sputtering. Another set of these samples were fabricated and then annealed ex-situ in Ar at 980°C to study the effect of annealing on the morphology of the thin film. Samples of 50W, 150W and 200W power using RF magnetron sputtering were also fabricated and these were annealed in-situ at 980°C in an atmosphere of pure Ar and pure CH4 to study the effects of gas composition during annealing. Different annealing temperatures were tested, in the range 700-1100 °C. Samples were characterized using SEM, Raman and XRD spectroscopies and AFM measurements. Linear sweep voltammetry, electrochemical impedance spectroscopy, cyclic voltammetry and chronoamperometry were employed to characterize thin films performance towards HER.

Results show correlations between sputtering power, surface roughness, crystallite sizes, effect of annealing and effect of gas composition during annealing. Thermally annealed samples exhibit enhanced performance, which can be contributed to better crystallinity of the material. Comparing the samples of different powers, results showed that 50W of pulsed DC magnetron sputtering performed better than the other powers for a 100nm thin film which was annealed at 980°C in an environment of pure Ar. Annealing temperature slightly affects the onset and overpotential values, with the sample annealed at 800°C exhibiting the lowest value, compared to the 700°C, 900°C and 1050°C annealed samples. These findings highlight the importance and influence of every single process used in the fabrication of thin films and how these parameters modify their physical and chemical properties.

REFERENCES
[1] Majumdar, S.; Chaitoglou, S.; Serafin, J.; Farid, G.; Ospina, R.; Ma, Y.; Amade Rovira, R.; Bertran-Serra, E. Enhancing Hydrogen Evolution: Carbon Nanotubes as a Scaffold for Mo_2C Deposition via Magnetron Sputtering and Chemical Vapor Deposition. Int. J. Hydrogen Energy 2024, https://doi.org/10.1016/j.ijhydene.2024.09.425
[2] Chaitoglou, S.; Ospina, R.; Ma, Y.; Amade, R.; Vendrell, X.; Rodriguez-Pereira, J.; Bertran-Serra, E. Deposition and In-Situ Formation of Nanostructured Mo2C Nanoparticles on Graphene Nanowalls Support for Efficient Electrocatalytic Hydrogen Evolution. J. Alloys Compd. 2024, https://doi.org/10.1016/j.jallcom.2023.172891
[3] Mir, R. A.; Upadhyay, S.; Pandey, O. P. A Review on Recent Advances and Progress in Mo_2C@C: A Suitable and Stable Electrocatalyst for HER. Int. J. Hydrogen Energy 2023, https://doi.org/10.1016/j.ijhydene.2022.12.179

P50
SUPERCAPACITIVE PERFORMANCE OF ELECTRODES BASED ON GRAPHENE NANOWALLS ANCHORED ON TITANIUM-MXENE

Yang Ma,*[1,2] Stefanos Chaitoglou,[1,2] Ghulam Farid,[1,2] Roger Amade,[1,2] Shubhadeep Majumdar,[1,2] and **Enric Bertran-Serra**,*[1,2]

[1] Department of Applied Physics, University of Barcelona, C/Martí i Franquès, 1, 08028 Barcelona, Catalunya, Spain

[2] ENPHOCAMAT Group, Institute of Nanoscience and Nanotechnology (IN²UB), University of Barcelona, C/Martí i Franquès, 1, 08028 Barcelona, Catalunya, Spain

* Corresponding authors: **ebertran@ub.edu**; y**mamaxxx147@alumnes.ub.edu**

Supercapacitors are considered the superior choice for energy storage in electric vehicles and wireless technology due to their exceptional power density, cycle stability, and charge-discharge efficiency compared to conventional batteries [1]. However, their low energy density limits their ability to serve as a primary energy source. As a result, current research efforts are focused on nanostructured materials, particularly carbon-based materials such as activated carbon, carbon nanotubes (CNTs), and carbon aerogels, to increase specific capacitance [2]. Supercapacitors work through electrochemical double-layer capacitors (EDLCs) and pseudocapacitors. EDLCs store energy at the electrode/electrolyte interface via ion adsorption, primarily using carbon-based electrodes [3]. Despite graphene's excellent electrical and thermal conductivity, its theoretical capacitance is limited, which recent studies aim to overcome by changing the graphene orientation from horizontal to vertical, resulting in a 38% increase in capacitance [4]. Vertical graphene nanowalls (GNWs) synthesised by plasma-enhanced chemical vapour deposition (PECVD) offer superior electrical conductivity and a three-dimensional structure, making them excellent scaffolds for supercapacitor electrodes. On the other hand, MXene has garnered considerable attention as a promising energy storage material attributed to its substantial specific surface area and high electrical conductivity [5]. It represents a general term for a class of transition metal carbide/nitride materials, commonly derived from the etching of the precursor MAX phase. Presently, numerous mono- and bimetallic MXenes have been confirmed to exist, with $Ti_3C_2T_x$ MXene being particularly prevalent in energy storage research due to its exceptional conductivity and hydrophilicity [6], However, MXene nanosheets suffer from self-accumulation during operation, which seriously affects their further application. To address this issue, researchers have developed more stable MXene materials through methods such as freeze-drying, electrostatic self-assembly, or the introduction of intercalation materials [7]. Among the various approaches, the simplest way to enhance MXene properties is by introducing intercalation materials. Different intercalation materials exhibit varying abilities to improve MXene films. Previous

studies have demonstrated the advantages of using graphene, due to its structural diversity, high specific surface area. The presence of graphene enables the creation of a stable 3D structure with MXene nanosheets, increases the layer spacing of MXene nanosheets, and establishes stable ion transport channels. As a result, the composite film demonstrates a fundamental enhancement in charge storage capacity.
In this investigation, we explore the potential of GNWs with Mxene as a promising open structure, providing ample surface area for active sites and facilitating rapid ion diffusion. To elevate their specific capacitance, we introduce a supercapacitive enhancement by arranging GNWs anchored onto the Mxene. This hierarchical configuration is synthesized through a multi-step process involving acid etching and inductively coupled plasma-chemical vapor deposition (ICP-CVD). When utilized as supercapacitor electrodes, the GNWs/Ti-Mxene hybrids are assessed in an aqueous KOH electrolyte solution, indicating an increase in capacitance compared to pure Ti-Mxene sheets. The GNWs/Ti-Mxene hybrid showcases outstanding electrochemical performance, underscoring its significant potential for energy storage applications. Our study is poised to offer valuable insights for enhancing electrochemical properties in various composite and hybrid materials.

REFERENCES

[1]] X. Li, J. Ren, D. Sridhar, B.B. Xu, H. Algadi, Z.M. El-Bahy, Y. Ma, T. Li, Z. Guo, Progress of layered double hydroxide-based materials for supercapacitors, Mater. Chem. Front. 7 (8) (2023) 1520–1561.
[2] Xu, T.; Yang, D. Z.; Fan, Z. J.; Li, X. F.; Liu, Y. X.; Guo, C.; Zhang, M.; Yu, Z. Z. Reduced graphene oxide/carbon nanotube hybrid fibers with narrowly distributed mesopores for flexible supercapacitors with high volumetric capacitances and satisfactory durability. Carbon 2019, 152, 134–143.
[3] L. Cao, C. Wang, Y. Huang, Structure optimization of graphene aerogel-based composites and applications in batteries and supercapacitors, Chem. Eng. J. 454 (2023) 140094.
[4] Zhang, Y.; Zou, Q.; Hsu, H. S.; Raina, S.; Xu, Y.; Kang, J. B.; Chen, J.; Deng, S.; Xu, N.; Kang, W. P. Morphology Effect of Vertical Graphene on the High Performance of Supercapacitor Electrode. ACS Appl. Mater. Interfaces. 2016, 8, 7363-7369.
[5] Q. Wu, P.F. Li, Y.H. Wang, F.F. Wu, Construction and electrochemical energy storage performance of free-standing hexagonal Ti3C2 film for flexible supercapacitor, Appl. Surf. Sci. 593 (2022), 153380.
[6] G. Wang, S. Guo, Y. Wu, J. Wu, F. Zhang, L.u. Li, M. Zhang, C. Yao, C.J. Gomez- ´ García, T. Wang, Y. Zhang, T. Chen, H. Ma, POMCPs with Novel Two Water Assisted Proton Channels Accommodated by MXenes for Asymmetric Supercapacitors, Small 18 (29) (2022) e2202087.
[7] S. Li, Z. Peng, Y. Huang, L. Tan, Y. Chen, Electrostatic self-assembly of MXene and carbon nanotube@MnO2 multilevel hybrids for achieving fast charge storage kinetics in aqueous asymmetric supercapacitors, J. Mater. Chem. A 10 (44) (2022) 23886–23895.

P51
NANOSTRUCTURED CNT@SINW HYBRID ANODES FOR NEXT-GENERATION LITHIUM-ION BATTERIES

Ghulam Farid[1,2,*], Roger Amade-Rovira[1,2], Yang Ma[1,2], J. Serafin[1,2,3], Stefanos Chaitoglou[1,2], Shubhadeep Majumdar[1,2], Enric Bertran-Serra[1,2]
[1]Department of Applied Physics, University of Barcelona, C/Martí i Franquès, 1, 08028 Barcelona, Catalunya, Spain
[2]ENPHOCAMAT Group, Institute of Nanoscience and Nanotechnology (IN²UB), University of Barcelona, C/ Martí i Franquès, 1, 08028 Barcelona, Catalunya, Spain
[3] Department of Inorganic and Organic Chemistry, University of Barcelona, 08028 Barcelona, Spain
* Corresponding author e-mail: **chaudhryghulamfarid@ub.edu**

The pursuit of high-performance lithium-ion batteries (LIBs) has driven significant interest in nanostructured anodes. In this study, we propose a novel CNT@SiNW hybrid structure fabricated by growing carbon nanotubes (CNTs) atop vertically aligned silicon nanowires (SiNWs) via a combination of metal-assisted chemical etching (MACE) and chemical vapor deposition (CVD). This structure addresses limitations of dense CNT growth by enhancing spacing, porosity, and surface area, thereby improving lithium-ion accessibility and electrochemical performance [1–3].

MATERIALS & METHODS

Vertically aligned SiNWs were fabricated on p-type silicon wafers using a MACE process involving $AgNO_3$/HF and H_2O_2/HF solutions. After removing residual Ag and oxides, Al and Fe catalytic layers were sputtered on the SiNW tips. CNTs were then synthesized using CVD with acetylene as a carbon source. Surface morphology was characterized by FE-SEM and TEM; structural properties by XRD and Raman spectroscopy; and surface area by nitrogen adsorption-desorption (BET) analysis [4–6].

RESULTS AND DISCUSSION

The CNT@SiNW hybrid structure demonstrated a significantly higher BET surface area (150 m^2/g) and larger average pore size (2.34 nm) compared to CNTs on flat Si substrates (101 m^2/g, 1.87 nm). FE-SEM and TEM imaging confirmed improved vertical alignment and spacing of CNTs due to the SiNW template. Electrochemical tests revealed an initial delithiation capacity of 1.47 $mA{\cdot}h{\cdot}cm^{-2}$ and sustained capacity of 0.42 $mA{\cdot}h{\cdot}cm^{-2}$ after 200 cycles, compared to 0.01 $mA{\cdot}h{\cdot}cm^{-2}$ for CNT-only electrodes. Impedance spectroscopy showed reduced charge-transfer resistance, and post-mortem XPS confirmed minimal Li_2CO_3 build-up, indicating better SEI stability [7–10].

CONCLUSION

This CNT@SiNW hybrid anode showcases a scalable method to integrate the advantages of CNTs and SiNWs, offering enhanced cycling stability and rate capability. The technique presents strong potential for next-generation energy storage applications requiring high capacity and long-term durability.

REFERENCES

[1] G. Farid et al., J. Alloys Compd., 968 (2023) 172109.
[2] G. Farid et al., J. Energy Storage, 78 (2024) 110104.
[3] G. Farid et al., Arab. J. Chem. (2024) 105631.
[4] G. Farid et al., Mater. Res. Express, 5 (2018) 055044.
[5] Y. Ma et al., Chem. Eng. J., 488 (2024) 151135.
[6] E. Bertran-Serra et al., Nanomaterials, 13 (2023) 2533.
[7] G. Farid et al., ACS Appl. Nano Mater., 5 (2022) 2779–2786.
[8] A. Mateen et al., ECS J. Solid State Sci. Technol. 11 (2022) 054006.
[9] C. Huo et al., Adv. Funct. Mater., 30 (2020) 2005744.
[10] A. Mateen, ChemSusChem 18 (2025) e202400777.

P52
Ru/CNTs PREPARED BY ELECTROLESS DEPOSITION FOR HETEROGENEOUS CATALYSIS APPLICATION

J. Lloreda[1,2,3,*], J. Rigual[1], V. Abad[3], E. Gómez[1,2], A. Serrà[1,2]
[1] Grup d'Electrodeposició de Capes Primes i Nanoestructures (GE-CPN), Departament de Ciència de Materials i Química Física, Universitat de Barcelona, Martí i Franquès 1, E-08028, Barcelona, Espanya
[2] Institut de Nanociència i Nanotecnologia (IN²UB), Universitat de Barcelona, Barcelona, Espanya
[3] Consorci per a la Gestió dels Residus del Vallès Oriental, Camí Ral s/n, E-08401, Granollers, Espanya
* juditlloreda@ub.edu

Supported metallic NPs play a key role in heterogeneous catalysis. This type of materials presents a large number of active sites over a support with great surface area, which boast even more the catalytic activity. Industrial processes such as methanation and reforming reactions benefit from the development of nanocatalysts. The synthesis of these materials requires an accurate tailoring of the process to obtain an optimal loading of the active metal. Under this scenario, electroless deposition enables the control of the particle size and morphology while being able to deposit on a broad array of supports. Electroless baths contain a metal precursor, a reducing agent, and additives, carefully balanced to achieve an effective autocatalytic reaction [1]. Phosphates and boranes are largely used as reducing agents, with its oxidation leading to P or B heteroatom co-deposition. Although its presence is beneficial for some applications, it can hinder the desired catalytic effect. Instead, hydrazine oxidation results in its complete decomposition into H_2 and N_2 without leaving any heteroatoms on the metal deposits.

In this work, a Ru-based electroless bath with hydrazine as reducing agent [2] was employed to prepare the catalytic materials using carbon nanotubes as support. Initially, the optimization of bath solution was performed over fluorine-doped tin oxide coated glass (FTO) substrates, and UV-vis spectrophotometry was used to track the electroless solution. After morphological and compositional characterization via scanning electron microscopy (SEM) coupled with energy-dispersive X-ray spectroscopy (EDS), the deposition conditions were assessed. Carbon nanotubes (CNTs) were successfully oxidized following a simple and effective acid attack etching combined with ultrafast sonication. This step contributed to the disaggregation of the CNTs and improved sensitization treatment prior to chemical deposition. A series of samples at different deposition times were prepared and characterized using transmission electron microscopy (TEM). Optimal conditions for Ru/CNTs synthesis were establish at 1 h, based on TEM results. The suitability of the prepared material as catalyst for dry reforming of methane reaction is currently under evaluation.

ACKNOWLEDGMENTS
With the support of the Industrial Doctorates Program of the Department of Research and Universities of the Generalitat de Catalunya (project 2022 DI 035). The authors would like to thank the CCiT-UB for the use of their equipment.

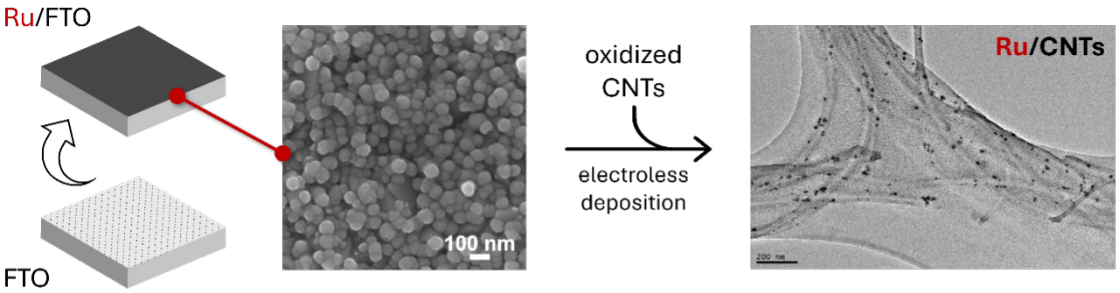

REFERENCES
[1] Muench, F. ChemElectroChem, 2021, 8, 2993. [2] R. Saida, R.; et al. J. Electron. Mater. 2023, 52, 6690

P53
MAGNETIC CONTROL OF DRIVEN COLLOIDS DISPERSED IN LIQUID CRYSTALS

J. Torres-Andrés[1,2,*], F. Sagués[1,2], J. Ignés-Mullol[1,2]
[1] Departament de Ciència de Materials i Química Física, Facultat de Química, Universitat de Barcelona, Barcelona, 08028.
[2] Institut de Nanociència i Nanotecnologia de la Universitat de Barcelona (IN²UB), Universitat de Barcelona, Barcelona, 08028.
* joel.torres@ub.edu

Liquid crystals (LCs) are complex fluids that feature long-range orientational order, and studying the propulsion of colloidal entities within them is of interest for their capacity to respond to external stimuli. When colloids are dispersed and driven in LCs, new propulsion phenomena emerge due to the inherent anisotropy of the liquid phase [1]. Furthermore, orientational waves (waves formed by changes in the orientation of molecules within the material) can be generated and propelled through the complex liquid [2,3]. Particularly, studies have shown the possibility of generating solitonic waves that exhibit behaviour close to that of colloidal inclusiong. While the motion of solitonic waves and solid particles within liquid crystals has been explored, there is a lack of in-situ control of their directionality using simple experimental strategies while performing observations.
In this work, we show simple arrangements based on the application of fixed external magnetic fields to control solid polystyrene (PS) particles and two types of solitary waves, both in confined and unconfined LCs. We demonstrate that degeneration in motion directionality can be broken by applying an in-plane fixed magnetic field while running experiments, showing that, for the case of some solitons, the magnetic field has a direct effect on their shape and velocity. In addition to this, we show how to attain dense regions of PS particles in the form of rotating mills, by generating topological defects on the surrounding LC using toroidal magnetic fields, enabling collective behaviour studies. Moreover, some of these colloidal entities are introduced and steered inside microfluidic channels. It is in these systems where we observe a dependency of propulsion velocity on the channel width, a clear phenomenon related to lateral confinement imposed by walls. Consequently, this work gives an approach to the field of colloidal control in complex fluids by magnetic fields.

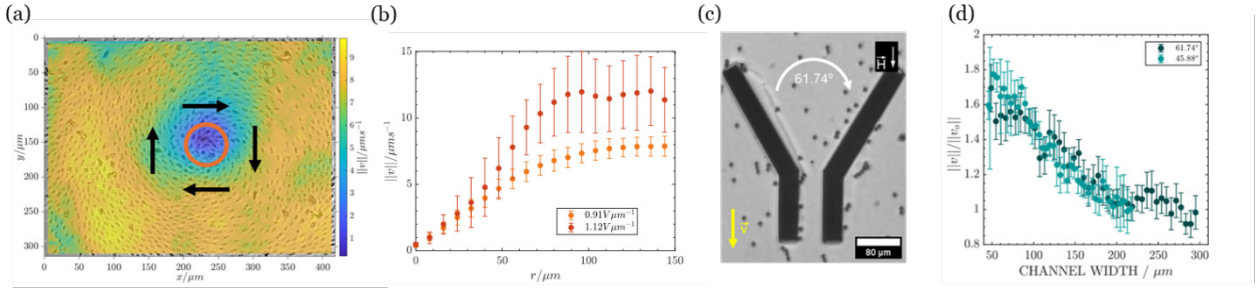

Figure 1. (a) Rotating mill conformed of polystyrene particles around a +1 defect inside a nematic LC cell. The background colour refers to the mean speed in the field of view. (b) Speed variation of the PS particles as a function of mill radius for different propelling electric field amplitudes. (c, d) Normalized velocity variation of solitonic waves passing through microfluidic channels with different aperture angles.

REFERENCES
[1] Peng, C.; et. al. Micromachines, 2019, 10(1):45p. 1-19.
[2] Ackerman, P.J.; et. al. Nat. Commun., 2017, 8:673, p. 1-13.
[3] Li, B.X.; et. al. Nat. Commun. 2019, 10:3749, p. 1-9.

P54
EXPLORING STRUCTURAL–PHOTOPHYSICAL PROPERTY RELATIONSHIPS IN GOLD(I)-PHOSPHINE COMPLEXES

Laura Mañas Roman, Anyie P. Atencio, Inmaculada Angurell, Laura Rodríguez

Department of Inorganic and Organic Chemistry, Universitat de Barcelona, Martí Franquès 1-11, 08028 Barcelona (Spain)
e-mail: aatences19@alumnes.ub.edu

Our previous investigation about the possibilities of tuning luminescent properties in gold(I)-phosphine complexes revealed that the coordination environment and chromophore position significantly influence intersystem crossing, phosphorescence, and aggregation behavior. Also, distinct photophysical trends were identified among the three series of compounds with triphenylene derivatives exhibiting aggregation-induced emission broadening and phenanthrene derivatives showing strong heavy atom effects[1].

Therefore, we present herein the synthesis, structural and photophysical characterization of four new series of gold(I) compounds (Figure 1), which differ in the type of chromophore and the position of coordination of the gold(I) atom. The main differences remain on the position of the chromophore, that can be: i) having the chromophore linked directly to the Au(I) metal centre; ii) having a chromophore at the phosphine unit; iii) having the chromophore in both coordination positions.

Additionally, to go a step further in this line of research, in each series we present a complex that combines two different types of chromophores in the same structure, that is, a complex that has one type of chromophore in the phosphine unit and another type of chromophore directly linked to the metal center.

For this study we selected pyrene and anthracene as chromophores due to their interesting photophysical properties[2],[3] with the objective of determining the relationship between the structural position of the chromophore and the change in the luminescent properties. We also want to know how the luminescent properties of these complexes change when combining two different classes of chromophores. So that the form and extent of the influence of the heavy atom on the system is determined.

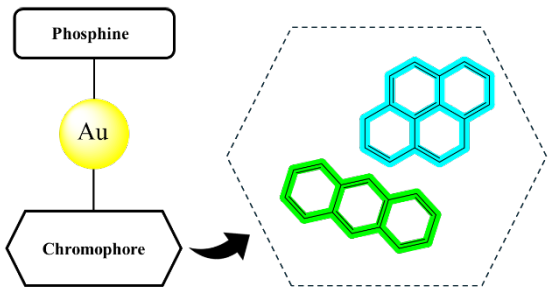

Figure 1: Chemical structure of the complexes with different chromophores.

REFERENCES

[1] Atencio, A. P.; Burguera, S.; Zhuchkov, G.; de Aquino, A.; Ward, J. S.; Rissanen, K.; Lima, J. C.; Angurell, I.; Frontera, A.; Rodríguez, L. Tuning Luminescence in Gold(I)-Phosphine Complexes: Structural, Photophysical, and Theoretical Insights. Inorg. Chem. Front., 2025, 12, 3041-3054.

[2] Mallesham, G.; Swetha, C.; Niveditha, S.; Mohanty, M. E.; Babu, N. J.; Kumar, A.; Bhanuprakash, K.; Rao, V. J. Phosphine Oxide Functionalized Pyrenes as Efficient Blue Light Emitting Multifunctional Materials for Organic Light Emitting Diodes. J. Mater. Chem. C. Mater., 2015, 3 (6), 1208–1224.

[3] Schillmöller, T.; Ruth, P. N.; Herbst-Irmer, R.; Stalke, D. Three Colour Solid-State Luminescence from Positional Isomers of Facilely Modified Thiophosphoranyl Anthracenes. Chem. Commun., 2020, 56 (54), 7479–7482.

P55
TUNING PHOTOPHYSICAL PROPERTIES OF Au(I) PILLARPLEXES THROUGH ANION VARIATION

A. de Aquino[1], J. Zuber[2], T. Pickl[2], J. C. Lima[3], L. Rodríguez[1], A. Pöthig[2]

[1] Departament de Química Inorgànica i Orgànica, Secció de Química Inorgànica, Universitat de Barcelona, Martí i Franquès 1-11, E-08028 Barcelona, Spain.
[2] Department of Chemistry and Catalysis Research Center, Technical University of Munich, Garching, Germany.
[3] LAQV-REQUIMTE, Departamento de Química, Universidade Nova de Lisboa, Monte de Caparica.
* adeaqusa7@alumnes.ub.edu

The exploration of supramolecular host compounds has led to the identification of a captivating class of complexes known as pillarplexes [1]. These distinctive structures are formed by coordinating cyclophane-based ligands with linearly binding metal centres such as Au(I). Pillarplexes are notable for three key features: (i) a selective pore capable of hosting linear guests, (ii) tuneable solubility through anion exchange, and (iii) intriguing photoluminescent behavior [2,3].
In this study, we investigate three different gold pillarplexes combined with different counteranions varying in their polarity (PF_6, OTf, and OAc). These complexes were synthesized and subsequently analysed through aggregation-induced emission (AIE) experiments in two different solvent systems, enabling a comparison of their photophysical behaviour under varying environmental conditions.
To further probe the nature of aggregation in solution, we employed Dynamic Light Scattering (DLS) and NMR spectroscopy. These techniques provided insights into the conformational behaviour and aggregation mechanisms of the pillarplexes, shedding light on their potential utility in the field of materials science.

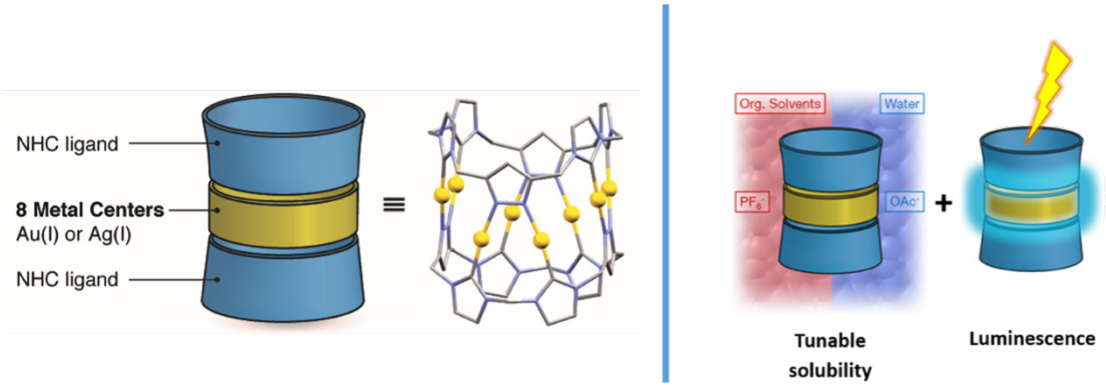

Figure 1. General structure of the pillarplex and representation of their main properties.

REFERENCES
[1] P. J. Altmann, A. Pöthig, J. Am. Chem. Soc., 2016, 138, 13171-13174.
[2] A. Pöthig, S. Ahmed, H. C. Winther-Larsen, S. Guan, P. J. Altmann, J. Kudermann, A. M. S. Andersen, T. Gjoen, O. A. H. Astrand, Front. Chem., 2018, 6, 584.
[3] S. Guan, T. Pickl, C. Jandl, L. Schuchmann, X. Zhou, P. J. Altmann, A. Pöhig, Org. Chem. Front., 2021, 8, 4061-4070.

P56
NEW ORGANOMETALLIC PRECURSORS FOR ENANTIOSELECTIVE CATALYSIS

J. Capdevila[1,2,*], J. Eusamio[1,2], A. Grabulosa[1,2]

[1] Universitat de Barcelona, Departament de Química Inorgànica i Orgànica, Secció de Química Inorgànica
[2] Institut de Nanociència i Nanotecnologia de la Universitat de Barcelona (IN²UB)
* jcapdere7@alumnes.ub.edu

Phosphorus-based ligands, particularly diphosphanes, have long played a central role in organometallic homogeneous catalysis due to their strong metal-coordination capabilities and versatility in asymmetric synthesis. Among these, P-stereogenic ligands have emerged as powerful tools in enantioselective catalysis [1], especially in hydrogenation. In this context, rhodium-phosphane complexes stand out for their exceptional catalytic performance. The present study presents the design, synthesis, and initial evaluation in catalysis of a novel non-symmetric, short-bridged diphosphane ligand—miniPAMP—which combines structural features from two established ligands, tBuMiniPHOS [2] and DIPAMP [3]. The goal of this project is to explore the coordination chemistry of miniPAMP with Rh(I) and assess the catalytic performance of the resulting complexes in enantioselective transformations.

MATERIALS AND METHODS

The synthesis of the miniPAMP ligand was performed using a one-pot procedure that involved the deprotonation and phosphination of enantiomerically pure methylphosphane–borane, a methodology well-established within our group [4]. The borane protecting group was removed under standard conditions to yield the free diphosphane, which was then reacted with Rh(I) precursors to form mono-chelated Schrock–Osborn-type complexes for further study.

RESULTS AND DISCUSSION

Both the miniPAMP ligand and its corresponding Rh(I) complex were successfully synthesized and fully characterized by NMR spectroscopy, confirming the desired structure. The coordination of miniPAMP to Rh(I) proceeded smoothly, yielding a stable mono-chelated complex. This was subsequently evaluated as catalysts in model enantioselective hydrogenation and hydroacylation reactions.

REFERENCES

[1] A. Grabulosa, P-Stereogenic Ligands in Enantioselective Catalysis, Royal Society of Chemistry, Cambridge, 2011. [2] Y. Yamanoi, T. Imamoto, J. Org. Chem. 1999, 64, 2988-2989. [3] W. S. Knowles, Adv. Synth. Catal. 2003, 345, 3-13. [4] J. Eusamio, Y. M. Medina, J. C. Córdoba, A. Vidal-Ferran, D. Sainz, A. Gutiérrez, M. Font-Bardia, A. Grabulosa, Dalton Trans. 2023, 52, 2424-2439.

P57
INKJET PRINTING OF METAL HALIDE PEROVSKITES: LINKING THIN FILM FORMATION TO PHOTODETECTOR DEVICE PERFORMANCE

K. Lobo[1], G. Vescio[1], J. Khan[1], J. Mari-Guaita[1], S. Hernandez[1], A. Cirera[1], Carmen Coya[2], and B. Garrido[1]

[1] OPERA Group, MIND-IN²UB, Universitat de Barcelona, Carrer Martí i Franquès 08028, Barcelona
[2] Escuela de Ingeniería de Fuenlabrada, Universidad Rey Juan Carlos, 28933 Madrid, Spain
* Correspondence: **kennethlobo@ub.edu**

Metal halide perovskites have emerged as promising materials for optoelectronic applications owing to several desirable attributes such as high photoluminescence quantum yield and tunable absorption/emission.[1] Additionally, when paired with solution-based methods like inkjet printing, a significant potential for high-resolution, mask-free patterning and scalable, feasible production of devices emerges.[2,3] This is typically achieved through the printing of inks containing nanoparticles in dispersion or through the deposition of precursor solutions, the latter providing greater control on the characteristics of optoelectronic active layers.[4] The rich chemistry of these materials enables crystal formation under undemanding conditions and has been well exploited with methods like spin coating, however an understanding into crystalline film formation and their correlation to the resultant optoelectronic performance in inkjet printed devices remains largely unexplored.[5] This work presents findings on structural, morphological, and electrical investigations on printed layers of methylammonium lead bromide ($MAPbBr_3$) for photodetector applications.

Precursor solutions containing methylammonium bromide and lead bromide in DMF/DMSO were inkjet printed onto glass/Si substrates and thermal treatment was carried out to drive crystallization. This method was found to progress the film formation without the typical use of an antisolvent, resulting in the formation of large grains up to tens of micrometers in size as suggested by electron microscopy. The films were found to exhibit strong photoluminescence at 550 nm, and time dependent studies were performed to evaluate the evolution of this emission as a function of time to understand film formation. The substantial absorption coefficient of the $MAPbBr_3$ films observed in UV-visible spectroscopy was leveraged for photodetection by printing onto interdigital contacts. Printing parameters were found to be crucial for controlling device characteristics, exhibiting a sharp rise in responsivity of several mA/W at the absorption edge and fast response times. Further, the printability was extended to polymeric substrates and the device performance investigated under flexure. These findings provide an insight into the crystallization dynamics of $MAPbBr_3$ for achieving a careful control on their incorporation in device fabrication steps for enhanced optoelectronic performance.

REFERENCES

[1] Akkerman, Quinten A., et al. "Genesis, challenges and opportunities for colloidal lead halide perovskite nanocrystals." Nat. Mater. 17.5 (2018): 394-405.
[2] Chirvony, Vladimir S., et al. "Achieving Inkjet-Printed 2D Tin Iodide Perovskites: Excitonic and Electro-Optical Properties." Adv. Funct. Mater. 34.39 (2024): 2405154.
[3] Vescio, Giovanni, et al. "Fully Inkjet-Printed Green-Emitting PEDOT: PSS/NiO/Colloidal $CsPbBr_3/SnO_2$ Perovskite Light-Emitting Diode on Rigid and Flexible Substrates." Adv. Eng. Mater. 25.21 (2023): 2300927.
[4] González, Sergio, et al. "Inkjet-Printed p-NiO/n-ZnO Heterojunction Diodes for Photodetection Applications." Adv. Mater. Interface. 10.15 (2023): 2300035.
[5] Vescio, Giovanni, et al. "2D PEA2SnI4 inkjet-printed halide perovskite LEDs on rigid and flexible substrates." ACS Energy Lett. 7.10 (2022): 3653-3655.

P58
ELECTRODEPOSITED Cu, Ni, Ru AND THEIR BINARY / TERNARY ALLOYS FOR ENHANCED ELECTROCATALYTIC REDUCTION OF LEVULINIC ACID INTO VALUE-ADDED CHEMICAL PLATFORMS

P. Vilariño[1,2,*], E. Gómez[1,2], A. Serrà[1,2]

[1] Grup d'Electrodeposició de Capes Primesi Nanoestructures(GE-CPN), Departament de Ciència de Materials i Química Física, Universitat de Barcelona, Martí i Franquès, 1, E-08028, Barcelona, Catalonia, Spain.
[2] Institute of Nanoscience and Nanotechnology (IN²UB), Universitat de Barcelona, Barcelona, Catalonia, Spain.
* Corresponing Author: **pol.vilarino@ub.edu**

The electrocatalytic hydrogenation (ECH) of levulinic acid (LA) presents a sustainable and energy-efficient approach for the production of high-value chemicals such as γ-valerolactone (GVL) and valeric acid (VA). This study investigates the electrochemical reduction of LA using electrodeposited catalysts based on Cu, Ni, and Ru, including binary (CuNi, CuRu, NiRu) and ternary (CuNiRu) systems, under both acidic and alkaline conditions. Catalysts were synthesized via electrodeposition from newly developed formulations. Among the materials examined, Ni-rich catalysts demonstrated the highest performance. In particular, CuNi and CuNiRu catalysts achieved faradaic efficiencies exceeding 80%, LA conversion rates above 85%, and GVL selectivity up to 94% in acidic media. Electrochemical characterisation revealed that the reaction pathway and product distribution were significantly affected by catalyst composition and solution pH. Acidic conditions favoured enhanced conversion and selectivity toward GVL, whereas alkaline environments led to reduced reaction rates and a shift in selectivity toward VA. Stability tests under acidic conditions confirmed the reusability of CuNi-based catalysts, showing only moderate performance decline over successive cycles and minimal catalyst leaching. A comparison with state-of-the-art electrocatalysts underscores the advantages of the developed materials, particularly in terms of efficiency and product selectivity. These results highlight the promise of electrodeposited Ni-rich catalysts for scalable, cost-effective, and environmentally sustainable biomass valorisation, offering a viable electrochemical alternative to conventional hydrogenation methods.

ACKNOWLEDGEMENTS
Ministerio de Ciencia e Innovación (MICIN) is acknowledged through Grant TED2021-129898B-C22 funded by NextGenerationEU and MICIU/AEI/10.13039/501100011033. The authors also would like to express their gratitude to the Departament de Recerca i Universitats, particularly the Departament d'Acció Climàtica, Alimentació i Agenda Rural, as well as the Fons Climàtic de la Generalitat de Catalunya (project 2023 CLIMA 00009 AGAUR) for theirsupport. Authorsthank the CCiT-UB for the use of their equipment.

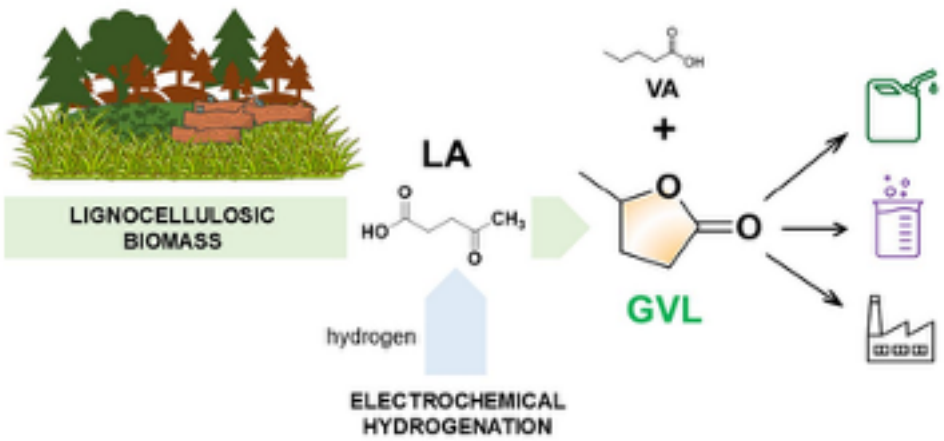

P59
WITHDRAWN

NanoEnergy

P60
DIELECTRIC-METAL-DIELECTRIC THIN FILM STRUCTURES AS TRANSPARENT ELECTRODES FOR SOLAR CELLS

U. Aziz[1]*, A. L. Muñoz-Rosas[1], J. M. Asensi[1], J. Bertomeu[1], J. L. Vidrier[1]

[1] Multiferroic and Photovoltaic Materials for Renewable Energies (MAMFER), Universitat de Barcelona, Barcelona (Spain)
* **umeraziz@ub.edu**

The carrier-selective contacts have emerged as a promising approach for achieving high-efficient crystalline silicon solar cells with economical and scalable materials. Previously, different electrode materials have been broadly studied as either electron or hole selective contacts such as oxides, nitrides, halides, and some organic molecules. To fabricate a complete solar cell, a proper transparent electrode is required which is capable of extracting the photogenerated charge while not compromising on its transmittance (T) and reflectance (R). In this regard, the indium-doped tin oxide is commonly used as conductive electron. However, because of its scarcity, elevated cost, among other reasons, dielectric-metal-dielectric (DMD) layered structures have emerged as candidates to substitute the ITO electrode in photovoltaics solar cells [1].

In this work, the performance of DMD structures has been investigated for solar cell applications. The ZnO and Al-doped ZnO films were selected as dielectric materials, whereas Ag and Al were employed as the metal. Magnetron sputtering technique was employed for depositing the layers on the glass substrates. Through simulations employing the transfer matrix method, the dielectric and metal layers thickness and compositions were optimized in terms of reflectance, transmittance and sheet resistance. Afterwards, a series of adequate dielectric/metal/dielectric (DMD) stacks has been fabricated. The T and R of the resulting samples were optically characterized by UV-Vis-NIR spectroscopy, and the electrical properties of the material were also tested using the transfer length method. Furthermore, the structural and elemental analysis of independent deposited layers on the substrate has been confirmed through X-ray diffraction, scanning electron microscope, energy dispersive X-ray, and atomic force microscope. Figure of merit of the different layered structures was obtained through Haacke method.

REFERENCES

[1] Tom, T., Ros, E., López-Pintó, N., Miguel Asensi, J., Andreu, J., Bertomeu, J., Puigdollers, J. and Voz, C., 2020. Influence of co-sputtered Ag: Al ultra-thin layers in transparent V2O5/Ag: Al/AZO hole-selective electrodes for silicon solar cells. Materials, 13(21), p.4905.

P61
EVALUATION OF TiO_2–HCl INKS FOR CHEMICAL SINTERING IN DIRECT INK WRITING (DIW) 3D PRINTING PROCESSES FOR WATER TREATMENT APPLICATIONS

José Antonio Padilla Sánchez[1], Paola Tirira[1], Pol Barcelona[1], Mònica Martínez[1], Elena Xuriguera[1], Ignasi Sires[1]
[1] Universitat de Barcelona, Departament de Ciència de Materials i Química Física, C/ Martí i Franquès 1, Barcelona, Spain
* **japadilla@ub.edu**

Climate change and the increasing scarcity of freshwater demand sustainable solutions for the treatment and reuse of urban wastewater. A key challenge is the removal of persistent organic pollutants (POPs), whose complete degradation is often costly and inefficient using conventional methods. Among Advanced Oxidation Processes (AOPs), heterogeneous photocatalysis with TiO_2 in its mixed-phase form (80-20% anatase/rutile), exhibits high photocatalytic activity under UV irradiation, generating hydroxyl radicals capable of degradation and mineralizing POPs [1].

Additive manufacturing (AM) via direct ink writing (DIW) improves filter design and also enables the integration of functional enhancements, which enhance the generation of hydroxyl radicals (OH•) and improve contaminant degradation efficiency. To address the issue of organic matter removal during the thermal sintering of DIW fabricated inks, this work applies chemical sintering (CS) Figure 1, which allows fabrication at significantly lower temperatures [2].

In this binder-free approach, oxygen bridges form between TiO_2 nanoparticles in an acidic medium at low temperatures, producing 3D objects without the need of high-temperature treatments.

MATERIALS AND METHODS

For the preparation of the inks, diferent comercial anatase nanopowder of TiO_2 was mixed with different acidic HCl solutions. After cooling in an ice bath at 0 °C, the mixtures were mixed using a planetary mixer. The inks were transferred to a 3 ml syringe. Printing was carried out using a BioX printer from CellInk. The printed samples measured 10 × 10 × 3 mm. Two thermal treatments were applied: an initial drying step at 50 °C for 48 h under vacuum, followed by a two-stage sintering process—first at 100 °C, then at the target working temperature. The heating rate was 5 °C/min, with dwell times of 1 h and 12 h at each respective temperature. Microstructural characterization of the samples was performed using scanning electron microscopy (SEM).

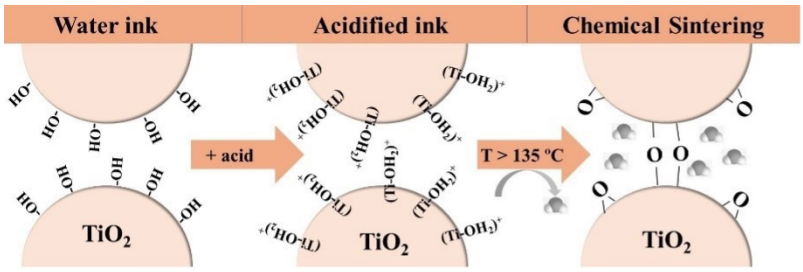

Figure 1. Chemical Sintering Process applied to DIW inks. Adapted from Elkoro et al.

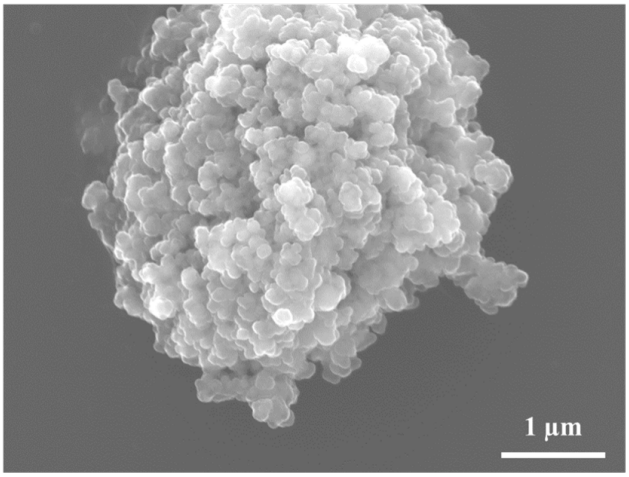

Figure 2 Starting nanopowder form Alfa Aesar.

RESULTS AND DISCUSSION

The various anatase powders used to prepare the inks have nanometric particle sizes. Figure 2 shows one of the powders used, with a particle size of 32 nm and a specific surface area (S.A.) of 45 m^2/g.

Not all the powders enabled the formulation of printable inks. As reported in the literature [1], there is an optimal pH range that maximizes the solid-to-liquid mass ratio, which lies between pH 0 and pH 1, in the case of TiO_2/HCl. This value depends on the specific oxide and the type of acidic compound used. This behavior has been observed across the different TiO_2 oxides studied.

From the analysis of the crystalline phase evolution, it was observed that the anatase-to-rutile transition began between 650 °C and 700 °C, which is 50 to 75 °C higher than expected. To achieve a composition of 80% anatase and 20% rutile, the thermal treatment temperature should be set between 650 °C and 700 °C. Since this temperature is relatively low—well below conventional sintering temperatures—both densification and porosity deviate from expectations: densification is lower, and porosity is higher than anticipated. The observed shrinkage is approximately 15%, with a mass loss of around 3%.

The application of relatively low temperatures (650–700 °C) allows to maintain the nanometric microstructure in the TiO_2 samples. Figure 3 shows a scanning electron microscopy image of a sample treated at 675 °C, where the particle size can clearly be seen to remain in the nanometric range. Maintaining a nanometric TiO_2 particle size is expected to enhance the catalytic performance of these samples.

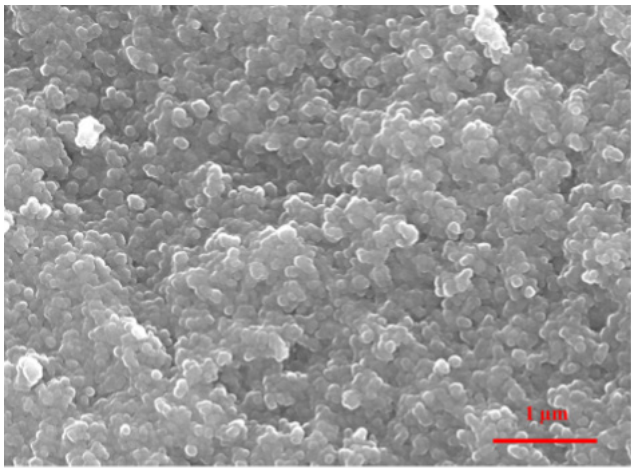

Figure 3 Particle size in the sample TiO2 at 675 °C.

REFERENCES

[1] Mendez-Arriaga, F.; Calleja, E.; Ruiz-Huerta L.; Caballero-Ruiz, A.; Almanza R., TiO2 3D structures for environmental purposes by additive manufacturing: Photoactivity test and reuse, Materials Science and Semiconductor Processing, 2019, 100, 35–41.

[2] Elkoro, A.; Casanova, I., 3D Printing of Structured Nanotitania Catalysts: A Novel Binder-Free and Low-Temperature Chemical Sintering Method, 3D Printing and Additive Manufacturing, 2018, 5 (3), 220–226.

P62
NEW TECHNOLOGIES OF TRANSPARENT SOLAR CELLS WITH OXIDES FOR ADVANCED PHOTOVOLTAIC INTEGRATIONS

Gustavo Álvarez[1,2,3], Pau Estarlich[3], Alex J. Lopez[1], José Miguel Asensi[4], Gerard Masmitja[3], Cristóbal Voz[3], Joaquim Puigdollers[3], Alejandro Pérez-Rodríguez[1,5]

[1] Institut de Recerca en Energia de Catalunya (IREC), Jardins de les Dones de Negre, 1, 2a pl, 08930, Sant Adrià del Besòs, Barcelona, Spain.
[2] Facultat de Física, Universitat de Barcelona (UB), C. Martí i Franquès 1-11, 08028 Barcelona, Spain.
[3] Departament Enginyeria Electrònica, Universitat Politècnica Catalunya, c/ Jordi Girona 3-1, 08034, Barcelona, Spain.
[4] IN²UB, Departament de Física Aplicada, Universitat de Barcelona, Carrer de Martí i Franquès 1-11, 08028, Barcelona, Spain.
[5] IN²UB, Departament d'Enginyeria Electrònica i Biomèdica, Universitat de Barcelona, Carrer de Martí i Franquès 1-11, 08028, Barcelona, Spain.
* corresponding author: **galvarez@irec.cat**

Transparent photovoltaic (TPV) technologies represent a significant advancement in the photovoltaic field, particularly suited advanced integration concepts that require additional device functionalities combining high optical transparency and high optical aesthetic quality, for applications in different emerging fields as those related to BIPV (Building-Integrated Photovoltaics), Agrivoltaics and PV of Things. TPV systems address conventional integration challenges by prioritizing not only energy efficiency but also transparency and aesthetic appeal, which inherently adds complexity to their device architectures. This work explores the efficiency and transparency limits—specifically, the light utilization efficiency (LUE) [1]—of TPV devices based on an ultra-thin hydrogenated amorphous silicon (a-Si:H) absorber layer[2], combined with charge-carrier selective layers and transparent electrodes.

MATERIALS & METHODS

The optimal device structure comprises vanadium oxide (V_2O_x) as the hole-transport layer (HTL), facilitating hole flow while blocking electrons, and phosphorus-doped hydrogenated amorphous silicon-carbon (a-SiC_x:H(n)) as the electron-transport layer (ETL), facilitating electron flow while blocking holes. Transparent conductive oxides (TCOs) such as fluorine-doped tin oxide (FTO) and aluminum-doped zinc oxide (AZO) serve as the back and front contacts, respectively, enabling external electrical connectivity. The fundamental device incorporates a nanometric layer of hydrogenated amorphous silicon (a-Si:H) sandwiched between the HTL and ETL, this configuration is structured as SLG/FTO/a-SiC_x:H(n)/a-Si:H/V_2O_x/AZO.

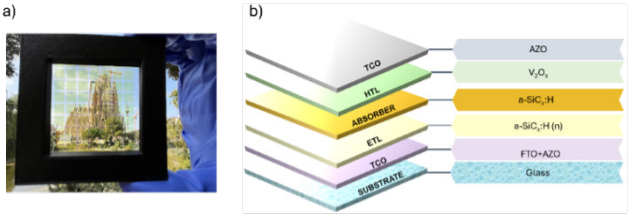

Figure 1. a).Picture of full device, taken outdoors in broad daylight. b) device structure

RESULTS AND DISCUSSION.

These optimized devices achieved power conversion efficiencies (PCE) exceeding 2.6% with average photopic transmittance (APT) of 50%, and a corresponding light utilization efficiency (LUE) of 1.3%. Comprehensive characterization included optical spectrophotometry, J–V measurements under AM1.5G illumination, spectral response analysis, and cross-sectional STEM-EDX mapping. Additionally, optoelectronic measurements revealed excellent bifacial performance, with a bifacial factor approaching unity. Furthermore, correction of reflection losses in the device architecture has allowed the estimation of LUE values up to 1.6%-1.7%, corresponding to PCE values up to 4% with AVT > 40%, which constitute the current world record LUE values reported up to now for inorganic TPV.

REFERENCES

[1] Traverse, C. J., Pandey, R., Barr, M. C., & Lunt, R. R. (2017). Emergence of highly transparent photovoltaics for distributed applications. Nature Energy, 2(11), 849-860.
[2] Alvarez-Suarez, G., Lopez-Garcia, A. J., Estarlich, P., Asensi, J. M., Masmitjà, G., Ortega, P., ... & Perez Rodriguez, A. (2025). Exploring the Limits and Balancing Efficiency, Transparency, and Esthetics in Ultrathin a-Si: H Transparent Photovoltaic Devices. Solar RRL, 2400816.

P63
CARBIDE-BASED MATERIALS AS CATALYSTS FOR THE CO_2 REDUCTION TO SYNGAS PROCESSES

A. Sánchez[1,2], P. Ramírez de la Piscina[1], N. Homs[1,2]

[1] Departament de Química Inorgànica i Orgànica, secció de Química Inorgànica & Institut de Nanociència i Nanotecnologia (IN²UB), Universitat de Barcelona, Martí i Franquès 1, 08028 Barcelona, Spain
[2] Catalonia Institute for Energy Research (IREC), Jardins de les Dones de Negre 1, 08930 Barcelona, Spain
* **adria.sanchez@qi.ub.edu**

The catalytic reduction of CO_2 to CO, which can result in syngas production, offers a valuable route for the recycling of CO_2, producing higher-value chemicals, i.e. via the Fischer-Tropsch or methanol synthesis processes. To reduce reliance on noble metals, transition metal carbides (3D CMTs) have emerged as promising alternatives in this process [1]. In general, 3D CMTs and related 2D compounds, MAXs and MXenes, are attracting interest due to their structural and electronic characteristics, which provide them properties that make them potentially applicable in different fields [2]. In this communication, we wish to present the developments carried out in our group using 3D CMTs and the related 2D MAXs and MXenes, as catalysts applied to CO_2 reduction through the reverse water gas shift reaction (RWGS). In this context, in recent years we have described different methods of preparing 3D CMTs that have allowed us to obtain materials with specific characteristics, which exhibit well-differentiated catalytic behaviors, in particular in the RWGS reaction; moreover, NbC and TaC (3D CMTs) materials have been found to be inactive [1,3]. Based on this background, we present in this paper the comparative study of 3D CMTs of Nb and Ta, MAXs (Nb2AlC, Ta2AlC) phases and the related MXene compounds (Nb2C and Ta2C), in the RWGS reaction.

MATERIALS & METHODS

MXenes Nb_2C and Ta_2C were synthesized from their respective MAX precursors (Nb_2AlC and Ta_2AlC) via an HF-free hydrothermal method. All materials were characterized by different physico-chemical techniques. Catalytic tests were conducted at atmospheric pressure and 300–500 °C in a fixed-bed reactor, using a CO_2:H_2 = 1:3 gas mixture. Reaction products were continuously monitored by gas chromatography. The catalytic study included the previously prepared 3D CMTs (NbC and TaC) [3], the commercial MAX phases (Nb_2AlC and Ta_2AlC), and the synthesized MXene materials (Nb_2C and Ta_2C).

RESULTS AND DISCUSSION

The Nb and Ta MAX and MXene materials showed catalytic activity under the RWGS conditions tested, in contrast with the NbC and TaC materials. This can be related to the structural differences and surface properties of the MAX and MXene phases. Moreover, the synthesised MXenes and the modified MAX phases displayed superior performance compared to the commercial MAX materials, an improvement that may be related to the increase of surface area and the presence of surface functional groups. In addition, the Nb-based catalysts are more selective towards CO than the corresponding Ta materials, which show a greater methanation activity. In conclusion, Nb and Ta MAXs and MXenes are capable of activate the CO_2 molecule and facilitate its catalytic hydrogenation, being particularly effective under the studied conditions of RWGS, compared to the stoichiometric 3D CMTs NbC and TaC. These results point Nb and Ta MXenes as promising materials for CO_2 reduction, via the RWGS reaction to syngas mixtures.

ACKNOWLEDGEMENTS

The authors thanks financial support from MICIN-EU, PID2020-116031RB I00/AEI/10.13039/501100011033/ FEDER and 2023 CLIMA 00009 AGAUR projects. A.S. thanks the MICIN and FSE+ for the PhD grant PRE2021-098422.

REFERENCES

[1] A. Pajares, X. Liu, J.R. Busacker, P. Ramírez de la Piscina, N. Homs, Nanomaterials, 12 (2022) 3165; Pajares, A., Ramírez de la Piscina, P., Homs, N., Appl. Catal A General 687 (2024) 119963.
[2] M. Dahlqvist, M.W. Barsoum, J. Rosen, Mater. Today, 72 (2024) 1; I. Gul, M. Sayed, T. Saeed, F. Rehman, A. Naeem, S. Gul, Q. Khan, K. Naz, M. ur Rehman, Coord. Chem. Rev. 511 (2024) 215870.
[3] A. Pajares, H. Prats, A. Romero, F. Viñes, P. Pilar Ramírez de la Piscina, R. Sayós, N. Homs, F. Illas, Appl. Catal. B Environ., 267 (2020) 118719; X. Liu, A. Pajares, DJ.D. Calinao Matienzo, P. Ramírez de la Piscina, N. Homs, Catal. Today, 356 (2020) 384; H. Prats, A. Pajares, F. Viñes, P. Ramírez de la Piscina, R. Sayós, N. Homs, F, Illas, ACS Appl. Mater. Interfaces, 16 (2024) 28505.

Research Areas Collaborations

P64
CORONA PERSONALISATION VIA ITERATIVE EXPOSURE TO MEDIA MODULATES NANOPARTICLE TOXICITY (NanoMet & NanoPharmaMed)

Alberto Martinez-Serra[1,2,3,*], Adriana S. Maddaleno[1,2], Asia Saorin[4], Marco P Monopoli[4], Giancarlo Franzese[1,3], Montserrat Mitjans[1,2]

[1] Institut de Nanociència i Nanotecnologia (IN²UB), Universitat de Barcelona, Av. Joan XXIII S/N, 08028, Barcelona, Spain
[2] Departament de Bioquímica i Fisiologia, Facultat de Farmàcia i Ciències de l'Alimentació, Universitat de Barcelona, Av. Joan XXIII 27-31, 08028 Barcelona, Spain
[3] Secció de Física Estadística i Interdisciplinària, Departament de Física de la Matèria Condensada, Facultat de Física, Universitat de Barcelona, Martí i Franquès 1, 08028, Barcelona, Spain
[4] Chemistry Department, RCSI (Royal College of Surgeons in Ireland), 123 St Stephen's Green, Dublin 2, Ireland
* Corresponding email: **amartise43@alumnes.ub.edu**

Blood plasma and serum have been widely used over the past decade as a relevant biological environment to investigate nanoparticle (NP) interactions, primarily due to its proteomic complexity and capacity to serve as a biomarker reservoir. [1] Despite containing thousands of proteins, the plasma proteome is dominated by a small subset of highly abundant proteins such as albumin, IgG, and fibrinogen. [2] However, NPs have emerged as promising tools for selective biomolecule enrichment, owing to their high surface area and the formation of a biomolecular corona—a layer of biomolecules that defines their biological identity. [3] While most corona studies rely on plasma, in vitro systems typically employ serum, such as foetal bovine serum (FBS), as the biomolecular source for cell cultures. In this sense, direct NP exposure to cell culture media (CCM) is also common in toxicity assays. [4,5]

In previous studies we have explored how after numerous cycles of NP exposure and isolation from human plasma, different types of biomolecules are progressively removed, and the biomolecular corona is enriched with low-abundance biomolecules. [6] However, this media-driven personalization of NP–protein interactions in cell culture conditions and its effects remains underexplored. In this work, we first analyse how multiple cycles of silica NP exposure and isolation from CCM containing 10% FBS form different biomolecular coronas, adsorbing distinct biomolecules onto the NP surface while the fluid is correspondingly fractionated. Then, we investigate how this repeated exposure of NPs to CCM affects NP toxicity. Using three human cell lines—3T3 (mouse fibroblasts), THP-1 (macrophage-like), and HaCaT (keratinocytes)—we examine how NPs with coronas from iterative incubation modulates cytotoxic responses. NPs are physiochemically and biomolecular characterised after each exposure cycle, and toxicity is assessed via standard viability assays, such as MTT.

Our preliminary findings indicate that repeated exposure of silica NPs to CCM results in the progressive remodelling of the biomolecular corona, characterized by selective enrichment of specific protein subsets. This temporal evolution not only reflects a depletion and fractionation of the surrounding media but also leads to marked differences in cellular responses. Distinct corona profiles generated through iterative exposure cycles induce variable cytotoxic effects across cell types, suggesting a direct link between corona composition and biological outcome. These results highlight the importance of considering dynamic exposure conditions in in vitro models and reveal how media-driven personalization of the corona can shape NP behaviour, toxicity, and potential as diagnostic or therapeutic platforms.

REFERENCES
[1] Monopoli, Marco P., et al. Journal of the American Chemical Society 133.8 (2011): 2525-2534. [2] Anderson, N. Leigh, et al. Molecular & cellular proteomics 1.11 (2002): 845-867. [3] Trinh, Duong N., et al. ACS nano 16.4 (2022): 5463-5475. [4] Saorin, Asia, et al. Materials Advances 5.12 (2024): 5106-5117. [5] Mitjans, Montserrat, et al. Nanomaterials 13.11 (2023): 1800. [6] Martinez-Serra, Alberto, et al. Analytical Chemistry (Accepted).

P65
DEVELOPMENT OF TRIPHENYLENE-DERIVED MOFs FOR THEIR USE IN GREEN CATALYSIS (NanosMat & NanoPhotoElectro)

Yuzelfy Mendoza-Gamero[1,2,3,*], Sergi Gonzalez-Martinez[1,2,3], Albert Romano-Rodriguez[1,2], Daniel Sainz-García[2,3]

[1] Institute of Nanoscience and Nanotechnology (IN²UB), Universitat de Barcelona, Barcelona.
[2] Dept Electronic and Biomedical Engineering Department, Universitat de Barcelona, Barcelona
[3] Dept Inorganic and Organic Chemistry Department, Universitat de Barcelona, Barcelona
* yuzelfymendoza@ub.edu

With the increasing need for sustainable chemical processes, heterogeneous catalysis emerges as a key strategy for developing cleaner and more efficient reactions. Within this context, metal-organic frameworks (MOFs) stand out due to their high porosity, structural stability, and versatility in incorporating active metal centers [1].

Our work focuses on the design and synthesis of triphenylene-based ligands, leveraging their rigid and planar structure to construct robust and functional MOFs. Functionalization of the triphenylene core enables the introduction of multiple coordination sites, facilitating the incorporation of metals [1,2] such as nickel, copper, and palladium for their efficiency in carbon–carbon coupling reactions, particularly the Suzuki–Miyaura reaction [2].

In this study, we synthesised hexaaminetriphenylene (HTAT), hexaanilinetriphenylene (HANT) and hexaphenoltriphenylene (HPTP) ligands by Buchwald-Hartwig and Suzuki-Miyaura reactions, according to the methods reported in literature [3,4], which allowed the formation of MOFs with high porosity and electrical conductivity. These MOFs were characterized by FTIR, ^{1}H-NMR, MS, SEM and PXRD techniques, to study their crystalline structure and morphological properties.

The development of these functionalized MOFs opens new opportunities to create selective, efficient and reusable catalytic systems, helping to drive more sustainable and environmentally friendly chemical processes [4,5]. The effectiveness of these MOFs as heterogeneous catalysts will be presented, focusing on their ability to promote key carbon-carbon coupling reactions under optimized conditions and green solvents.

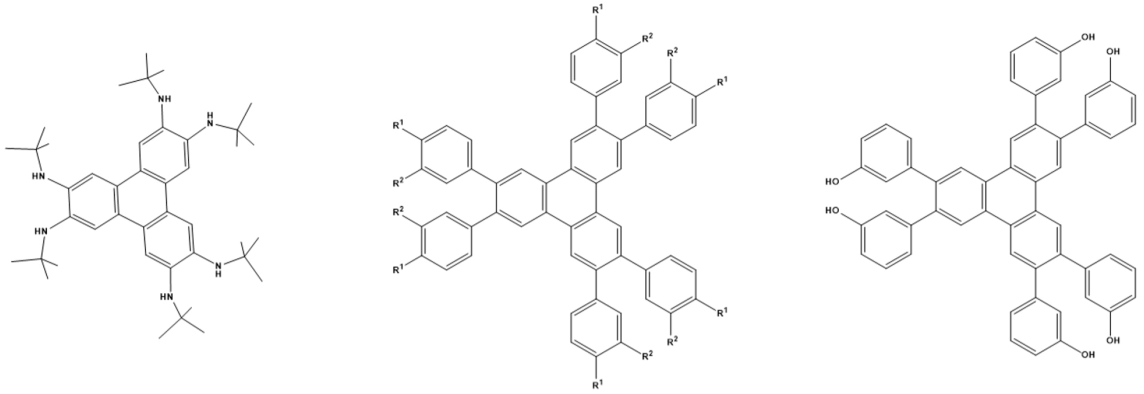

Figure 1. Chemical structures of the triphenylene-based ligands synthesized: hexaaminotriphenylene (HTAT), para-hexaanilinotriphenylene (R^1-HANT), meta-hexaanilinotriphenylene (R^2-HANT) and meta-hexaphenoltriphenylene

REFERENCES
[1] Mircea Dincă, et al. J. Am. Chem. Soc. 2020, 142 , 12367-12373. [2] Dorian Sonet, et al. Tetrahedron Lett. 2019, 60 , 1234-1238. [3] Sergio Gonell, et al. Angew. Chem. Int. Ed. 2013, 52, 7009–7013. [4] Belén Martín-Matute, et al. J. Am. Chem. Soc. 2019, 141, 7223–7234. [5] Rao, Ravulakollu Srinivasa, et al. Heliyon, 2024, 10,23, e40571

AUTHOR INDEX

AUTHOR INDEX

A
Abad, V. 56
Aguilà, D. 60, 68, 71
Alff, L. 29
Álvarez, G. 70, 99
Amabilino, D. B. 18, 41
Amade, R. 84, 85, 87
Amorós, J. 13
Angurell, I. 90
Ara, J. 11, 64
Arfa, C. 61
Aromí, G. 60, 63, 68, 71
Arteaga, O. 79, 81
Asensi, J. M. 96, 99
Atencio, A. P. 90
Aziz, U. 96,

B
Badosa, Q. 62, 72
Bagherpour, S. 39, 43, 47
Bantysh, O. 27,
Barcelona, P. 97
Barneo, D. 19
Barrios, L. A. 63, 69
Batlle, X. 11, 12, 64, 66, 70
Bertomeu, J. 96
Bertran-Serra, E. 84, 85, 87
Bescós, L. 40
Bian, S. 81
Blanco, A. 70
Borrell, J. 32
Borrisé, X. 70
Botet-Carreras, A. 32
Brancart, J. 49
Brion, N. 49
Bruylants, G. 49
Buch-Palasi, J. 67
Burguera, S. 22
Busquets, Ma. A. 11, 34, 36

C
Caballero, A. B. 11
Caballero, S. 74
Calpena, A. 50
Capdevila, J. 92
Casals, B. 25, 59, 62, 72
Castaño, O. 17, 33, 35
Castellví-Picanyol, A. 59, 62
Catalán, G. 25
Cerrato-Serrano, P. 52
Chaitoglou, S. 84, 85, 87
Cirera, A. 76, 78, 93
Cirisano, F. 37
Ciudad, C. J. 34, 36
Colchero, A. 31
Coll, C. 29
Costache, M. V. 52, 54, 56
Coya, C. 93
Cuartiella, M. 13

D
David, C. 70
de Aquino, A. 91
de Melo, R. 39
del Morán, Ma. C. 11
del Pozo, D. 29
Del Río, J. A. 33, 35
Delgado, A. 36
Díaz-Torres, R. 60, 71
Domènech-Gil, G. 75, 80
Domènech, Ò. 32
Dong, Y. 17
Dosta, J. 13
Duch, M. 43
Dupkalová, D. 18

E
Engel, E. 17
Escribano, E. 48
Escuer, A. 12, 53, 65, 74
Estany-Macià, A. 75
Estarlich, P. 99
Estradé, S. 29
Eusamio, J. 83, 92

F
Farid, G. 84, 85, 87
Fasna, A. 41
Fazio, S. 34
Ferrando-Huertas, P. 33
Ferrari, M 37
Figueroa, A. I. 12, 64
Forero, J. D. 76
Fort-Grandas, I. 75, 80
Fraile-Rodríguez, A. 12
Franzese, G. 23, 103
Frontera, A. 22

G
Gaja-Capdevila, N. 45
Galceran, R. 25, 62
Gamez, P. 11
García Celma, M. J. 48
García-Martín, A. 70
García-Santiago, A. 52, 54, 56
García, M. 22, 64
Garrido, B. 76, 78, 93
Gómez, E. 24, 88, 94
González-Martínez, S. 75, 104
Grabulosa, A. 83, 92
Gracia, C. 35
Griera, R. 36
Guardia-Escoté, L. 40
Guerrero, A. 70
Gupta, M. 41

H
Hay, J. 34
Hernández-Mínguez, A. 59, 62, 72
Hernàndez, J. M. 25, 52, 54, 56, 59, 62, 67, 72
Hernandez, S. 76, 78, 93
Herrando-Grabulosa, M. 45
Homs, N. 101
Huguet, J. 33, 35
Huidobro, L. 24,
Ibáñez-Insa, J. 20
Iborra, M. 13
Ignés-Mullol, J. 27, 89
Isanta, B. 36
Iwasaki, S. 20
Jabin, I. 49
Jiménez-Franco, A. 20
Kaiser, N. 29
Kakabadze, T. 48
Khan, J. 76, 93

L
Labarta, A. 11, 12, 64, 66, 70
Lakshmi, N. V. 47
Lambíes Asensio, A. 54
Langenberg, E. 19
Lázaro, A. 22
Leborán, V. 19
Leone, F. 39
Lima, J. C. 91
Llor, N. 36
Lloreda, J. 88
Lobo, K. 76, 93
Logothetou, G. 20
López-Aguilar, E. 34
López-Conesa, L. 29
López-Sánchez, J. 35
Lopez, A. J. 99
Luis, F. 68

M
Ma, Y. 84, 85, 87
Macià, F. 25, 59, 62, 72
Maddaleno, A. S. 40, 103
Majumdar, S. 84, 85, 87
Mallandrich, M. 50
Mañas, L. 90
Marí-Guaita, J. 76, 93
Martinez-Serra, A. 23, 103
Martínez, J. 63
Martínez, M. 13, 97
Martínez, O. 71
Masmitja, G. 99
Massaro, M. 39
Mayans, J. 12, 53, 57, 65, 74
Mendoza-Gamero, Y. 104
Mitjans, M. 40, 103
Mohammadi, R. 50
Molina-Luna, L. 29

Monopoli, M. P. 23, 103
Montero, M. T. 32
Mora-Blanco, D. 70
Mora, I. 78
Morán, M. C. 37
Moreno-Sereno, M. 75, 80
Morral, G. 48
Moya, C. 11, 49, 64, 66
Mueller, P. A. 34
Muñoz-Rosas, A. L. 96

N
Nandi, P. 29
Nasiou, D. 29
Navarro-Urrios, D. 52
Neylubina, Y. 68
Nicolopoulos, S. 20
Noé, V. 34, 36
Noguera-Monteagudo, A. 17, 33
Noto, R. 39
Novikov, T. 63, 69

O
Òdena, J. 59, 62, 72

P
Pacheco-Velázquez, S. C. 34
Padilla, J. A. 97
Palacio, F. 76, 78
Pamir, N. 34
Pardo, I. 79
Pardo, J. A. 19
Pascual, E. 79
Pastor, I. 31
Pecharromán, C. 70
Peiró, F. 29
Pellegrino, P. 77, 80
Pérez-García, Ll. 18, 38, 39, 41, 43, 47
Pérez-Murano, F. 70
Pérez-Rodríguez, A. 99
Pesquera, D. 25
Pickl, T. 91
Pinto, A. 22
Plana-Ruiz, S. 20
Plaza, J. A. 43
Pöthig, A. 91
Poulopoulos, V. 20
Puigdollers, J. 99

R
Ramirez, E. 13
Ramírez, P. 101
Ramos, R. 19
Raymo, F. M. 39
Riela, S. 39
Rigual, J. 88
Ritort, F. 31
Rivadulla, F. 19
Rodríguez-Álvarez, J. 70
Rodríguez, A.F. 64
Rodríguez, L. 22, 90, 91
Rodríguez, R. 33, 35
Romano-Rodríguez, A. 75, 80, 104
Romero, H. 19
Roqué-Rosell, J. 20
Rosales Rivera, L. C. 48
Roubeau, O. 60, 63, 68, 71
Rovirola, M. 59, 62, 72
Ruiz Torres, J. A. 11, 66

S
Sagués, F. 21, 27, 89
Sainz-García, D. 75, 104
Sainz, D. 80
Sánchez-Espejo, R. 39
Sánchez-López, E. 45
Sánchez, A. 101
Sánchez, R. 78
Sañudo, E. C. 55, 58, 61
Saorin, A. 103
Serafin, J. 87
Serrà, A. 24, 88, 94
Serra, J. 65
Serrano-Guarinos, J. 68
Sires, I. 97
Sotirakopoulos, K. 69
Soto, R. 13
Stefanova, M. 20
Suárez, T. 43

T
Teixidó, E. 40
Tema, E. 20
Tirira, P. 97
Torrent, J. 12, 57
Torres-Andrés, J. 89
Troian-Gautier, L. 49

U
Ullah, Z. 41

V
Van Durme, B. 17
Van Vlierberghe, S. 17, 33
Varela-Domínguez, N. 19
Vargas, B. 29
Vázquez, P. 43
Vergés, I. 77
Vergés, M. 21
Vescio, G. 76, 78, 93
Vidal-Ferran, A. 80
Vidrier, J. L. 96
Vila-Comamala, J. 70
Vilanova, O. 23
Vilariño, P. 60, 94
Vinardell, M. P. 40
Viseras, C. 39
Voz, C. 99

W
Wang, J. 38

X
Xuriguera, E. 97

Y
Yanac-Huertas, R. E. 33, 35
Yedra, L. 29

Z
Zuber, J. 91
Zymi, E. 20


Institut de Nanociència
i Nanotecnologia
UNIVERSITAT DE
BARCELONA

UNIVERSITAT DE BARCELONA
IN²UB - Institut de Nanociència i Nanotecnologia

in2ub@ub.edu
www.ub.edu/in2ub